CHARACTERISATION AND TRIBOLOGICAL BEHAVIOUR OF ALUMINA-TITANIA COATINGS

A THESIS SUBMITTED IN PARTIAL FULFILMENT

OF THE REQUIREMENTS FOR THE DEGREE OF

Master of Technology

in

Metallurgical and Materials Engineering

By

ANUPAMA SAHU

Department of Metallurgical and Materials Engineering

National Institute of Technology

Rourkela

2007

CHARACTERISATION AND TRIBOLOGICAL BEHAVIOUR OF ALUMINA-TITANIA COATINGS

A THESIS SUBMITTED IN PARTIAL FULFILMENT
OF THE REQUIREMENTS FOR THE DEGREE OF

Master of Technology

in

Metallurgical and Materials Engineering

By

ANUPAMA SAHU

Under the Guidance of

Prof. S. SEN

&

Under the Co-Guidance of

Prof. S. C. MISHRA

Department of Metallurgical and Materials Engineering

National Institute of Technology

Rourkela

2007

National Institute of Technology
Rourkela

CERTIFICATE

This is to certify that thesis entitled, "CHARACTERISATION AND TRIBOLOGICAL BEHAVIOUR OF ALUMINA-TITANIA COATINGS**"** submitted by Ms. ANUPAMA SAHU in partial fulfillment of the requirements for the award of Master of Technology Degree in Metallurgical and Materials Engineering at National Institute of Technology, Rourkela (Deemed University) is an authentic work carried out by her under our supervision and guidance.

To the best of our knowledge, the matter embodied in this thesis has not been submitted to any other university/ institute for award of any Degree or Diploma.

Prof. S.C.Mishra
Date:
Dept. of Metallurgical and Materials Engineering
National Institute of Technology
Rourkela-769008

Prof. S.Sen
Date:
Dept. of Metallurgical and Materials Engineering
National Institute of Technology
Rourkela-769008

ACKNOWLEDGEMENT

I avail this opportunity to extend my hearty indebtedness to my guide **Prof. S. Sen &** my co-guide **Prof. S. C. Mishra, Dept. of Metallurgical and Materials Engineering, NIT, Rourkela** for their invaluable guidance, motivation, untiring efforts and meticulous attention at all stages during my course of work.

I express my sincere thanks to **Prof. G. S. Agarwal**, **Head of the Department of Metallurgical and Materials Engineering, NIT, Rourkela** for providing me the necessary facilities in the department. I am also grateful to **Prof. K. N. Singh**, **M. Tech. co-ordinator**, for his constant concern and encouragement for execution of this work.

I also express my sincere gratitude to **Prof. Alok Satapathy**, **Dept. of Mechanical Engineering** for his timely help during the course of work.

I thankful to **Sri Rajesh Pattnaik, Sri Samir Pradhan** & **Sri Udayanath Sahu,** Metallurgical & Materials Engineering, Technical assistants, for their co-operation in experimental work.

Special thanks to **Ms. Rojaleena Das**, department of Metallurgical and Materials Engineering for being so supportive and helpful in every possible way.

Date :

Anupama Sahu

Roll No. : 20504001

CONTENTS

ABSTRACT

Alumina-Titania coatings are excellent candidates for providing protection against abrasive wear and resistant to high temperature erosion. Such coatings are desirable in electrical insulation and anti-wear applications; viz. as protective coatings for sleeve shafts, thermo-couples jackets, pump shafts e.t.c.

Plasma spraying is gaining acceptance as a development of quality coatings of various materials on a wide range of substrates. Coatings made with plasma route exhibit excellent wear, corossion resistance and high thermal shock resistance etc. Alumina pre-mixed with Titania powder (Al_2O_3-13%TiO_2) is deposited on mild steel and copper substrates by atmospheric plasma spraying at various operating power level ranging from 11 to 21kW.

The properties of the coatings depend on the materials used, operating condition and the process parameters. The plasma spraying process is controlled by the parameter interdependencies, co-relations and individual effect on coating characteristics. The particle sizes of the raw materials used for coating are characterized using Laser particle size analyzer of Malvern Instruments make. To characterize the coating, Coating interface bond strength is measured using coating pull out method with Instron 1195 confirming to ASTM C-633 standard. Micro-hardness measurement is done on the polished cross section of the samples on the optically distinguishable phases Using Leitz Micro-Hardness Tester.

To ascertain the phases present and phase changes / transformation taking place during plasma spraying, X-ray diffractograms is taken on the raw material and on coatings. The coating quality and behaviour depends on coating morphology and inter-particle bonding of the sprayed powders. The surface and interface morphology of the coatings is observed by Scanning Electron Microscope. Measurement of porosity is made using the image analysis technique. To ensure the coatability of alumina- titania on different substrates, coating thickness is measured on the polished cross-sections of the samples, using an optical microscope. Coating deposition efficiency is also calculated.

To study the suitability of the coatings for wear resistance application, wear properties of these coatings are studied. The erosion wear behaviour of these coatings is evaluated with solid particle erosion tests under various operating conditions. In order to control the wear

loss in such a process, one of the challenges is to recognize parameter interdependencies; correlations and their individual effects on wear so that the coating can be useful for tribolgical application.

Statistical analysis of the experimental results using Taguchi experimental design is presented. Spraying parameters such as impact angle, impact velocity, stand off distance, size of the erodent are identified as the significant factors affecting the coating erosion wear. A prediction model using artificial neural networks is also employed to simulate property-parameter correlations and a fairly good agreement in the experimental and predicted values is obtained. This analysis makes it clear that by appropriate choice of processing conditions, a sound and adherent ceramic coating is achievable with alumina and titania.

LIST OF FIGURES

LIST OF TABLES

Chapter 1

INTRODUCTION

- Background
- Objectives of the present piece of investigation

CHAPTER 1
INTRODUCTION

1.1 BACKGROUND

Increasing demand for engineering products to work in severe operating environments calls for apt to surface design. Surface design is usually concerned with surface texture and surface chemistry to counter possible wear modes. While surface texture is achieved by mechanical treatment, chemistry is usually controlled by surface modification in the form of coating/deposition.

Surface modification is a generic term now applied to a large field of diverse technologies that can be gainfully harnessed to achieve increased reliability and enhanced performance of industrial components. The incessant quest for higher efficiency and productivity across the entire spectrum of manufacturing and engineering industries has ensured that most modern-day components are subjected to increasingly harsh environments during routine operation. Critical industrial components are, therefore, prone to more rapid degradation as the parts fail to withstand the rigors of aggressive operating conditions and this has been taking a heavy toll of industry's economy. In an overwhelmingly large number of cases, the accelerated deterioration of parts and their eventual failure has been traced to material damage brought about by hostile environments and also by high relative motion between mating surfaces, corrosive media, extreme temperatures and cyclic stresses. Simultaneously, research efforts focused on the development of new materials for fabrication are beginning to yield diminishing returns and it appears unlikely that any significant advances in terms of component performance and durability can be made only through development of new alloys.

As a result of the above, the concept of incorporating engineered surfaces capable of combating the accompanying degradation phenomena like wear, corrosion and fatigue to improve component performance, reliability and durability has gained increasing acceptance in recent years. The recognition that a vast majority of engineering components fail catastrophically in service through surface related phenomena has further fuelled this approach and led to the development of the broad interdisciplinary area of surface modifications. A protective coating deposited to act as a barrier between the surfaces of the component and the aggressive environment that it is exposed to during operation is now

globally acknowledged to be an attractive means to significantly reduce/suppress damage to the actual component by acting as the first line of defense. Coating is a layer of material formed naturally or synthetically or deposited artificially on the surface of an object made of another material with the aim of obtaining required technical or decorative properties.

Existing surface treatment processes fall under three broad categories:

(a) Overlay Coatings:

This category incorporates a very wide variety of coating processes wherein a material different from the bulk is deposited on the substrate. The coating is distinct from the substrate in the as-coated condition and there exists a clear boundary at the substrate/coating interface. The adhesion of the coating to the substrate is a major issue.

(b) Diffusion Coatings:

Chemical interaction of the coating-forming element(s) with the substrate by diffusion is involved in this category. New elements are diffused into the substrate surface, usually at elevated temperatures so that the composition and properties of outer layers are changed as compared to those of the bulk.

(c) Thermal or Mechanical Modifications of Surfaces:

In this case, the existing metallurgy of the component surface is changed in the near-surface region either by thermal or mechanical means, usually to increase its hardness. The type of coating to be provided depends on the application. There are many techniques available, e.g. electroplating, vapour depositions, thermal spraying etc. Of all these techniques, thermal spraying is popular for its wide range of applicability, adhesion of coating with the substrate and durability. It has gradually emerged as the most industrially useful method of developing a variety of coatings, to enhance the quality of new components as well as to reclaim worn/wrongly machined parts.

The increasing utility and industrial adoption of surface engineering is a consequence of the significant recent advances in the field. Very rapid strides have been made on all fronts of science, processing, control, modeling, application developments etc. and this has made it an invaluable tool that is now being increasingly considered to be an integral part of component design. Surface modification today is best defined as “the design of substrate and surface together as a system to give a cost effective performance enhancement, of which

neither is capable on its own". The development of a suitable high performance coating on a component fabricated using an appropriate high mechanical strength metal/alloy offers a promising method of meeting both the bulk and surface property requirements of virtually all imagined applications. The newer surfacing techniques, along with the traditional ones, are eminently suited to modify a wide range of engineering properties. The properties that can be modified by adopting the surface engineering approach include tribological, mechanical, thermo-mechanical, electrochemical, optical, electrical, electronic, magnetic/acoustic and biocompatible properties.

The development of surface engineering has been dynamic largely on account of the fact that it is a discipline of science and technology that is being increasingly relied upon to meet all the key modern day technological requirements: material savings, enhanced efficiencies, environmental friendliness etc. The overall utility of the surface engineering approach is further augmented by the fact that modifications to the component surface can be metallurgical, mechanical, chemical or physical. At the same time, the engineered surface can span at least five orders of magnitude in thickness and three orders of magnitude in hardness.

Driven by technological need and fuelled by exciting possibilities, novel methods for applying coatings, improvements in existing methods and new applications have proliferated in recent years. Surface modification technologies have grown rapidly, both in terms of finding better solutions and in the number of technology variants available, to offer a wide range of quality and cost. The significant increase in the availability of coating process of wide ranging complexity that are capable of depositing a plethora of coatings and handling components of diverse geometry today, ensures that components of all imaginable shape and size can be coated economically.

Although there are different techniques available for the deposition of materials on suitable substrates, thermal spraying process is being widely used for depositing thick coatings for various industrial applications. The type of thermal spraying depends on the type of heat source employed and consequently flame spraying (FS), high velocity oxy-fuel spraying (HVOF), plasma spraying (PS) etc. come under the umbrella of thermal spraying. Plasma spraying utilizes the exotic properties of the plasma medium to impart new functional properties to conventional and non-conventional materials and is considered as one highly versatile and technologically sophisticated thermal spraying technique instead of having relatively high price of the sprayable consumables.

Plasma spraying, one of the thermal spraying processes, is increasingly popular owing to its versatility in spraying a large number of materials and is being researched well. It is a very large industry with applications in corrosion, abrasion and temperature resistant coatings and the production of monolithic and near net shapes [**1**]. The process can be applied to coat on variety of substrates of complicated shape and size using metallic, ceramic and /or polymeric consumables. The production rate of the process is very high and the coating adhesion is also adequate. Since the process is almost material independent, it has a very wide range of applicability, e.g., as thermal barrier coating, wear resistant coating etc. Thermal barrier coatings are provided to protect the base material, e.g., internal combustion engines, gas turbines etc. at elevated temperatures. Zirconia (ZrO_2) is a conventional thermal barrier coating material. As the name suggests, wear resistant coatings are used to combat wear especially in cylinder liners, pistons, valves, spindles, textile mill rollers etc. alumina (Al_2O_3), titania (TiO_2) and zirconia (ZrO_2) are the some of the conventional wear resistant coating materials [**2**].

One major limitation of the process is a relatively high price of the plasma sprayable consumables. Plasma spraying has certain unique advantages over other competing surface engineering techniques. By virtue of the high temperature (10,000-15,000^{0}K) and high enthalpy available in the thermal plasma jet, any powder, which melts without decomposition or sublimation, can be coated keeping the substrate temperature as low as 50^{0}C. The coating process is fast and the thickness can go from a few tens of microns to a few mm. Very intricate shapes of the materials can be coated by this method. Plasma spraying is extensively used in hi-tech industries like aerospace, nuclear energy as well as conventional industries like textiles, chemicals, plastics and paper mainly as wear resistant coatings in crucial components.

Plasma spraying is a surface modification technique that combines particle melting, rapid solidification and consolidation in a single process. Because of their higher strength-to-weight ratio and superior wear-resistant properties, ceramics are preferred in most tribological applications. The ceramic materials can be applied for the overlay coating due to the higher gas enthalpy of the thermal plasma jet. The suitability of a ceramic coating on metal substrates depends on (i) the adherence strength at coating-substrate interface, and (ii) stability at operating conditions.

Critical components in high-tech industries operate under extremely hostile conditions of temperature, gas flow, heat flux and corrosive media, which severely limit their service life. This problem can be minimized by using composite structures consisting of the core material to with stand the load and with a suitable surface coating to improve the component life span at operating environment. Plasma spray technology, the process of preparing overlay coating on any surface, is one of the most widely used techniques to prepare such complex structural parts with improved properties and increased life span [**3**].

Alumina–titania coating, which is one of the material largely manufactured, used the atmospheric plasma sprayed (APS) process. This material is known for its wear, corrosion and erosion resistance applications. These types of coatings can be prepared by blending the matrix powder with reinforcement and by plasma spraying [**4, 5**]. The coating process is based on the creation of a plasma jet to melt a feedstock powder [**3**]. Powder particles are injected with the aid of a carrier gas; they gain their velocity and temperature by thermal and momentum transfers from the plasma jet. At the surface of the substrate, particles flatten and solidify rapidly forming a stack of lamellae.

The use of the composite in preference to pure aluminum oxide has certain advantages. TiO_2 is a commonly used additive in plasma sprayable alumina powder. TiO_2 has a relatively low melting point and it effectively binds the alumina grains leading to higher density and wear resistance coating [**6**]. However, a success of an Al_2O_3 - TiO_2 coating depends upon a judicious selection of the arc current, which can melt the powders effectively. This results in a good coating adhesion along with high wear resistance [**7**]. Al_2O_3 with low wt. %. of TiO_2 coatings provide high electric resistance and are suitable where good insulating properties and high electric strength are required [**8**]. But the coatings of mixtures with high wt. %. TiO_2 possess good electrical conductivity due to its manufacturing process of powder and preparation of coatings [**9**].

Here the coatings (alumina 13% titania) have been characterized for their hardness, porosity, adhesion strength and microstructure. The significant phase changes associated with the plasma processing during the coating deposition have been studied. In addition, the coating deposition efficiencies at various operating conditions have also been evaluated.

To study the suitability of the coatings for wear resistance application, wear properties of these coatings is evaluated. The erosion wear behaviour of these coatings is evaluated using a solid particle erosion test. One less studied area in case of ceramic coatings is their

resistance to solid particle erosion. This aspect is studied in the present work by subjecting the coatings to solid particle impact at different impact angles. The capabilities of the coatings to sustain the erosive attack have been assessed. Erosion wear tests were carried out on the coatings to ensure its applicability under various operating conditions. In order to control the wear loss in such a process, one of the challenges is to recognize parameter interdependencies; correlations and their individual effects on wear so that the coating can be useful for tribological application.

A qualitative analysis of the experimental results with regard to erosion wear rate using statistical techniques is presented. The analysis is aimed at identifying the operating variables/factors significantly influencing the erosion wear rate of alumina titania on metals. Factors are identified in accordance to their influence on the coating erosion wear rate. A prediction model based on artificial neural network is also presented considering the significant factors. Neural computation is used since plasma spraying is a complex process that has many variables and multilateral interactions. This technique involves construction of a database, training, and validation and then provides a set of predicted results related to the coating adhesion strength and erosion wear rate at various operating parameters.

1.2 OBJECTIVES OF THE PRESENT PIECE OF INVESTIGATION

The objective of the present investigation is as follows:

a. To explore the coating potential of alumina 13% titania on metal substrates by plasma spraying.

b. To develop a series of plasma sprayed coatings from alumina 13% titania on metal substrates and to find coating deposition efficiency, porosity and thickness.

c. X-ray diffractogram for phase analysis.

d. Micro-structural characterization to evaluate the soundness of the coatings.

e. Mechanical characterization to evaluate the micro-hardness and interface bond strength of the coatings.

f. To asses the capabilities of the coatings to combat wear with a special reference solid particle erosion wear.

g. To analyze the experimental results using statistical techniques so as to identify significant factors/interactions influencing the coating erosion wear rate.

h. Complementing the experimental results, in regard to coating adhesion strength and erosion wear rate, by predicted results obtained from an artificial neural network analysis.

Chapter 2

LITERATURE SURVEY

- Preamble
- Surface Modification
- Techniques of surface modification
- Thermal Spraying
- Plasma Spraying
- Industrial Applications of Plasma Spraying
- Wear
- Types of wear
- Symptoms of wear
- Recent trends in metal wear research
- Wear resistant Coatings
- Erosion wear of ceramic coatings

CHAPTER 2
LITERATURE SURVEY

2.1 PREAMBLE

This chapter deals with the literature survey of the broad topic of interest namely the development of surface modification technology for tribological applications. This treatise embraces various coating techniques with a special reference to plasma spraying, the coating materials and their characteristics. The performances of wear resistant coatings under various conditions have been reviewed critically along with the corresponding failure mechanisms. It also presents a review of the wear, types of wear, symptoms of wear and recent trends in metal wear research along with erosion wear behaviour of ceramic coatings, which is the material of interest in this work.

At the end of the chapter a summary of the literature survey and the knowledge gap in the earlier investigations are presented.

2.2 SURFACE MODIFICATION

Surface modification is a relatively new term that has come up in the last two decades or so to describe interdisciplinary activities aimed at tailoring the surface properties of engineering materials. The object of surface engineering is to upgrade their functional capabilities keeping the economic factors in mind [**10**]. 'Surface Engineering' is the name of the discipline - surface modification is the philosophy behind it. To elucidate the matter an example can be taken. Tungsten carbide cobalt composite is a very popular cutting tool material, and is well known for its high hardness and wear resistance. If a thin coating of TiN is applied on to the WC-Co insert, its capabilities increase considerably [**11**]. Actually a cutting tool, in action, is subjected to a high degree of abrasion, and TiN is more capable of combating abrasion. On the other hand, TiN is extremely brittle, but the relatively tough core of WC-Co composite protects it from fracture. Thus through a surface modification process we assemble two (or more) materials by the appropriate method and exploit the qualities of both [**12**]. It is a very versatile tool for technological development provided it is applied judiciously keeping the following restrictions in mind:

(i) The technological value addition should justify the cost.

(ii) The choice of technique must be technologically appropriate.

(iii)The coating-surface treatment should not impair the properties of the bulk material.

2.3 TECHNIQUES OF SURFACE MODIFICATION

Today a large number of commercially available technologies are present in the industrial scenario [**12**]. An overview of such technologies is presented below.

SURFACE MODIFICATION TECHNOLOGIES:

2.3 a) Plating

- Electro-deposition
- Electroless deposition
- Electro-chemical Conversion coating
- Electro-forming

2.3 b) Diffusion Processes

- Carburising
- Nitriding
- Carbonitriding
- Aluminising
- Siliconising
- Chromising
- Boronising

2.3 c) Surface Hardening

- Flame Hardening
- Induction Hardening
- Electron-beam Hardening
- Laser-beam Hardening
- Ion Implantation

2.3d) Thin Film Coating

- PVD
- CVD

2.3e) Hardfacing by Welding

- SMAW
- GTAW
- GMAW
- Submerged Arc Welding
- Plasma Welding

- Laser Beam Welding
- Electron beam Welding

2.3 f) Thermal Spraying

- Flame Spraying
- Electric arc Spraying
- Plasma Spraying
- D-gun Coating

2.4 THERMAL SPRAYING

It is the generic category of material processing technique that apply consumables in the form of a finely divided molten or semi molten droplets to produce a coating onto the substrate kept in front of the impinging jet. The melting of the consumables may be accomplished in a number of ways, and the consumable can be introduced into the heat source in wire or powder form. Thermal spray consumables can be metallic, ceramic or polymeric substances. Any material can be sprayed as long as it can be melted by the heat source employed and does not undergo degradation during heating [**13]**.

The nature of bonding at the coating-substrate interface is not completely understood. It is normally assumed that bonding occurs by the mechanical interlocking. Under this circumstance it is generally possible to ignore the metallurgical compatibility [**12**]. This is an extremely significant feature of thermal spraying. Another interesting aspect of thermal spraying is that the surface temperature seldom exceeds 200^0 C. Hard metal or ceramic coating can be applied to thermosetting plastics. Stress related distortion problems are also not so significant. The spraying action is achieved by the rapid expansion of combustion gases (which transfer the momentum to the molten droplets) or by a separate supply of compressed air. There are two basic ways of generating heat required for melting the consumables [**14, 15**]. They are (i) combustion of a fuel gas and (ii) high energy electric arc, shown in fig.2.1.

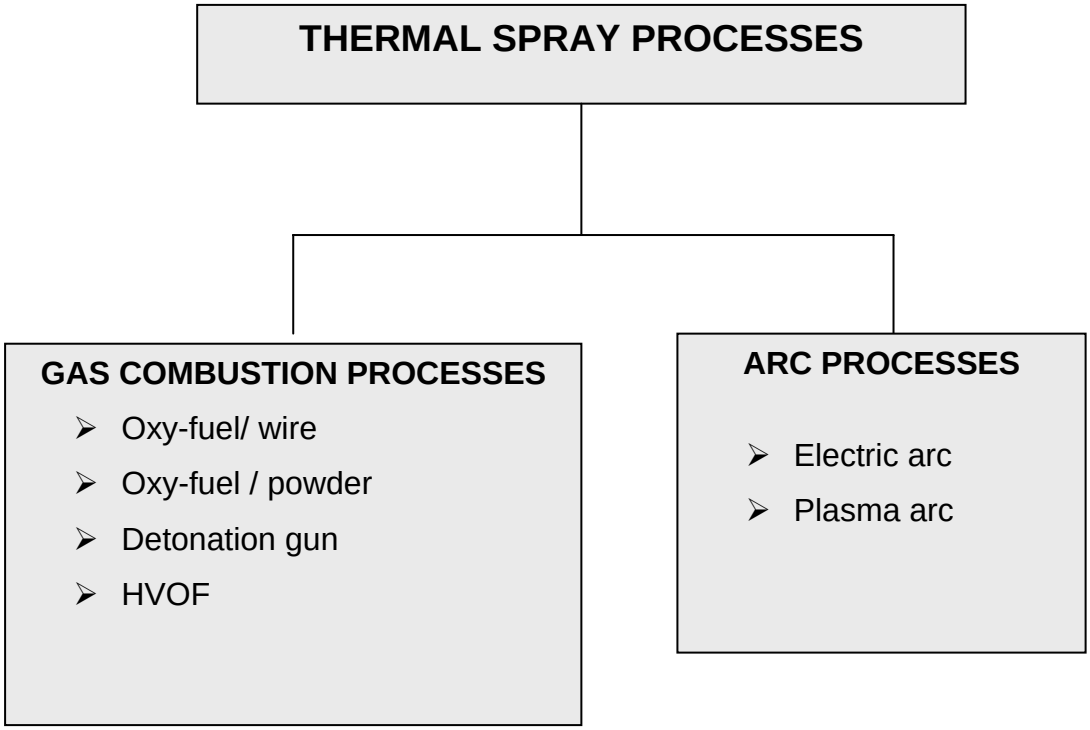

Fig. 2.1 Categorization of common thermal spray processes.

Processes available for thermal spraying have been developed specifically for a purpose and fall into two categories-high and low energy processes. The key processes and their energy sources are summarized in table 2.1 [**15**].

Processes		Energy sources	Different nomenclature
Low energy processes	Flame spraying	Chemical	Oxyfuel gas-powder spraying
			Oxyfuel gas-wire spraying
			Metallizing
	Arc spraying	Electrical	Electric arc spraying
			Twin-wire arc spraying
			Metallizing
High energy processes	**Plasma spraying**	Electrical	Air plasma spraying (APS)
			Vacuum plasma spraying (VPS)
			Low pressure plasma spraying (LPPS)
			Water stabilized plasma spraying (UWS)
			Inductive plasma spraying
	Detonation flame spraying	Chemical	D-gun
	High velocity oxyfuel spraying	Chemical	HVOF spraying
			High velocity oxygen fuel spraying
			High velocity flame spraying (HVFS)
			High velocity air fuel

Table 2.1 Thermal-spraying processes.

2.5 PLASMA SPRAYING

Plasma spraying is the most versatile thermal spraying process as shown in fig.2.2. An arc is created between thoriated tungsten cathode and an annular copper anode (both water cooled). Plasma generating gas is forced to pass through the annular space between the electrodes. While passing through the arc, the gas undergoes ionization in the high temperature environment resulting plasma. The ionization is achieved by collisions of electrons of the arc with the neutral molecules of the gas. The plasma protrudes out of the electrode encasement in the form of a flame. The consumable material, in the powdered form, is poured into the flame in metered quantity. The powders melt immediately and absorb the momentum of the expanding gas and rush towards the target to form a thin deposited layer.

The next layer deposits onto the first immediately after, and thus the coating builds up layer by layer [**10, 12**]. The temperature in the plasma arc can be as high as 10,000^{0}C and it is capable of melting anything.

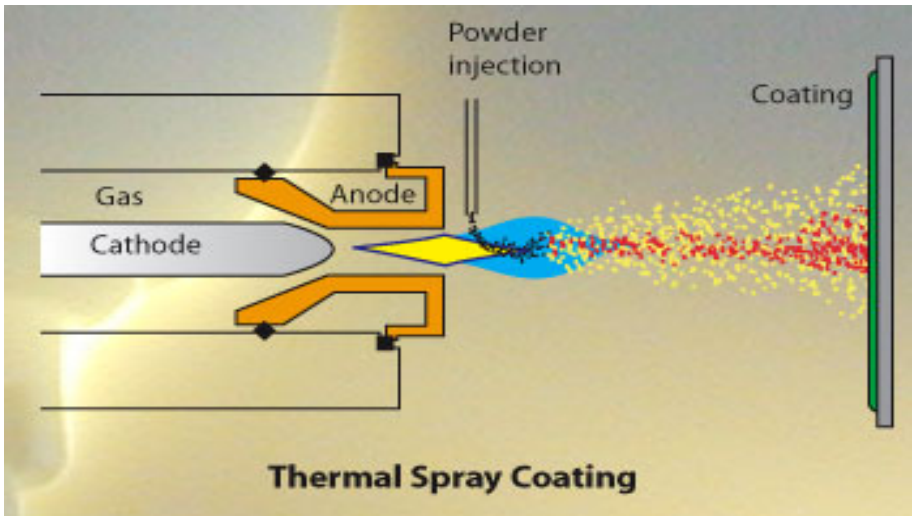

Fig. 2.2 Schematic of Plasma spraying.

2.6 INDUSTRIAL APPLICATIONS OF PLASMA SPRAYING

i) Textile Industry
ii) Paper and printing industry
iii) Automotive Industry and the production of Combustion engines
iv) Glass Industry
v) Electrochemical Industry
vi) Hydraulic machines and mechanisms
vii) Rolling mills and foundry
viii) High Temperature wears resistance coatings on Slide Gate Plates
ix) Chemical Plants
x) Aircraft Jet engines

There has been a steady growth in the number of applications of thermally sprayed coatings. Availability of hardware and adaptability of the technique are the most important factors for this growth. Plasma spraying has been successfully applied to a wide range of industrial technologies. Automotive industry, aerospace industry, nuclear industry, textile industry, paper industry and iron and steel industry are some of the sectors that have successfully exploited thermal plasma spray technology [**16**].

2.6 i) Textile Industry

Plasma spraying was for the first time employed in textile industry in Czechoslovakia. Plasma spraying has replaced the classical technologies of chrome plating, anodization and chemical surface hardening. Advantages of this technique are a lot, all of which add to the quality and quantity of textile production.

- Critical machinery parts**:** Different thread guiding & distribution rollers, ridge thread brakes, distribution plates, driving & driven rollers, gallets, tension rollers, thread brake caps, lead-in bars etc.

- Coatings and advantages**:** High wear resistance coatings are required on textile machinery parts, which are in contact with synthetic fibers. For this purpose especially Al_2O_3 + 3% TiO_2, Al_2O_3 + 13% TiO_2, Cr_2O_3, WC + Co are applied. These coatings with hardness ranging from 1800 to 2600 HRV are extraordinarily dense, have high wear resistance and provide excellent bonding with the substrate. Plasma spraying has following advantages in textile industries:

  - Replacement of worn out parts is minimized and hence reduces the idle times.
  - Physical and mechanical properties of fibers are improved.
  - Revolution speed of these lighter parts can be increased.
  - Shelf life of the textile machinery parts with plasma sprayed coating last 5 to 20 times longer than parts coated by chrome plating or another classical technique.
  - Economic savings are realized considerably by substituting heavy steel or cast iron parts with aluminum or durable ones with wear- resistant coatings.

2.6 ii) Paper and printing industry

The machinery in the paper and printing industry is usually quite large and is subjected to considerable wear from the sliding and friction contact with the paper products.

- Critical machinery parts**:** Paper drying rolls, sieves, filters, roll pins etc.in paper machines, printing rolls, tension rolls and other parts of printing machines.

- Coatings and advantages**:** Spraying of oxide layers is an available economical solution which can be employed right in place in the production shop. Here again

oxide layers composed of Al_2O_3 with 3 to 13 % additions of TiO_2, Cr_2O_3 or MnO_2 are applied. Cast iron rolls are typically first sprayed with NiCr 80/20, 50μm thick and then over it 0.2mm thick Al_2O_3 + 13% TiO_2 layer is coated. The special advantages are mentioned below:

- Ensures corrosion resistance of rolls i.e. the base metal
- Resistance of oxide layers against printing inks extends the life of machine parts
- Production cost is reduced considerably
- Coating resulted to the so-called "orange peel" phenomena, surface finishing obtainable that prevents paper foil, dyes etc.from sticking and allows their proper stretching.

2.6 iii) Automotive Industry and the production of Combustion engines

Plasma sprayed coatings used, in automotive industries of many industrially advanced countries, endure higher working pressure and temperature to improve wear resistance, good friction properties, resistance against burn-off and corrosion due to hot combustion products and resistance against thermal loading. Some of the several applications developed for the automotive industry at the Slovak Academy of Sciences (SAV) in Bratislava are spraying torsion bars with aluminium coatings against corrosion. The plasma spraying technology is introduced in the production of gearshift forks for gear boxes in fiat car factory and on the critical parts of big Diesel engines.

2.6 iv) Glass Industry

Molten glass quickly wears the surface of metal which comes in contact with it. In order to protect the metal tools, plasma sprayed coatings are made on to it.

2.6 v) Electrochemical Industry

In the electromechanical and computer industries the electrically conductive Cu, Al, W and the semi-conductive and insulating ceramic layers are widely used. Some contacts of electrodes, e.g. the spark gaps of nuclear research equipment, are produced of massive tungsten. Such electrodes can be replaced by modern electrodes with a sprayed tungsten

coating about 0.5mm thick. This electrode ensures short- time passages of 300,000A current with a life of several hundred switching.

2.6 vi) Hydraulic machines and mechanisms

The range of possible applications in this field is very extensive, mainly in water power plants, in production and work of pumps, where many parts are subjected to combined effects of wear, corrosion, erosion and cavitations.

2.6 vii) Rolling mills and foundry

In Rolling mills and pressing shops the wear resistant coatings are used to renovate the heavy parts of heavy duty machines whose replacement would be very costly. Several applications in this field are presented herewith:

- Rolling strand journals being repaired by giving a coating layer of stainless steel. Blooming roll mill journal renovated with a NiCrBSi layer.
- Gears of rolling mill gear box being renovated by a wear resistance coating.
- To repair a rolling mill slide and the plungers of a forging press a hard wear resistance is applied.
- Heat resistant plasma coating is widely used for foundry and metallurgical equipment where molten metal or very high temperatures are encountered. This equipment includes the sliding plugs of steel ladles with alumina or zirconia coatings.
- Conveyer rollers in plate production with zirconia based refractory coatings.
- Oxygen tubes, cast iron moulds in continuous casting of metals, with Al_2O_3+TiO_2,$ZrSiO_4$+ZrO_2+MgO.

2.6 viii) High Temperature wears resistance coatings on Slide Gate Plates

In steel plants severe erosion of refractory teeming plates (slide gate plates) and generation of macro-micro cracks during teeming of steel is observed, rendering the plates unstable for reuse. Plasma sprayed ceramic coatings on refractory plates is made to minimize the damage and hence increase the life of slide gate plate. Al_2O_3, $MgZrO_3$, ZrO_2, TiO_2, Y_2O_3 and calcia stabilized. Zirconia can be coated.

2.6 ix) Chemical Plants

The base metal of machine parts is subjected to different kind of wear in chemical plants. In such cases plasma sprayed coatings are applied to protect the base metal. They can be used for various blades, shafts, bearing surfaces, tubes, burners, parts of cooling equipments etc.

2.6 x) Aircraft Jet engines

The working parts of Aircraft jet engines are subjected to serve mechanical, chemical and thermal stresses. A jet engine has a number of construction nodes where plasma coating is employed with much success in order to protect them. There are for example, face of the blower box, compressor box and disc, guide bearing, fuel nozzles, blades, combustition chambers.

2.7 WEAR

Wear occurs as a natural consequence when two surfaces with a relative motion interact with each other. Wear may be defined as the progressive loss of material from contacting surfaces in relative motion. Scientists have developed various wear theories in which the Physico-Mechanical characteristics of the materials and the physical conditions (e.g. the resistance of the rubbing body and the stress state at the contact area) are taken in to consideration. In 1940 Holm [**17**] starting from the atomic mechanism of wear, calculated the volume of substance worn over unit sliding path.

Wear of metals is probably the most important yet at least understood aspects of tribology. It is certainly the youngest of the tri of topics, friction, lubrication and wear, to attract scientific attention, although its practical significance has been recognizes throughout the ages.

Wear is not an intrinsic material property but characteristics of the engineering system which depend on load, speed, temperature, hardness, presence of foreign material and the environmental condition [**18**]. Widely varied wearing conditions causes wear of materials. It may be due to surface damage or removal of material from one or both of two solid surfaces in a sliding, rolling or impact motion relative to one another. In most cases wear occurs through surface interactions at asperities. During relative motion, material on contacting

surface may be removed from a surface, may result in the transfer to the mating surface, or may break loose as a wear particle. The wear resistance of materials is related to its microstructure may take place during the wear process and hence, it seems that in wear research emphasis is placed on microstructure [**19**]. Wear of metals depends on many variables, so wear research programs must be planned systematically. Therefore researchers have normalized some of the data to make them more useful. The wear map proposed by Lim and Ashby [**18**] is very much useful in this regard to understand the wear mechanism in sliding wear, with or without lubrication.

2.8 TYPES OF WEAR

In most basic wear studies where the problems of wear have been a primary concern, the so-called dry friction has been investigated to avoid the influences of fluid lubricants.

Dry friction' is defined as friction under not intentionally lubricated conditions but it is well known that it is friction under lubrication by atmospheric gases, especially by oxygen [**20**].

A fundamental scheme to classify wear was first outlined by Burwell and Strang [**21**]. Later Burwell [**22**] modified the classification to include five distinct types of wear, namely (1) Abrasive (2) Adhesive (3) Erosive (4) Surface fatigue (5) Corrosive.

2.8.1 Abrasive wear

Abrasive wear can be defined as wear that occurs when a hard surface slides against and cuts groove from a softer surface. It can be account for most failures in practice. Hard particles or asperities that cut or groove one of the rubbing surfaces produce abrasive wear. This hard material may be originated from one of the two rubbing surfaces. In sliding mechanisms, abrasion can arise from the existing asperities on one surface (if it is harder than the other), from the generation of wear fragments which are repeatedly deformed and hence get work hardened for oxidized until they became harder than either or both of the sliding surfaces, or from the adventitious entry of hard particles, such as dirt from outside the system.

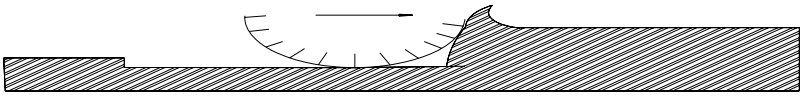

Fig. 2.3 Schematic representations of the abrasion wear mechanism.

Two body abrasive wear as shown in fig. 2.3 occurs when one surface (usually harder than the second) cuts material away from the second, although this mechanism very often changes to three body abrasion as the wear debris then acts as an abrasive between the two surfaces. Abrasives can act as in grinding where the abrasive is fixed relative to one surface or as in lapping where the abrasive tumbles producing a series of indentations as opposed to a scratch. According to the recent tribological survey, abrasive wear is responsible for the largest amount of material loss in industrial practice [**23**].

2.8.2 Adhesive wear

Adhesive wear can be defined as wear due to localized bonding between contacting solid surfaces leading to material transfer between the two surfaces or the loss from either surface. For adhesive wear as shown in fig. 2.4 to occur it is necessary for the surfaces to be in intimate contact with each other. Surfaces, which are held apart by lubricating films, oxide films etc. reduce the tendency for adhesion to occur.

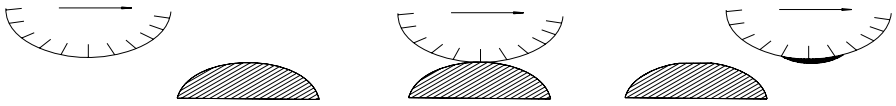

Fig. 2.4 Schematic representations of the adhesive wear mechanism.

2.8.3 Erosive wear

Erosive wear can be defined as the process of metal removal due to impingement of solid particles on a surface. Erosion is caused by a gas or a liquid, which may or may not carry, entrained solid particles, impinging on a surface. When the angle of impingement is small, the wear produced is closely analogous to abrasion. When the angle of impingement is

normal to the surface, material is displaced by plastic flow or is dislodged by brittle failure. The schematic representation of the erosive wear mechanism is shown in fig.2.5.

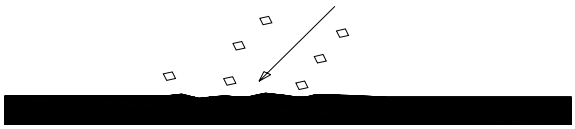

Fig. 2.5 Schematic representations of the erosive wear mechanism.

2.8.4 Surface fatigue wear

Wear of a solid surface caused by fracture arising from material fatigue. The term 'fatigue' is broadly applied to the failure phenomenon where a solid is subjected to cyclic loading involving tension and compression above a certain critical stress. Repeated loading causes the generation of micro cracks, usually below the surface, at the site of a pre-existing point of weakness. On subsequent loading and unloading, the micro crack propagates. Once the crack reaches the critical size, it changes its direction to emerge at the surface, and thus flat sheet like particles is detached during wearing. The number of stress cycles required to cause such failure decreases as the corresponding magnitude of stress increases. Vibration is a common cause of fatigue wear. The schematic representation of the surface fatigue wear mechanism is shown in fig. 2.6.

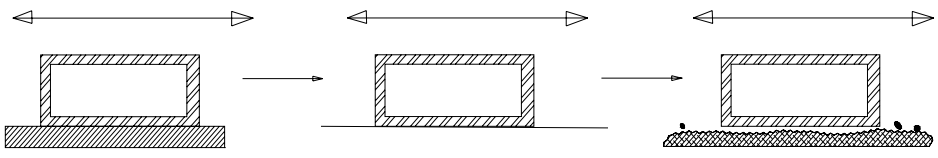

Fig. 2.6 Schematic representations of the surface fatigue wear mechanism.

2.8.5 Corrosive wear

Most metals are thermodynamically unstable in air and react with oxygen to form an oxide, which usually develop layer or scales on the surface of metal or alloys when their interfacial bonds are poor. Corrosion wear is the gradual eating away or deterioration of unprotected metal surfaces by the effects of the atmosphere, acids, gases, alkalis, etc. This type of wear creates pits and perforations and may eventually dissolve metal parts.

2.9 SYMPTOMS OF WEAR

Literature available on the rate controlling wear mechanism demonstrated that it may change abruptly from one another at certain sliding velocities and contact loads, resulting in abrupt increases in wear rates. The conflicting results in the wear literature arise partly because of the differences in testing conditions, but they also make clear that a deeper understanding of the wear mechanism is required if an improvement in the wear resistances of the coating is to be achieved. This in turn requires a systematic study of the wear under different stresses, velocities and temperatures. It is generally recognized that wear is a characteristic of a system and influenced by many parameters. Laboratory scale investigation if designed properly allows careful control of the tribo system where by the effects of different variables on wear behaviour of the coating can be isolated and determined. The data generated through such investigation under controlled conditions may help in correct interpretation of the results.

A summary of the appearance and symptoms of different wear mechanism is indicated in Table 2.2 and the same is a systematic approach to diagnose the wear mechanisms.

Types of wear	Symptoms	Appearance of the worn-out surface
Abrasive	Presence of clean furrows cut out by abrasive particles	Grooves
Adhesive	Metal transfer is the prime symptoms	Seizure, catering rough and torn-out surfaces.
Erosion	Presence of abrasives in the fast moving fluid and short abrasion furrows	Waves and troughs.
Corrosion	Presence of metal corrosion products.	Rough pits or depressions.
Fatigue	Presence of surface or subsurface cracks accompanied by pits and spalls	Sharp and angular edges around pits.
Impacts	Surface fatigue, small sub micron particles or formation of spalls	Fragmentation, peeling and pitting.
Delamination	Presence of subsurface cracks parallel to the surface with semi-dislodged or loose flakes	Loose, long and thin sheet like particles
Fretting	Production of voluminous amount of loose debris	Roughening, seizure and development of oxide ridges
Electric attack	Presence of micro craters or a track with evidence of smooth molten metal	Smooth holes

Table 2.2 Symptoms and appearance of different types of wear [**24**].

A typical model, exemplifying the rate of erosion depending on size and velocity of particle on impacting the substrate is shown in fig.2.7. The increase in impact velocity or particle diameter clearly accelerates erosion damage. From the fact that an increase in particle velocity or size leads to larger or deeper indentations as schematically shown in Fig. 2.7, deviations in $k2$ and $k3$ values from the theoretical ones (k_2 =2, k_3 = 0) indicate the true effects of impact velocity and particle diameter which are connected with the relative aggressiveness of indentation. The larger or deeper is the indentation the greater amount of material is removed from the rim of the indentation.

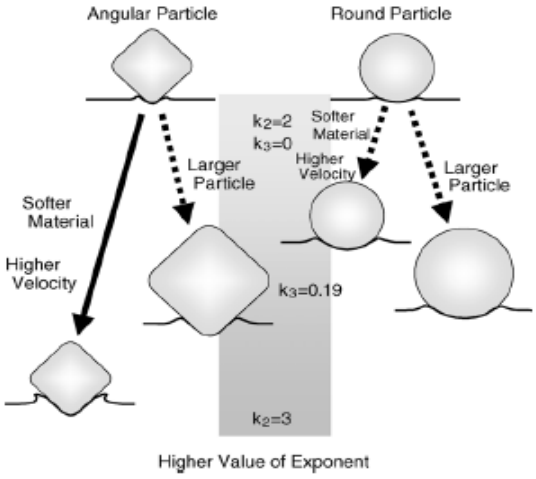

Fig. 2.7 Model of the effects of impact parameters on exponents k_2 and k_3.

2.10 RECENT TRENDS IN METAL WEAR RESEARCH

Much of the wear researches carried out in the 1940's and 1950's were conducted by mechanical engineers and metallurgists to generate data for the construction of motor drive, trains, brakes, bearings, bushings and other types of moving mechanical assemblies [**25**].

It became apparent during the survey that wear of metals was a prominent topic in a large number of the responses regarding some future priorities for research in tribology. Some 22 experienced technologists in this field, who attended the 1983 'Wear of Materials Conference' in Reston, prepared a ranking list [**26**]. Their proposals with top priority were further investigations of the mechanism of wear and this no doubt reflects the judgments that particular effects of wear should be studied against a background of the basic physical and chemical processes involved in surface interactions. The list proposed is shown in table 2.3.

Peterson [**27**] reviewed the development and use of tribo-materials and concluded that metals and their alloys are the most common engineering materials used in wear applications. Grey cast iron for example has been used as early as 1388. Much of the wear research conducted over the past 50 years is in ceramics, polymers, composite materials and coatings [**28**].

Ranking	Topics
1.	Mechanism of Wear
2.	Surface Coatings and treatments
3.	Abrasive Wear
4.	Materials
5.	Ceramic Wear
6.	Metallic Wear
7.	Polymer Wear
8.	Wear with Lubrication
9.	Piston ring-cylinder liner Wear
10.	Corrosive Wear
11.	Wear in other Internal Combustion Machine Components

Table 2.3 Priority in wears research [**26**].

Wear of metals encountered in industrial situations can be grouped into categories shown in table 2.4. Though there are situations where one type changes to another or where two or more mechanism plays together.

Type of wear in Industry	Approximate percentage involved
Abrasive	50
Adhesive	15
Erosion	8
Fretting	8
Chemical	5

Table 2.4 Type of wear in industry [**25**]**.**

2.11 WEAR RESISTANT COATINGS

The choice of a material depends on the application. However, the ceramic coatings are very hard and hence on an average offer more abrasion resistance than their metallic counterparts Today a variety of materials, e.g., carbides, oxides, metallic, etc., belonging to the above category are available commercially. The coatings with these materials can be grouped into the following categories: [**10]**

(i) Carbides: WC, TiC, SiC, ZrC, Cr_2C_3 etc.
(ii) Oxides: Al_2O_3, Cr_2O_3, TiO_2, ZrO_2 etc.
(iii) Metallic: NiCrAlY, Triballoy etc.
(iv) Diamond

2.11.1 Oxide Coatings

Metallic coatings and metal containing carbide coatings sometime are not suitable in high temperature environments in both wear and corrosion applications. Often they fail owing to oxidation or decarburization. In such case the material of choice can be an oxide ceramic coating, e.g., $Al_2O_3.Cr_2O_3$, TiO_2, ZrO_2 or their combinations. However, a high wear resistance, and chemical and thermal stability of these materials are counterbalanced by the disadvantages of low values of thermal expansion coefficient, thermal conductivity, mechanical strength, fracture toughness and somewhat weaker adhesion to substrate material. The thickness of these coatings is also limited by the residual stress that grows with thickness. Therefore, to obtain a good quality coating it is essential to exercise proper choice of bond coat, spray parameters and reinforcing additives [**10**].

2.11.1a) Chromia (Cr_2O_3) Coatings

These coatings are applied when corrosion resistance is required in addition to abrasion resistance. It adheres well to the substrate and shows an exceptionally high hardness 2300 $HV_{0.5\ kg}$ [**10**]. Chromia coatings are also useful in ship and other diesel engines, water pumps, and printing rolls [3]. A Cr_2O_3- 40 wt% TiO_2 coating provides a very high coefficient of friction (0.8), and hence can be used as a brake liner [**29**]. The wear mode of chromia coatings has been investigated under various conditions. Depending on experimental conditions, the wear mode can be abrasive [**29**], plastic deformation [**30**], micro fracture [**31**] or a conglomerate of all of these [**32**]. This material has also been tested under lubricated conditions, using inorganic salt solutions (NaCl, $NaNO_3$, Na_3PO_4) as lubricants and also at a

high temperature. The wear rate of self-mated chromia is found to increase considerably at 450°C, and plastic deformation and surface fatigue are the predominant wear mechanisms [**33**]. Under lubricated condition, the coatings exhibit tribochemical wear [**34**]. It has also been tested for erosion resistance [**35**].

2.11.2b) Zirconia (ZrO_2) Coatings

Zirconia is widely used as a thermal barrier coating. However, it is endowed with the essential qualities of a wear resistant material, i.e., hardness, chemical inertness, etc. and shows reasonably good wear behaviour. In the case of a hot pressed zirconia mated with high chromium containing iron (martensitic, austenitic, or pearlitic), it has been found that in course of rubbing the iron transfers on to the ceramic surface and the austenitic material adheres well to the ceramic as compared to their martensitic or pearlitic counterparts [**36**]. The thick film improves the heat transfer from the contact area keeping the contact temperature reasonably low; thus the transformation of ZrO_2 is prevented. On the other hand with the pearlitic or martensitic iron the material transfer is limited. The contact temperature is high enough to bring about a phase transformation and related volume change in ZrO_2 causing a stress induced spalling. In a similar experiment the wear behaviour of sintered, partially stabilized zirconia (PSZ) with 8 wt% yttria against PSZ and steels has been tested at 200°C. When metals are used as the mating surface, a transferred layer soon forms on the ceramic surface (coated or sintered) [**37**]. In ceramic-ceramic system the contact wear is abrasive in nature. However, similar worn particles remain entrapped between the contact surfaces and induce a polishing wear too. In the load range of 10 to 40 N, no transformation of ZrO_2 occurs [**37,38**]. However, similar tests conducted at 800°C show a phase transformation from monoclinic ZrO_2 to tetragonal ZrO_2 [**39**]. The wear debris of ZrO_2 sometimes get compacted in repeated loading and gets attached to the worn surface forming a protective layer [**40**]. During rubbing, pre-existing or newly formed cracks may grow rapidly and eventually interconnect with each other, leading to a spallation of the coating [**41**]. The worn particles get entrapped between the mating surfaces and abrade the coating. The wear performance of ZrO_2-12 mol% CeO_2 and ZrO_2-12 mol% CeO_2 -10 mol% Al_2O_3 coatings against a bearing steel under various loads has been studied [**42**]. Introduction of alumina as a dopant, has been found to improve the wear performance of the ceramic significantly. Here plastic deformation is the main wear mode. The wear performance of zirconia at 400°C and 600°C has been reported in the literature [**43**]. At these temperatures the adhesive mode of wear plays the major role.

2.11.2c) Titania (TiO_2) Coatings

Titania coating is known for its high hardness, density, and adhesion strength. It has been used to combat abrasive, erosive and fretting wear either in essentially pure form or in association with other compounds [**44,45**]. The mechanism of wear of TiO_2 at 450°C under both lubricated and dry contact conditions has been studied. It has been found to undergo a plastic smearing under lubricated contact, where as it fails owing to the surface fatigue in dry condition. TiO_2-stainless steel couples in various speed load conditions have also been investigated in details [**46**]. At a relatively low load, the failure is owing to the surface fatigue and adhesive wear, whereas at a high load the failure is attributed to the abrasion and delamination associated with a back and forth movement [**47**]. At low speed the transferred layer of steel oxidizes to form Fe_2O_3 and the wear progresses by the adhesion and surface fatigue. At a high speed, Fe_3O_4 forms instead of Fe_2O_3 [**48**]. The TiO_2 top layer also softens and melts owing to a steep rise in temperature, which helps in reducing the temperature subsequently [**49**]. The performance of the plasma sprayed pure TiO_2 has been compared with those of Al_2O_3 – 40 wt% TiO_2 and pure Al_2O_3 under both dry and lubricated contact conditions [**50**]. TiO_2 shows the best results. TiO_2 owing to its relatively high porosity can provide good anchorage to the transferred film and also can hold the lubricants effectively [**51**]. Table 2.5shows some physical properties of Titania.

Properties	TiO2
Composition	TiO2(Rutile)
Density, g/c.c.	4.10
Melting point, ^0C	1900
Hardness, HV. Kgf/mm^2	942
Co-efficient of thermal expansion, $\mu m/m.^0C$	7.5

Table 2.5 Physical properties of Titania.

2.11.2d) Alumina (Al_2O_3) Coatings

Alumina is obtained from a mineral called bauxite, which exists in nature as a number of hydrated phases, e.g., boehmite (γ-Al_2O_3, H_2O), hydragillate , diaspore (α-Al_2O_3. $3H_2O$). It also exists in several other metastable forms like β, δ, θ, η, κ and X [**52**]. α -Al_2O_3 is known to be a stable phase and it is available in nature in the form of corundum. In addition, α-Al_2O_3 can be extracted from the raw materials by fusing them.

Boehmite→450^0C→γ-Al_2O_3→750^0C→δ-Al_2O_3→1000^0C→υ-Al_2O_3→1200^0C→α-Al_2O_3

Bayererite→230^0C→ η- Al_2O_3 →850^0C→ υ-Al_2O_3→1200^0C→ α-Al_2O_3

The phase transformation during freezing of the plasma sprayed alumina droplets has been studied in details [**53,54**]. From the molten particles, γ-Al_2O_3 tends to nucleate, since liquid to γ transformation involves a low interfacial energy. The phase finally formed upon cooling depends on the particle diameter. For particle diameter less than 10 μm, the metastable form is retained (γ, δ, β or θ). Plasma spraying of alumina particles having a mean diameter of 9 μm results in the development of the gamma phase in the coating after cooling [**55**]. The α form is found in the large diameter particle. In fact larger is the diameter; greater is the fraction of α-Al_2O_3 in the cooled solid. This form is desirable for its superior wear properties. Other than the cooling rate, one way to achieve the phase finally formed is to vary the temperature of the substrate. If the substrate temperature is kept at 900^0C, the δ phase forms. The α-Al_2O_3 can be formed by raising the temperature of the substrate to 1100^0 C resulting a slow cooling. During freezing the latent heat of solidification is absorbed in the still molten pool. If this heat generation is balanced by the heat transfer to the substrate, columnar crystals grow. On the other hand, if the aforesaid heat transfer is faster than the heat injection rate from the growing solidification front, equi-axed crystals are supposed to form. In reality columnar crystals are generally found. Table 2.6 shows some physical properties of Alumina.

Properties	Alumina (99.9%)
Composition	Al_2O_3(corundum)
Density,g/c.c.	3.90
Melting point,^{0}C	2015
Thermal conductivity, J/kg. K	35.60
Hardness, HV. Kgf/mm^2	1500
Flexural strength, MPa	380
Tensile strength, MPa	262
Poisson's ratio	0.26
Young's modulus, Gpa	370
Co-efficient of thermal expansion,μm/m.^{0}C	8
Heat capacity, J/kg.K	880

Table 2.6 Physical properties of Alumina.

There are several advantages of alumina as a structural material, e.g., availability, hardness, high melting point, resistance to wear and tear etc. It bonds well with the metallic substrates when applied as a coating on them. Some of the applications of alumina are in bearings, valves, pump seals, plungers, engine components, rocket nozzles, shields for guided missiles, vacuum tube envelops, integrated circuits, etc. Plasma sprayed alumina-coated railroad components are presently being used in Japan [**56**]. Properties of alumina can be further complemented by the particulate (TiO_2, TiC) or whisker (SiC) reinforcement [**57**]. TiC reinforcement limits the grain growth, improves strength and hardness, and also retards crack propagation through the alumina matrix [**58**]. The sliding wear behaviour of both monolithic and SiC whisker reinforced alumina has been studied [**59**]. The whisker reinforced composite has been found to have good wear resistance. The monolithic alumina has a brittle response to sliding wear, whereas the worn surface of the composite reveals signs of plastic deformation along with fracture. The whiskers also undergo pullout or fracture.

The sliding wear behaviour of plasma sprayed alumina against AISI-D2 steel under different speed load conditions has been reported. Within the load range used (45N-133N), the wear vs. load plot shows a maxima. In the initial phase, the wear volume increases with the load for a given number of sliding cycles. Beyond a certain load, owing to both load and frictional heating, a major plastic flow occurs on the coating surface. The plastic flow leads to an increase in real area of contact and a corresponding reduction of normal stress, though the normal load increases. As a result, wear decreases with an increase in load beyond a critical normal load. On the other hand, the wear vs. sliding speed plot also displays a maxima within the speed range used (0.31 to 8 m/s). At a low speed range, the asperities move against each other and deform each other in the process. As the speed is increased, the asperities are subjected to heavy impacts and tend to get fractured from the root producing a higher volume of debris. At a very high velocity the friction related temperature rise becomes high enough to soften the asperities and thereby to protect them from fracture. The wear rate keeps low under such circumstances. Therefore, the plastic deformation and brittle fracture form the failure mechanisms.

2.11.2e) Alumina Titania Coatings

TiO_2 is a commonly used additive in plasma sprayable alumina powder. TiO_2, has a relatively low melting point and it effectively binds the alumina grains. However, a success of an Al_2O_3 - TiO_2 coating depends upon a judicious selection of the arc current, which can melt the powders effectively. This results in a good coating adhesion along with high wear

resistance. The wear performance of Al_2O_3 and Al_2O_3 -50 wt% TiO_2 has been reported in the literature [**59]**. In dry sand abrasion testing, alumina outperformed others presumably owing to its high hardness. In dry sliding at low velocity range, the tribocouple (ceramic and hardened stainless steel) exhibits stick-slip. At relatively high speed range, the coefficient of friction drops owing to the thermal softening of the interface [**60**]. The wear of alumina is found to increase appreciably beyond a critical speed and a critical load. Alumina has been found to fail by plastic deformation, shear and grain pullout. In dry and lubricated sliding as well, the mixed ceramic has been found to perform better than pure alumina. A coating of Al_2O_3 -50 wt% TiO_2 is quite porous and hence is quite capable of holding the transferred metallic layer which protects the surface [**61**]. Wear performance of such coatings can further be improved by a sealing of the pores by polymeric substances. A low thermal diffusivity of the alumina coatings results in a high localized thermal stress on the surface. The mode of wear of alumina is mainly abrasive. The pore size and pore size distribution also play a vital role in determining the wear properties. The Al_2O_3 - TiO_2 coating has a high thermal diffusivity and hence it is less prone to wear.

Alumina-Titania coatings are excellent candidates for providing protection against abrasive wear, and are resistant to high temperature erosion. Such coatings are desirable in electrical insulation and anti-wear applications, for example in protective coatings for sleeve shafts, thermo-couples jackets, pump shafts e.t.c. These coatings exhibit wear, corossion and thermal shock resistance. Alumina-Titania powder is deposited on graphite using vacuum spraying to minimize porosiy of the sprayed coating. With addition of titania wear resistance increases, adhesion strength increases but hardness decreases [**62**]. TiO_2 is the most wear resistance, with least friction coefficient and is less hard than Al_2O_3 coating. Wear resistance is measured by POD test [**63**]. The erosion, abration rates increased by three orders of magnitude when increasing the size of the erodent from 75 to 600 mm and wearing particles, with increasing titania erosion and abrasion rate decreases [**64**]. Porosity of Al_2O_3-40%TiO_2 ranges within 4 to 6%, an agglomerated powder allows to improve the homogeneity of the coating, with the formation of a new compound, Al_2TiO_5.In ball on disc situation wear resistance of an agglomerated powder coating is more improved, thermal expansion coefficient of alumina and tiania are 8 and 7.5($10^{-6}k^{-1}$)[**65**]. Nanostructured alumina–titania coatings exhibits superior wear resistance adhesion, toughness. Post treated deposits exhibit higher resistance to indentation; post treatment induces spray deposite properties with high densification. An improvement in surface properties of treated deposits by way of reduced indentation diameter due to enhanced surface hardness and densification of microstructure

[**66**]. The coatings deposited by HVOF are significantly harder and tougher, and their abrasion resistance is two–threefold higher with less porosity. Bead width and thickness increases with increasing hydrogen fraction in the plasma gas, argon gas fraction increases the bead symmetry. Bond strength of the coating, coating thickness, micro hardness, and porosity depend on gas enthalpy i.e. on H_2.At lower power levels, titania particles are melted, where as alumina particles remain unmelted. As the power is increased, the aluminium oxide content in the coating increases and the coating composition progressively approaches that of the feedstock powder, hardness and wear resistance increase with the torch power [**67**]. The friction coefficient determination from POD (Pin-On-Disk) test is 0.5-0.6 [**68**]. XRD, SEM, TEM results showed that Nanostructured coating exhibits a bimodal microstructure. SO, mechanichal properties increases, the splat lamellae consisted of γ -Al2O3 grains and most of them were less than 200 nm in diameter. Equiaxed grains took the modification of ∝-Al2O3 and ranged from 150 to 800 nm in size. The micro hardness of both kinds of coating was similar and about 820HV0.2. However, the adhesion strength of the Nan structured coating increased by 33 %, as compared with those of the conventional coating. The wear rate of the nanostructured coating was lower than that of the conventional coating [**69**]. Wear behaviour of atmospheric plasma sprayed (APS) alumina–titania coating is investigated using Pin-On-Disc (POD), friction coefficient decreases with increase of sliding velocity and applied load. In the running-in period, the friction coefficient increases because of the contact surface increase as low roughness. Then, the value of the friction coefficient stabilizes representing the wear behavior of the considered material couple [**70**]. Porosity decreases with increase of arc current, hydrogen fraction, with decrease of powder feed rate micro structural observations showed that the multilayers contain some inhomogeneities such as porosity, crack-like defects, unmelted particles, oxides and inclusions, which decreases the microhardness, it decreases from surface to substrate. The porosity content of the ceramic top coating and bond layer were approximately 6% and 2%. The HV values on the cross section of as-sprayed deposits varied over the range of 490T84 HVN for the bond coat and of 666 T68 HVN for the ceramic top layer. The hardness values of $Al_2O3–TiO_2$/Mo layers are higher than that of substrate. The elastic modulus of the as-sprayed Mo and $Al_2O3–TiO_2$ coating layers are 180 and 236 Gpa. The corresponding average strength for the Mo bond layer and $Al_2O_3–TiO_2$ coating were 40 and 31Mpa respectively [**71**]. Coating is having low density, with increasing titania porosity, hardness, melting point decrease, abrasive wear resistance increases with hardness [**72**].

2.12 EROSION WEAR OF CERAMIC COATINGS

Surface damage can result in changes in surface condition and dimension of a mechanical component, and this may sometimes cause disastrous failure of an entire mechanical system. One of cost-effective approaches against surface failure is coating. Various coating techniques have been successfully applied in industry to protect machinery and equipment from surface damage respectively caused by corrosion, oxidation and wear. However, when used in a harsh environment involving two or more damage modes, such as corrosion-wear or corrosion-erosion, many coatings perform poorly due to the synergistic action of wear and corrosion. Considerable efforts have been continuously made to develop high-performance coatings that can resist corrosive wear encountered in various industries such as mining, oilsand, petroleum and chemical industries [**73**]. It has been reported that the thermal spray is a technique that produces a wide range of coatings for diverse applications [**74**]. Coatings of a wide variety of materials are commonly applied to substrates for many purposes. Often, coatings are applied to improve tribological performance. These may include the enhancement of mechanical properties, visual appearance or corrosion resistance or may provide special magnetic and optical properties [**75**]. Plasma sprayed coatings are used today as thermal barriers and abrasion, erosion or corrosion resistant coatings in a wide variety of applications [**76**]. Plasma spraying is the most flexible and versatile thermal spray process with respect to the sprayed materials. Almost any material can be used for plasma spraying on almost any type of substrate. The high temperatures of plasma spray processes permit the deposition of coatings for applications in areas of liquid and high temperature corrosion and wear protection and also special applications for thermal, electrical and biomedical purposes [**77,78**].

The loss of material caused by the impingement of tiny, solid particles, which have a high velocity and impact on the material surface at defined angles, is called erosive wear [**79**]. Particulates ingested into the engine or formed as a result of incomplete combustion are known to cause erosion problems in gas turbines [**80,81**]. Erosion is a serious problem in many engineering systems, including steam and jet turbines, pipelines and valves used in slurry transportation of matter, and fluidized bed combustion systems [**82**]. Gas and steam turbines operate in environments where the ingestion of solid particles is inevitable. In industrial applications and power generation, such as coal-burning boilers, fluidized beds, and gas turbines, solid particles are produced during the combustion of heavy oils, synthetic fuels, and pulverized coal and causes erosion of materials. In such environments, protective

coatings on the surface of superalloys are frequently used [**83,84**]. Erosion tests on coatings have been widely reported. However, the mechanisms of coating damage in this type of test depend on the coating material and its thickness, the properties of the interface, the substrate material and the test conditions [**85**].

Liquid impact erosion is a well knownphenomenon in hydro and low-pressure steam turbine blades, and also in aircraft or missiles traveling at high speed through rain [**86–88**]. The material damage is caused mainly by the high pressure caused by the impact of liquid droplets and the micro-jetting action due to the asymmetrical collapse of bubbles on or near the surface. The surface damage can be minimized by heat treatment or surface modification and substantial advances have been made in this field. Lee et al. [**89**] investigated the liquid impact erosion resistance of 12Cr steel and stellite 6B coated with TiN by reactive magnetron sputter ion plating. The stresses generated by droplet impact were stated to have been decreased by the TiN as a result of stress attenuation and stress wave interactions.

Solid Particle Erosion (SPE) is a wear process where particles strike against surfaces and promote material loss. During flight a particle carries momentum and kinetic energy, which can be dissipated during impact, due to its interaction with a target surface. Different models have been proposed that allow estimations of the stresses that a moving particle will impose on a target [**90**]. It has been experimentally observed by many investigators that during the impact the target can be locally scratched, extruded, melted and/or cracked in different ways. The imposed surface damage will vary with the target material, erodent particle, impact angle, erosion time, particle velocity, temperature and atmosphere.

Plasma sprayed coatings are used today as erosion or abrasion resistant coatings in a wide variety of applications. Extensive research shows that the deposition parameters like energy input in the plasma and powder properties affect the porosity, splat size, phase composition, hardness etc. of plasma sprayed coatings [**91**]. These in turn, have an influence on the erosion wear resistance of the coatings. Quantitative studies of the combined erosive effect of repeated impacts are very useful in predicting component lifetimes, in comparing the performance of materials and also in understanding the underlying damage mechanisms involved.

Resistance of engineering components encountering the attack of erosive environments during operation can be improved by applying ceramic coatings on their surfaces. Alonso et. al. [**92**] experimented with the production of plasma sprayed erosion-

resistant coatings on carbon-fiber-epoxy composites and the studied of their erosion behaviour. The heat sensitivity of the composite substrate requires a specific spraying procedure in order to avoid its degradation. In addition, several bonding layers were tried to allow spraying of the protective coatings. Two different functional coatings; a cermet (WC-12 Co) and a ceramic oxide (Al_2O_3) were sprayed onto an aluminium-glass bonding layer. The microstructure and properties of these coatings were studied and their erosion behaviour determined experimentally in an erosion-testing device. Tabakoff and Shanov [**93**] designed a high temperature erosion test facility to provide erosion data in the range of operating temperatures experienced in compressors and turbines. In addition to the high temperatures, the facility properly simulates all the erosion parameters important from the aerodynamics point of view. These include particle velocity, angle of impact, particle size, particle concentration and sample size. They reported the erosion behavior of titanium carbide coating exposed to fly ash and chromite particles. Chemical vapor deposition technique (CVD) was used to apply a ceramic coating on nickel and cobalt based super-alloys (M246 and X40). The test specimens were exposed to particle-laden flow at velocities of 305 and 366ms^{-1} and temperatures of 550°C and 815°C.

A good number of reports are available on erosion behaviour of alumina coatings. The resistance to erosion of such coatings depends upon intersplat cohesion, shape, size, and hardness of erodent particles, particle velocity, angle of impact and the presence of cracks and pores [**94**]. The slurry (SiC and SiO_2) and airborne particle (Al_2O_3 and SiO_2) erosions of flame sprayed alumina coatings have also been reported in the literature. SiC and Al_2O_3 are found to cause significant amount of erosion in slurry and airborne erosion testing respectively. High particle velocity enhances the erosion rate and the erosion rate is maximum for an impact angle of 90^0. The failure is by the progressive removal of splats and can be attributed to the presence of defects and pores in the inter-splat regions. Similar observation has been made for the plasma sprayed alumina coatings subjected to an erosive wear caused by the SiO_2 particles [**95**].

Branco *et. al*. [**96**] examined room temperature solid particle erosion of zirconia and alumina-based ceramic coatings, with different levels of porosity and varying microstructure and mechanical properties. The erosion tests were carried out by a stream of alumina particles with an average size of 50 μm at 70m/s, carried by an air jet with impingement angle of 90^0. The results indicate that there is a strong relationship between the erosion rate and the coating porosity.

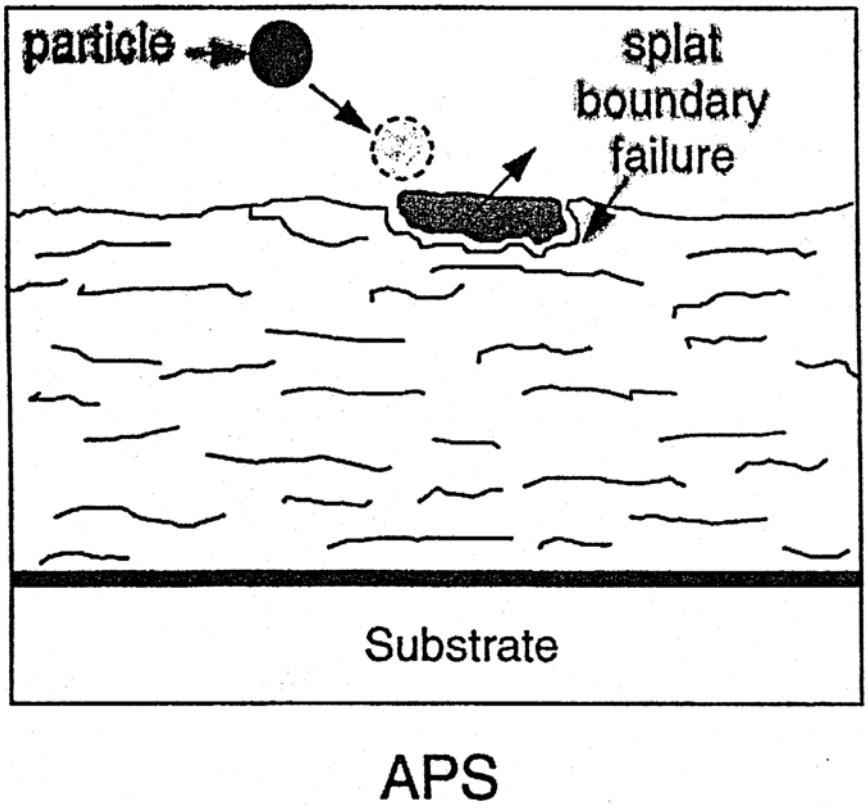

Fig. 2.8 A schematic diagram of the failure modes for an APS TBC.

The improved erosion behaviour is associated with the modes of failure for the APS ceramic coatings. As depicted in Fig.2.8, the APS coating fails by propagation of cracks around splat boundaries and through the microcrack network, that are inherent as part of the APS microstructure, and which provide a degree of strain tolerance.

Chapter 3

EXPERIMENTAL SET UP AND METHODOLOGY

- Introduction
- Development of the coatings
- Characterization of powder
- Characterization of Coatings
- Erosion wear behaviour of coatings

CHAPTER 3

EXPERIMENTAL SET UP & METHODOLOGY

3.1 INTRODUCTION

This chapter deals with the details of the experimental procedures followed in this study. The coating procedure itself requires some basic preparation, i.e., shot blasting and cleaning. After plasma spraying, the coated materials have been subjected to a series of tests, e.g., microstuctural characterization of the surfaces and cross sections, microhardness measurement, X - ray diffraction studies, adhesion test, erosion wear test etc. The details of each process are described here.

3.2 DEVELOPMENT OF THE COATINGS

3.2.1 Preparation of powders

In this study, alumina and titania powders (alumina with 13 wt% titania) are mechanically milled in a FRITSCH-Planetary ball mill for 3 hours to get a homogeneous mixture. The planetary ball mill has 4 numbers of zirconia balls (20g) and 20 numbers of zirconia balls (2g) for milling. The powders obtained were sieved to proper particle size range with the help of a roto-tap sieve shaker machine by using Laboratory test sieves (ISO R565). The particle size the powders considered in the study range 40 to100 micrometer mostly about 50 micrometer are used as raw materials for coating deposition on various substrates.

3.2.2 Preparation of substrate

Commercially available copper and mild steel have been chosen as different substrate materials. The specimens are circular i.e. 1 inch dia disc, 3mm thick. The specimens are grit blasted at a pressure of 3 kg/cm^2 using alumina grits having a grit size of 60. The standoff distance in shot blasting is kept between 120-150 mm. The average roughness of the substrates is 6.8 μm. The grit blasted specimens are cleaned with acetone in an ultrasonic cleaning unit. Spraying is carried out immediately after cleaning.

3.2.3 Plasma spray coating deposition

3.2.3.1 The Requirements for Plasma Spraying

Roughness of the substrate surface:

A rough surface provides a good coating adhesion. A rough surface provides enough room for anchorage of the splats facilitating bonding through mechanical interlocking. A rough surface is generally created by shot blasting technique. The shots are kept inside a hopper, and compressed air is supplied at the bottom of the hopper. The shots are taken afloat by the compressed air stream into a hose and ultimately directed to an object kept in front of the exit nozzle of the hose. The shots used for this purpose are irregular in shape, highly angular in nature, and made up of hard material like alumina, silicon carbide, etc. Upon impact they create small craters on the surface by localized plastic deformation, and finally yield a very rough and highly worked surface. The roughness obtained is determined by shot blasting parameters, i.e., shot size, shape and material, air pressure, standoff distance between nozzle and the job, angle of impact, substrate material etc. [**97**]. The effect of shot blasting parameters on the adhesion of plasma sprayed alumina has been studied [**98**]. Mild steel serves as the substrate material. The adhesion increases proportionally with surface roughness and the parameters listed above are of importance. A significant time lapse between shot blasting and plasma spraying causes a marked decrease in bond strength [**99**].

Cleanliness of the substrates:

The substrate to be sprayed on must be free from any dirt or grease or any other material that might prevent intimate contact of the splat and the substrate. For this purpose the substrate must be thoroughly cleaned (ultrasonically, if possible) with a solvent before spraying. Spraying must be conducted immediately after shot blasting and cleaning. Otherwise on the nascent surfaces, oxide layers tend to grow quickly and moisture may also affect the surface. These factors deteriorate the coating quality drastically [**99]**.

Bond coat:

Materials like ceramic cannot be sprayed directly onto metals, owing to a large difference between their thermal expansion coefficients. Ceramics have a much lower value of α and hence undergo much less shrinkage as compared to the metallic base to form a surface in compression. If the compressive stress exceeds a certain limit, the coating gets peeled off. To alleviate this problem a suitable material, usually metallic of intermediate a

value is plasma sprayed on to the substrate followed by the plasma spraying of ceramics. Bond coat may render itself useful for metallic topcoats as well. Molybdenum is a classic example of bond coat for metallic topcoats. Molybdenum adheres very well to the steel substrate and develops a somewhat rough top surface ideal for the topcoat spraying. The choice of bond coats depends upon the application. For example, in wear application, an alumina and Ni-AI top and bond coats combination can be used [**100**]. In thermal barrier application, CoCrAlY or Ni-AI bond coat [**101**] and zirconia topcoat are popular. Ceramic coatings when subjected to hertzian loading deform elastically and the metallic substrate deforms plastically. During unloading, elastic recovery of the coating takes place, whereas for the metallic substrate a permanent set has already taken place. Owing to this elastoplastic mismatch the coating tends to spall off at the interface. A bond coat can reduce this mismatch as well.

Cooling water:

For cooling purpose distilled water should be used, whenever possible. Normally a small volume of distilled water is recirculated into the gun and. it is cooled by an external water supply from a large tank. Sometime water from a large external tank is pumped directly into the gun [**102**].

3.2.3.2 Plasma spraying

The plasma spraying is done at the Laser and Plasma Technology Division, Bhabha Atomic Research Center, Mumbai. A conventional 40kW atmospheric plasma spraying (APS) set up is used. The plasma input power is varied from 11 to 21 kW by controlling the gas flow rate, voltage and the arc current. The powder feed rate is kept constant at 15 gm/min, using a turntable type volumetric powder feeder.

The general arrangement of the plasma spraying equipment is shown in fig.3.1.

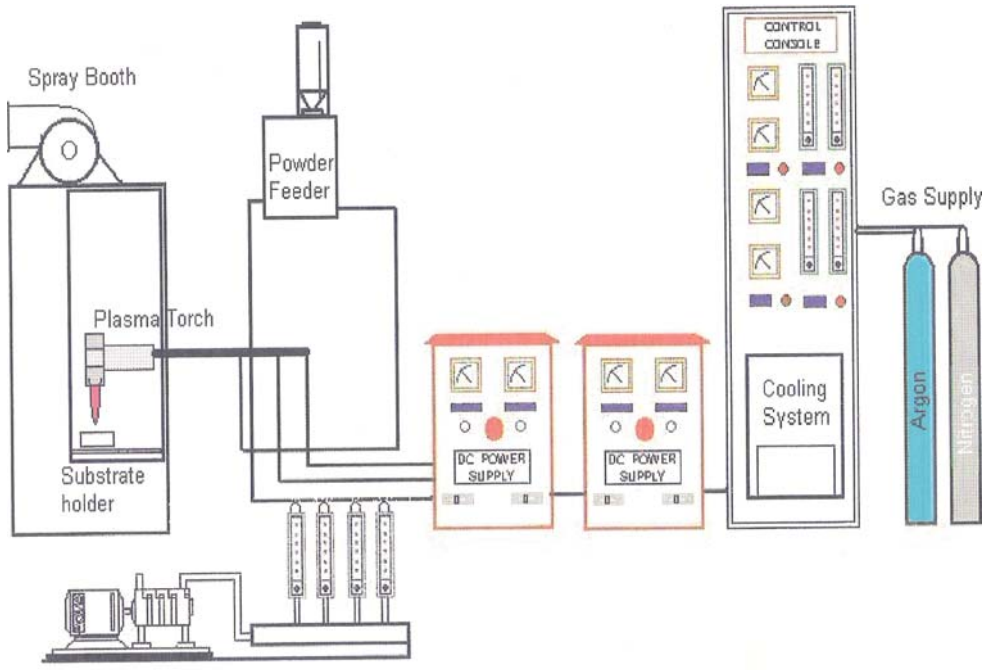

Fig. 3.1 General arrangement of the plasma spraying equipment.

The equipment consists of the following units [**102**]:

1. Plasma torch
2. Control console
3. Powder feeder
4. Power supply unit
5. Water cooling system
6. Gas cylinders and accessories

- **The plasma torch:**

It is the device which houses the electrodes and in which the plasma reaction takes place. It has the shape of a torch and it is connected to the water-cooled power supply cables, powder supply hose and gas supply hose.

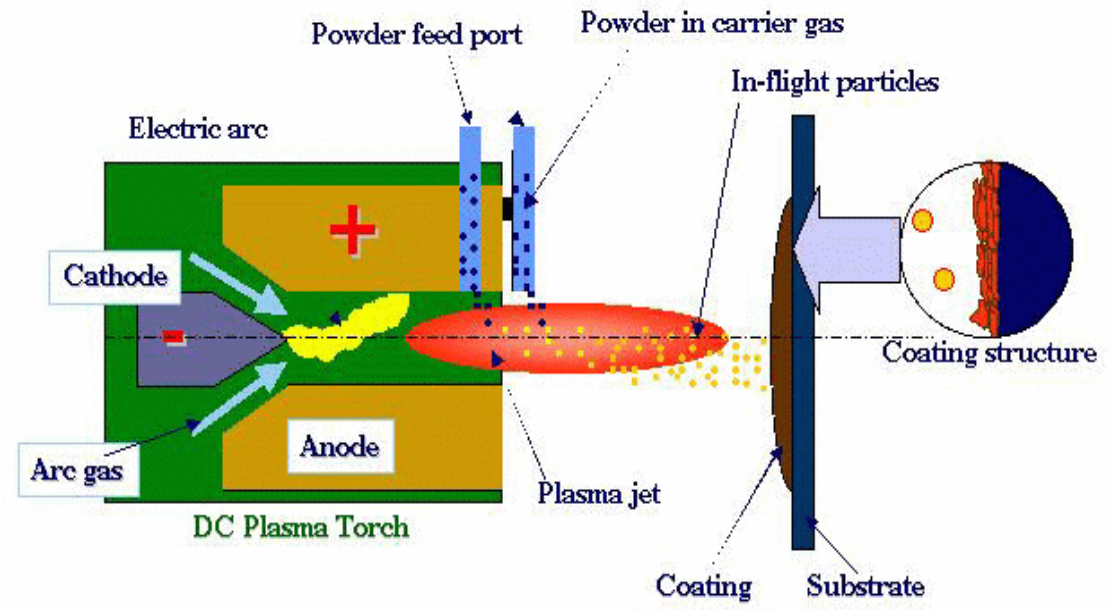

Fig. 3.2 The schematic of coating development by plasma spraying.

The plasma torch as shown in fig.3.2 consists of a cathode, made of thoriated tungsten for better thermo ionic emission and a nozzle shaped copper anode for high velocity plasma jet. The dimensions are: nozzle diameter: 6 mm, gap between the cathode and anode fixed at 12 mm and cathode length: 50 mm. Both the electrodes are water-cooled. The electrodes are separated by an insulating block made of teflon that has provision for gas injection. Powder to be spray deposited is injected through an injection port located at the nozzle exit. An arc is created between cathode and anode (both water cooled). Plasma generating gas is forced to pass through the annular space between the electrodes. While passing through the arc, the gas undergoes ionization in the high temperature environment resulting plasma. The ionization is achieved by collisions of electrons of the arc with the neutral molecules of the gas. The plasma protrudes out of the electrode encasement in the form of a flame. The consumable material, in the powdered form, is poured into the flame in metered quantity. The powders melt immediately and absorb the momentum of the expanding gas and rush towards the target with velocity 100m/sec to form a thin deposited layer. The next layer deposits onto the first immediately after, and thus the coating builds up layer by layer. The temperature in the plasma arc can be as high as $10{,}000^0$C,velocity 600-800m/sec and it is capable of melting anything. Elaborate cooling arrangement is required to protect the plasma torch (i.e., the plasma generator) from excessive heating.

- **The control unit:**

Important functions (current control, gas flow rate control etc.) are performed by the control unit. It also consists of the relays and solenoid valves and other interlocking arrangements essential for safe running of the equipment. For example the arc can only be started if the coolant supply is on and water pressure and flow rate is adequate.

- **The powder feeder:**

A turntable type powder feeder, designed and developed at the L&PT Division, BARC is used for injecting the powders into the plasma jet. The powder is kept inside a hopper. Powder flow rate could be varied by motor speed. The flow rate of the powder can be controlled precisely A separate gas line directs the career gas which fluidizes the powder and carries it to the plasma arc. The carrier gas flow rate is chosen such that the powder particles enter the plasma core. At lower flow rate, the particles may not be able to enter the core of the plasma leading to poor coating quality. On the other hand, if the carrier gas flow is very large, the powder particles will cross the central plasma zone without proper melting leading to poor quality of coating. The carrier gas flow rate needs to be optimized for each particular powder.

- **The power supply unit :**

Normally plasma arc works in a low voltage (30-60 volts) and high current (300-700 Amperes), DC ambient. The available power (AC, 3 phase, 440 V) must be transformed and rectified to suit the reactor. This is taken care of by the power supply unit. The power supply has a full control HF unit consisting of a HF (1 MHz) transformer.

- **The coolant water supply unit:**

It circulates water into the plasma torch, the power supply unit, and the power cables. Units capable of supplying refrigerated water are also available.

- **The Gas feeding system:**

The gas feeding system consists of gas cylinders, pressure gauges and gas tubes. The cylinders each have $7m^3$ capacities. The pressure was maintained at 75 kg/cm^2. There is a gas feeding arrangement for primary gas, secondary gas and carrier gas. Appropriate gas flow rates can be selected depending on the operating power and nature of the material to be coated.

A four stage closed loop centrifugal pump at a pressure of 10 kgf/cm^2 supplies cooling water for the system. Argon is used as the primary plasmagen gas and nitrogen as the secondary gas. The primary plasma gas (argon) and the secondary gas (nitrogen) are taken from normal cylinders at an outlet pressure of 4 kgf/cm^2 .The powders are deposited at spraying angle of 90°. The powder feeding is external through a turntable type power feeder. The properties of the coatings are dependent on the spray process parameters. The operating parameters during coating deposition process are listed in table 3.1.

Operating Parameters	Values
Plasma Arc Current (amp)	280, 360, 425, 500
Arc Voltage (volt)	40, 40 , 44 , 44
Torch Input Power (kW)	11,15,18,21
Plasma Gas (Argon) Flow Rate (lpm)	28
Secondary Gas (N_2) Flow Rate (lpm)	3
Carrier Gas (Argon) Flow Rate (lpm)	12
Powder Feed Rate (gm/min)	15
Torch to Base Distance TBD (mm)	100

Table 3.1 Operating parameters during coating deposition.

The coating is incrementally built up by impact of successive particles by the process of flattening, cooling and solidification as in fig.3.3. By virtue of the high cooling rates, typically 10^5 to 10^6 K/sec., the resulting microstructures are fine-grained and homogeneous.

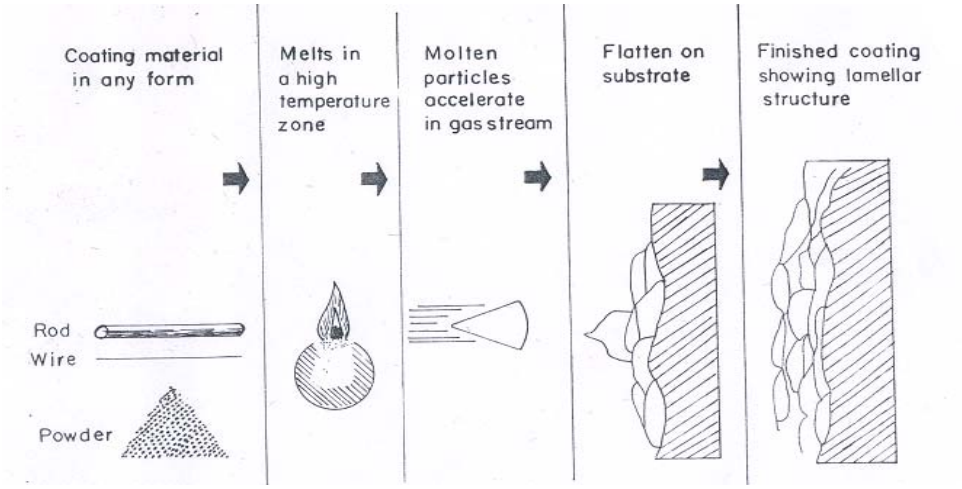

Fig. 3.3 Schematic of coating formation.

3.2.3.3 Process parameters in plasma spraying

In plasma spraying one has to deal with a lot of process parameters, which determine the degree of particle melting, adhesion strength and deposition efficiency of the powder. Deposition efficiency is the ratio of amount of powder deposited to the amount fed to the gun. An elaborate listing of these parameters and their effects are reported in the literature [**103**]

Some important parameters and their roles are listed below:

Arc power:

It is the electrical power drawn by the arc. The power is injected in to the plasma gas, which in turn heats the plasma stream. Part of the power is dissipated as radiation and also by the gun cooling water. Arc power determines the mass flow rate of a given powder that can be effectively melted by the arc. Deposition efficiency improves to a certain extent with an increase in arc power, since it is associated with an enhanced particle melting [**99,103,104**]. However, increasing power beyond a certain limit may not cause a significant improvement. On the contrary, once a complete particle melting is achieved, a higher gas temperature may prove to be harmful. In the case of steel, at some point vaporization may take place lowering the deposition efficiency.

Plasma gas:

Normally nitrogen or argon doped with about 10% hydrogen or helium is used as a plasma gas. The major constituent of the gas mixture is known as primary gas and the minor is known as the secondary gas. The neutral molecules are subjected to the electron bombardment resulting in their ionization. Both temperature and enthalpy of the gas increase as it absorbs energy. Since nitrogen and hydrogen are diatomic gases, they first undergo dissociation followed by ionization. Thus they need higher energy input to enter the plasma state. This extra energy increases the enthalpy of the plasma. On the other hand, the mono-atomic plasma gases, i.e. argon or helium, approach a much higher temperature in the normal enthalpy range. Good heating ability is expected from them for such high temperature [**105**]. In addition, hydrogen followed by helium has a very high specific heat, and therefore is capable of acquiring very high enthalpy. When argon is doped with helium the spray cone becomes quite narrow which is especially useful for spraying on small targets.

Carrier gas:

Normally the primary gas itself is used as a carrier gas. The flow rate of the career gas is an important factor. A very low flow rate cannot convey the powder effectively to the plasma jet, and if the flow rate is very high then the powders might escape the hottest region of the jet. There is an optimum flow rate for each powder at which the fraction of unmelted powder is minimum and hence the deposition efficiency is maximum [**103**].

Mass flow rate of powder:

Ideal mass flow rate for each powder has to be determined. Spraying with a lower mass flow rate keeping all other conditions constant results in under utilization and slow coating buildup. On the other hand, a very high mass flow rate may give rise to an incomplete melting resulting in a high amount of porosity in the coating. The un-melted powders may bounce off from the substrate surface as well keeping the deposition efficiency low [**103**].

Torch to base distance:

It is the distance between the tip of the gun and the substrate surface. A long distance may result in freezing of the melted particles before they reach the target, whereas a short standoff distance may not provide sufficient time for the particles in flight to melt [**99,103**]. The relationship between the coating properties and spray parameters in spraying alpha alumina has been studied in details. It is found that the porosity increases and the thickness of the coating (hence deposition efficiency) decreases with an increase in standoff distance. The usual alpha-phase to gamma-phase transformation during plasma spraying of alumina has also been restricted by increasing this distance. A larger fraction of the un-melted particles go in the coating owing to an increase in torch to base distance.

Spraying angle:

This parameter is varied to accommodate the shape of the substrate. In coating alumina on mild steel substrate, the coating porosity is found to increase as the spraying angle is increased from 30° to 60°. Beyond 60° the porosity level remains unaffected by a further increase in spraying angle. The spraying angle also affects the adhesive strength of the coating. The influence of spraying angle on the cohesive strength of chromia, zirconia 8-wt% yittria and molybdenum has been investigated, and it has been found that the spraying angle does not have much influence on the cohesive strength of the coatings [**106**].

Substrate cooling:

During a continuous spraying, the substrate might get heated up and may develop thermal-stress related distortion accompanied by a coating peel-off. This is especially true in situations where thick deposits are to be applied. To harness the substrate temperature, it is kept cool by an auxiliary air supply system. In addition, the cooling air jet removes the unmelted particles from the coated surface and helps to reduce the porosity [**99**].

Powder related variables:

These variables are powder shape, size and size distribution, processing history, phase composition etc. They constitute a set of extremely important parameters. For example, in a given situation if the powder size is too small it might get vaporized. On the other hand a very large particle may not melt substantially and therefore will not deposit. The shape of the powder is also quite important. A spherical powder will not have the same characteristics as the angular ones, and hence both could not be sprayed' using the same set of parameters [**107**].

Angle of powder injection:

Powders can be injected into the plasma jet perpendicularly, coaxially, or obliquely. The residence time of the powders in the plasma jet will vary with the angle of injection for a given carrier gas flow rate. The residence time in turn will influence the degree of melting of a given powder. For example, to melt high melting point materials a long residence time and hence oblique injection may prove to be useful. The angle of injection is found to influence the cohesive and adhesive strength of the coatings as well [**102**].

3.3 CHARACTERIZATION OF POWDER

3.3.1 Particle Size Analysis

The particle sizes of the raw materials used for coating (alumina, 13 wt% titania powder) are characterized using Laser particle size analyzer of Malvern Instruments make.

3.4 CHARACTERIZATION OF COATINGS

3.4.1 Coating Thickness Measurement

Thickness of the alumina titania coatings on different substrates are measured on the polished cross-sections of the samples, using an optical microscope. Five readings are taken on each specimen and the average value is reported as the mean coating thickness.

3.4.2 Evaluation of Coating Deposition Efficiency

Deposition efficiency is defined as the ratio of the weight of coating deposited on the substrate to the weight of the expended feedstock. Weighing method is accepted widely to measure this. Each specimen is weighed before and after coating deposition. The difference is the weight (Gc) of coating deposited on the substrate. From the powder feed rate and time of deposition the weight of expended feed stock (Gp) is determined. The deposition efficiency (η) is then calculated using the following equation [**108**].

$$\eta = (Gc / G_p \text{ X } 100) \%$$

Weighing of samples is done using a precision electronic balance with $\pm$ 0.1 mg accuracy.

3.4.3 Evaluation of Coating Interface Bond Strength

To evaluate the coating adhesion strength, a special type jig (fig.3.4) is fabricated. Cylindrical mild steel dummy samples (length 25 mm, top and bottom diameter 12 mm) are prepared. The surfaces of the dummies are roughened by punching. These dummies are then fixed on top of the coating with the help of a polymeric adhesive (epoxy 900-C) and pulled with tension after being mounted on the jig (fig.3.5). The coating pullout test is carried out using the set up Instron 1195 at a crosshead speed of 1 mm/minute.

Fig. 3.4 Jig used for the test

Fig. 3.5 Specimen under tension

Fig. 3.6 Adhesion test with Instron 1195 UTM.

The moment coating gets torn off from the specimen, the reading (of the load), which corresponds to the adhesive strength of the coating, is recorded. A typical test set up (during testing) is shown in figure.3.6. The test is performed as per ASTM C-633.

3.4.4 Porosity Measurement

Measurement of porosity is done using the image analysis technique. The porosity of the coatings was measured by putting polished cross sections of the coating sample under a microscope (Neomate) equipped with a CCD camera (JVC, TK 870E). This system is used to obtain a digitized image of the object [**109**]. The digitized image is transmitted to a computer equipped with VOIS image analysis software. The total area captured by the objective of the microscope or a fraction thereof can be accurately measured by the software. Hence the total area and the area covered by the pores are separately measured and the porosity of the surface under examination is determined.

3.4.5 Microhardness Measurement

Small specimens are sliced from the coated samples. Samples containing Coating cross-sections are mounted and polished for the microhardness measurement. Microscopic observation under optical microscope of the polished section of the coatings exhibits three distinctly different regions/ phases namely grey, dark and spotted/mixed. Vickers

Microhardness measurement is made on these optically distinguishable phases using Leitz Microhardness Tester equipped with a monitor and a microprocessor based controller, with a load of 0.245N and a loading time of 20 seconds. About twelve or more readings are taken on each sample and the average value is reported as the data point.

3.4.6 X-Ray Diffraction Studies

X-ray diffraction technique is used to identify the different (crystalline) phases present in the coatings [**110**]. XRD analysis is done using Ni-filtered Cu-Kα radiation in a Philips X-ray diffractometer. The characteristic d-spacing of all possible values are taken from JCPDS cards and are compared with d-values obtained from XRD patterns to identify the various X-ray peaks obtained.

3.4.7 Scanning Electron Microscopic Studies

Plasma sprayed coated specimens and plasma processed powders are studied by JEOL JSM-6480 LV scanning electron microscope mostly using the secondary electron imaging. The surface as well as the interface morphology of all coatings are observed under the microscope. Small specimens are sliced from the coated samples and were mounted using thermosetting molding powders. Coating cross-sections are polished in three stages using SiC abrasive papers of reducing grit sizes and then with diamond pastes on a wheel for coating interface analysis under SEM. These specimens are also utilized for the microhardness measurement.

3.5 EROSION WEAR BEHAVIOUR OF COATINGS

Solid particle erosion (SPE) is usually simulated in laboratory by one of two methods. The ‘sand blast’ method, where particles are carried in an air flow and impacted onto a stationary target. The schematic diagram of the sand blast type of erosion test rig is shown in fig.3.7 and the ‘whirling arm’ method, where the target is spun through a chamber of falling particles.

Schematic diagram of the erosion test rig

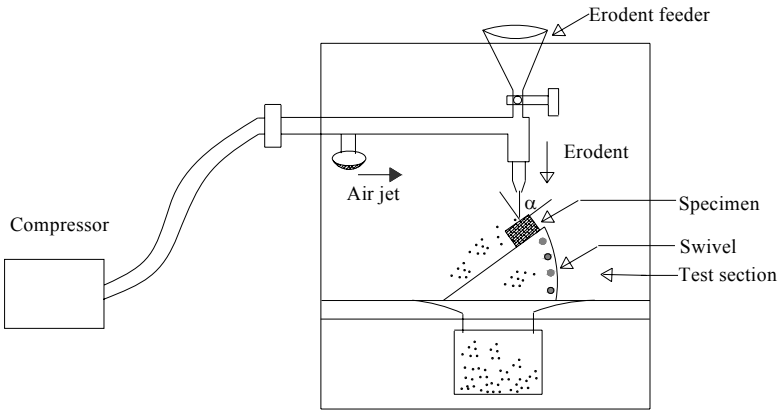

Fig. 3.7 Schematic diagram of the erosion test rig.

In the present investigation, an erosion apparatus (fabricated in laboratory) of the 'sand blast' type is used as shown in fig.3.8. It is capable of creating highly reproducible erosive situations over a wide range of particle sizes, velocities, particles fluxes and incidence angles, in order to generate quantitative data on materials and to study the mechanisms of damage. The test is conducted as per ASTM G76 standards.

(a) **(b)**

Fig. 3.8 Erosion test set up

The jet erosion test rig used in this work employs a 300 mm long nozzle of 3 mm bore and 300 mm long. This nozzle size permits a wider range of particle types to be used in the course of testing, allowing better simulations of real erosion conditions. The mass flow rate is measured by conventional method. Particles are fed from a simple hopper under gravity into the groove. Velocity of impact is measured using double disc method [**111**]. Some of the features of this test set up are:

- Vertical traverse for the nozzle: provides variable nozzle to target standoff distance, which influences the size of the eroded area.
- Different nozzles may be accommodated: provides ability to change the particle plume dimensions and the velocity range.
- Large test chamber with sample mount (typical sample size 25 mm x 25 mm) that can be angled to the flow direction: by tilting the sample stage, the angle of impact of the particles can be changed in the range of 0^0 – 90^0 and this will influence the erosion process.

In this work, room temperature solid particle erosion test on mild steel substrate coated with Alumina +13% titania as feed materials (coated at 11 kW, 18 kW) is carried out. The coating made at 11kW power level, is eroded at different impact angles 30°and 90°. The nozzle (2.2 mm ID) is kept at 100mm, 125mm, 150mm, 175mm &200mm standoff distances from the target. Dry silica sand particles of 200,300 and 400µm average particle size at a feed rate of 50gm/min are used as erodent with an average velocity of 32m/s (as measured by double disc method [**111**]) and pressure 4kgf/cm^2. The coating deposited at18 kW power level is eroded at 30°, 45^o, 60^o, 75^o and 90°angle at SOD of 100mm, 150mm. Here, 200 & 400µm size dry silica sand particles are used as erodent with different velocities i.e. of 32m/sec, 38m/sec 45m/sec, 52m/sec and 58m/sec and at pressures of 4kgf/cm^2, 4.7kgf/cm^2, 5.5kgf/cm^2, 6.1kgf/cm^2, 6.5kgf/cm^2 with feed rate 50gm/min, 54gm/min, 58gm/min, 60gm/min and 62 gm/min. Amount of wear is determined on 'mass loss' basis [**112,113**]. It is done by measuring the weight change of the samples at regular intervals during the test duration. A precision electronic balance with + 0.01 mg accuracy is used for weighing. Erosion rate, defined as the coating mass loss per unit erodent mass (gm/gm) is calculated. The erosion rates are calculated at different erodent size, different erodent velocities, impingement angles, erodent dose and stand off distances.

Chapter 4

RESULTS AND DISCUSSION

- Introduction
- Particle Size Analysis
- Measurement of coating thickness
- Coating Deposition Efficiency
- Coating Adhesion Strength
- Coating Porosity
- Coating hardness
- X-Ray Phase Composition Analysis
- Solis Particle Erosion Wear Behaviour
- Microstructural Investigation
- Discussion

CHAPTER 4

RESULTS AND DISCUSSION

4.1 INTRODUCTION

Plasma sprayed coatings of alumina 13wt% titania were developed on two different metals substrates (copper, mild steel) using a 40 kW atmospheric plasma spray system supplied by M/s Ion Arc Machines (India) Pvt. Ltd. at the Laser and Plasma Tech. Division, Bhabha Atomic Research Center, Mumbai. Spraying was done at different input power level to the dc plasma torch in the range from 11 kW to 21 kW. Characterization of the coatings was done with respect to their quality and tribological performance. The results of various tests are presented and discussed in this chapter.

4.2 PARTICLE SIZE ANALYSIS

The particle sizes of the alumina titania powder (after mixing in ball mill) are characterized using Laser particle size analyzer of Malvern Instruments make. Figure.4.1 shows the particle size distribution of alumina titania powder mix before plasma spraying. It can be seen that majority of particles are in the range of 40 to 100 micron. The mean particle diameter is found to be 35.44 micron. Maximum particles are in the range of 50 micron.

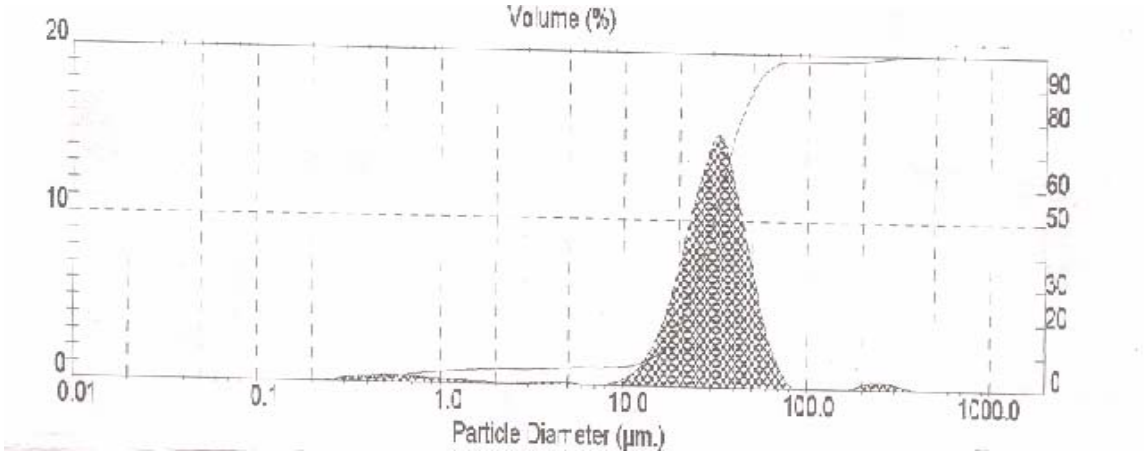

Fig. 4.1 Particle size distribution of Al_2O_3-13%TiO_2 feed stock.

4.3 MEASUREMENT OF COATING THICKNESS

To ensure the coatability of alumina titania on different substrates, coating thickness was measured on the polished cross-sections of the samples, using an optical microscope. The thickness values obtained for coatings deposited at different power levels for Copper and Mildsteel substrates are presented in table 4.1. Each data point on the curves is the average of at least five readings/measurements.

Sl. No.	Specimen	Substrate	Power level (kW)	Coating Thickness(~Micron)
1	Al_2O_3-TiO_2 Coating	Mild steel	11	120
2	do	Mild steel	15	150
3	do	Mild steel	18	190
4	do	Mild steel	21	180
5	do	Copper	11	125
6	do	Copper	15	160
7	do	Copper	18	200
8	do	Copper	21	190

Table 4.1 Thickness values of alumina titania coatings made at different power level for copper and mildsteel substrates.

The variation of alumina titania coating thickness values with torch input power for Copper and Mildsteel substrates are presented in Fig.4.2.Maximum coating thickness of ~ 200 micron on copper and ~ 190 micron on mild steel substrates deposited at 18 kW power levels are obtained. From the figure it is evident that there is an increase in coating thickness with increase in input power to the plasma torch; up to about 18 kW and then for further higher input power, no improvement in coating thickness is recorded. It is also seen from the

figure that there is a difference in thickness obtained for different substrates. Coating thickness is higher in case of copper than that of mild steel substrate, at all power levels.

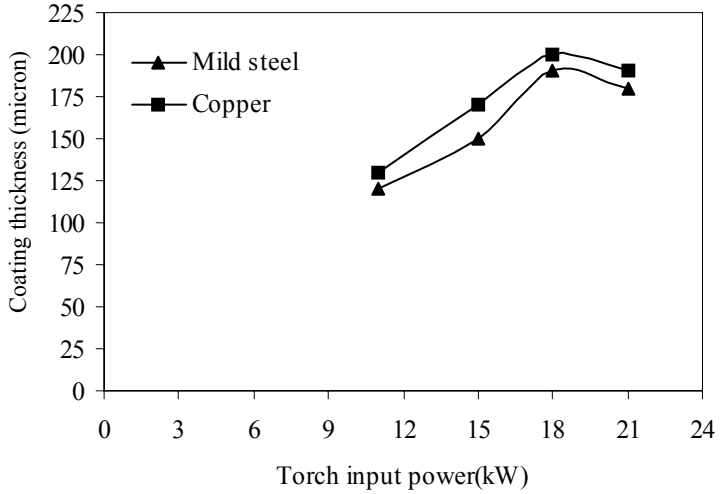

Fig. 4.2 variation of alumina titania coating thickness values with torch input power for Copper and Mildsteel substrates

This difference may be attributed to thermal conductivity of the substrate material, i.e. for materials with higher conductivity (i.e. copper), the heat transfer from the sprayed particles (reaching on the substrate) occurs at a faster rate than in case of materials with relatively lower conductivity (i.e. Mild steel). This might be enhancing the deposition rate and hence the coating thickness.

4.4 COATING DEPOSITION EFFICIENCY

Deposition efficiency is an important factor that determines the techno-economics of the process. Deposition efficiency of all coatings made within the scope of this investigation is evaluated. Coating deposition efficiency is defined as the ratio of the weight of coating deposited on the substrate to the weight of the expended feedstock. Weighing method is accepted widely to measure this. It can be described by the equation [**108**]

$$\eta = (G_c/G_p) \text{ X } 100 \text{ \%}$$

Where η is the deposition efficiency

Gc is the weight of coating deposited on the substrate and

Gp is the weight expended feedstock

Deposition efficiency depends on many factors that include the input power to the plasma torch, material properties, such as melting point, grain size and heat capacity of the powder being sprayed, stand off distance (torch to base distance) etc. For a given stand off distance and given material with specific particle size, torch power appears to be an important factor for the deposition efficiency. The deposition efficiency is a measure of the fraction of the powder that has melted, but that has not vaporized or decomposed into gaseous products. Deposition efficiency values of alumina titania coating made at different operating power levels on different substrates are shown in table 4.2. For example, deposition efficiency for alumina titania coatings ranges from 21.6% to 41.73% in case of mild steel substrate and from 25.2% to 43.34% in the case of copper substrate. It is interesting to note that the deposition efficiency, in all cases, has increased in a step up fashion with the increase in torch input power.

Sl. No.	Specimen	Substrate	Power level (kW)	Deposition efficiency (%
1	Al_2O_3-TiO_2 Coating	Mild steel	11	21.6
2	do	Mild steel	15	26.95
3	do	Mild steel	18	36.52
4	do	Mild steel	21	41.73
5	do	Copper	11	25.2
6	do	Copper	15	31.95
7	do	Copper	18	39.13
8	do	Copper	21	43.34

Table 4.2 Coating deposition efficiency values of alumina titania coating made at different operating power levels on different substrates.

Fig. 4.3 shows the variation of deposition efficiency of alumina titania coating with operating power level on different substrates. It is interesting to note that the deposition

efficiency, in all cases, is increased in a sigmoidal fashion with the torch input power. It reveals that efficiency of coating deposition is significantly influenced by the input power of the torch. The trend of variation is similar for all substrates to the same coating material considered in this work.

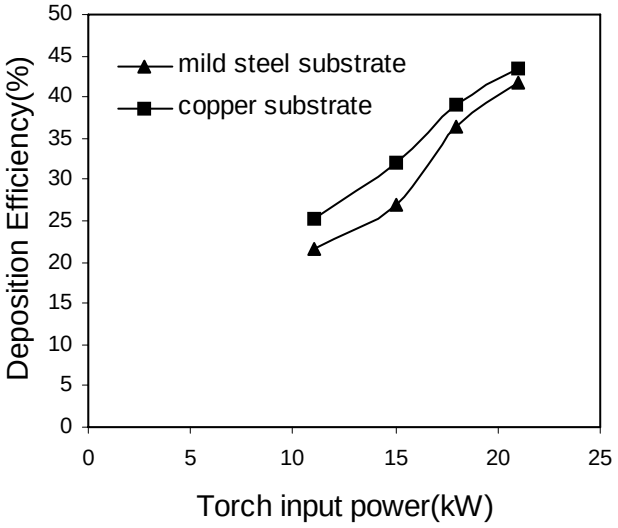

Fig. 4.3 Deposition efficiency of alumina titania coatings made at different power level on different substrates.

Plasma spray deposition efficiency of a given materials depends on its melting point, thermal heat capacity and particle size of the powder. At lower input power to the plasma torch, the plasma jet temperature is not high enough to melt the entire powder particles that enter the plasma jet. As the power is increased, the average plasma temperature increases melting a larger fraction of the powder. The spray efficiency, therefore, increases with plasma power. However, beyond a certain power level of plasma, the temperature of the plasma gas is very high, leading to vaporization/dissociation of the powder particles. This causes the deposition efficiency to decrease at higher power levels and hence coating thickness. This tendency is generally observed in plasma spray coatings. However, the plasma operating power above which the efficiency decrease depends on the chemical nature of the feed material i.e. powder and its particle size.

4.5 COATING ADHESION STRENGTH

From the microscopic point of view, adhesion is due to physico-chemical surface forces (Vander-walls, Covalent, ionic…), which can be established at the coating-substrate interface [**114**] and corresponds to the work of adhesion. From the mechanical point of view, adherence can be estimated by the force corresponding interfacial fracture and is macroscopic in nature. Coating adherence tests have been carried out by many investigators with various coatings. It has been stated that the fracture mode is adhesive if it takes place at the coating-substrate interface and that the measured adhesion value is the value of practical adhesion, which later is strictly an interface property, depending exclusively on the surface characteristics of the adhering phase and the substrate surface condition. [**115,116**].

In this work, evaluation of coating interface bond strengths is done using coating pullout method, conforming to ASTM C-633 standard. It is found that in all the samples fracture occurred at the coating-substrate interface. The results obtained for coatings made with Alumina-Titania on mild steel and copper substrates at different power levels are tabulated in table 4.3. The low value of adhesion strength of alumina titania may be due to difference in coefficient of thermal expansion of substrate and coating and/or formation of pores, cracks, voids in the coating and at along coating-substrate.

Sl.No	Specimen	Power level (kW)	Substrate	Adhesion strength (MPa)
1	Al2O3-TiO2	11	Mild steel	4.2
2	do	15	Mild steel	4.89
3	do	18	Mild steel	5.1
4	do	21	Mild steel	4.35
5	do	11	Copper	2.58
6	do	15	Copper	2.93
7	do	18	Copper	3.5
8	do	21	Copper	2.98

Table 4.3 Adhesion strength values of alumina titania coating on mild steel and copper substrates at different power levels.

.

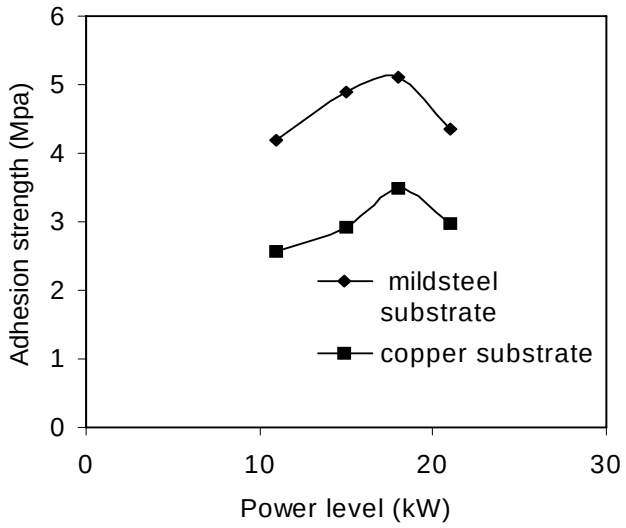

Fig. 4.4 Adhesion strength of alumina titania coatings made at different Power level on different substrates.

The variation of adhesion strength of alumina titania coating to the mild steel and copper substrate at different power levels is shown in fig.4.4. From the figure, it is clear that the adhesion strength varies with operating power of the plasma torch. Maximum adhesion strength of 5.1 MPa on mild steel substrate and of 3.5 Mpa on copper substrate is recorded at 18 kW. It can be visualized that, the interface bond strength increases with the input power of the torch up to a certain power level and then shows a decreasing trend in coating adhesion, irrespective of the substrate material. This might be due to the fact that, when the operating power level is increased, larger fraction of particles attain molten state as well as the velocity of the particles also increase. Therefore there is better splat formation and mechanical inter-locking of molten particles on the substrate surface leading to increase in adhesion strength [**117**]. But, at a much higher power level, the amount of fragmentation and vaporization of the particles increase. There is also a greater chance to fly off of smaller particles during in-flight traverse during plasma spraying and results in poor adhesion strength of the coatings. Coating adhesion strength is more in case of mild steel substrate than that of copper substrate may be due to the dependence of thermal conductivity for melted particle, dissipation of heat at metal interface and also may be due to thermal expansion coefficient mismatch at the ceramic metal interface [**118**].

4.6 COATING POROSITY

Porosity measurement is done using the image analysis technique. The polished interfaces of various coatings are studied under optical microscope (Neomate) equipped with a CCD camera (JVC, TK 870E). From the digitized image obtained by this system, coating porosity is determined using VOIS image analysis software for different power levels. The results are tabulated in table 4.4.

Sl.No	Specimen	Power level (kW)	Porosity (%)
1	Al2O3-TiO2	11	4.5
2	do	15	4.1
3	do	18	4
4	do	21	5.47

Table 4.4 Porosity of coating for different power levels.

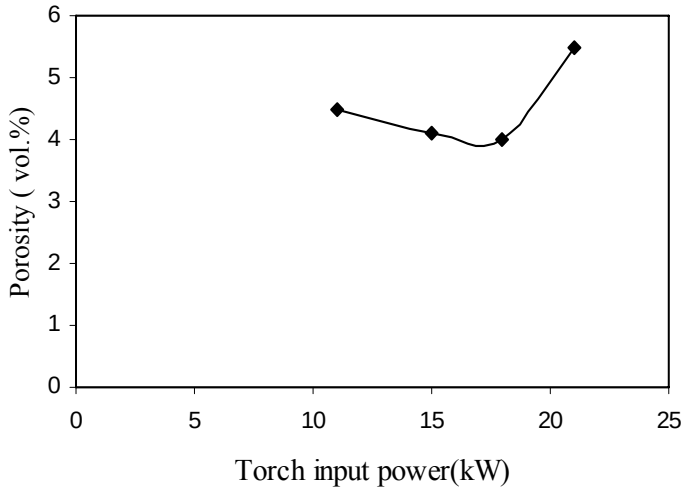

Fig. 4.5 Variation of coating porosity of alumina titania with torch input power.

Variation of coating porosity of alumina titania with torch input power is shown in fig.4.5. It is observed that porosity volume fraction of these coatings lie in the range of from ~ 4 to ~ 6 %. The amount of porosity is more in the case of coatings made at lower (11kW) and at higher (21kW) power levels. However; porosity is minimum at 18kW power for the

coatings made under this study. It may be mentioned that in the conventional plasma sprayed ceramic coatings, porosity of about 3 – 10 % is generally observed [**119**]. Thus the values obtained in the coatings under this study are well with in acceptable range for a good quality coating. The increased value of porosity may be the reason of low adhesion strength of the coatings deposited at at high power level i.e. at 21kW.

4.7 COATING HARDNESS

Microscopic observation of the polished cross section of the coatings was studied under optical microscope. Three distinctly different regions/ phases namely grey, dark and spotted/mixed are visible. Micro-hardness measurement is done on these optically distinguishable phases with Leitz Micro-Hardness Tester using 25Pa (0.245N) load. The results are summarized in table 4.5 to 4.8.

Sl.No	Coating	Power level (kW)	Phase	Micro Hardness (HV)
1	Al2O3-TiO2	11	Mixed	81.4
2	do	11	Mixed	173.49
3	do	11	Dark	143.88
4	do	11	Dark	160.27
5	do	11	Grey	120.37
6	do	11	Grey	126.50

Table 4.5 Hardness on the coating cross section for the coating deposited at 11 kW.

Sl.No	Coating	Power level (kW)	Phase	Micro Hardness (HV)
1	Al2O3-TiO2	15	Mixed	142.29
2	do	15	Mixed	154.88
3	do	15	Dark	106.60
4	do	15	Dark	206.50
5	do	15	Grey	203.39
6	do	15	Grey	194.14

Table 4.6 Hardness on the coating cross section for the coating deposited at 15 kW.

Sl.No	Coating	Power level (kW)	Phase	Micro Hardness (HV)
1	Al2O3-TiO2	18	Mixed	362.93
2	do	18	Mixed	397.31
3	do	18	Dark	626.59
4	do	18	Dark	597.12
5	do	18	Grey	649.03
6	do	18	Grey	672.70

Table 4.7 Hardness on the coating cross section for the coating deposited at 18 kW.

Sl.No	Coating	Power level (kW)	Phase	Micro Hardness (HV)
1	Al2O3-TiO2	21	Mixed	287.77
2	do	21	Mixed	332.92
3	do	21	Dark	459.11
4	do	21	Dark	477.95
5	do	21	Grey	591.71
6	do	21	Grey	567.92

Table 4.8 Hardness on the coating cross section for the coating deposited at 21 kW.

The results show that these three structurally different phases bear three different ranges of hardness that may depend on different phases present/formation in the coating, which is clear from X-ray diffraction analysis. High hard ness values may be due to the presence of different phase forms (i.e. allotropic transformations) of alumina phase having high hardness value. Low hard ness values may be of the titania phases. With increase in power level there is an increase in hardness values of some phases, which may be due to the formation of different allotropic phases and their composition variations during spray formation.

4.8 XRD PHASE COMPOSITION ANALYSIS

Micro-hardness test shows different hardness values on different optically distinct regions on the coating cross-sections. Therefore, to ascertain the phases present and phase

changes / transformation taking place during plasma spraying, the X-ray diffractograms are taken on the raw material and on some selected coatings using a Philips X Ray Diffractometer and with CuKα. The XRD results are shown in figures 4.6 to 4.10.

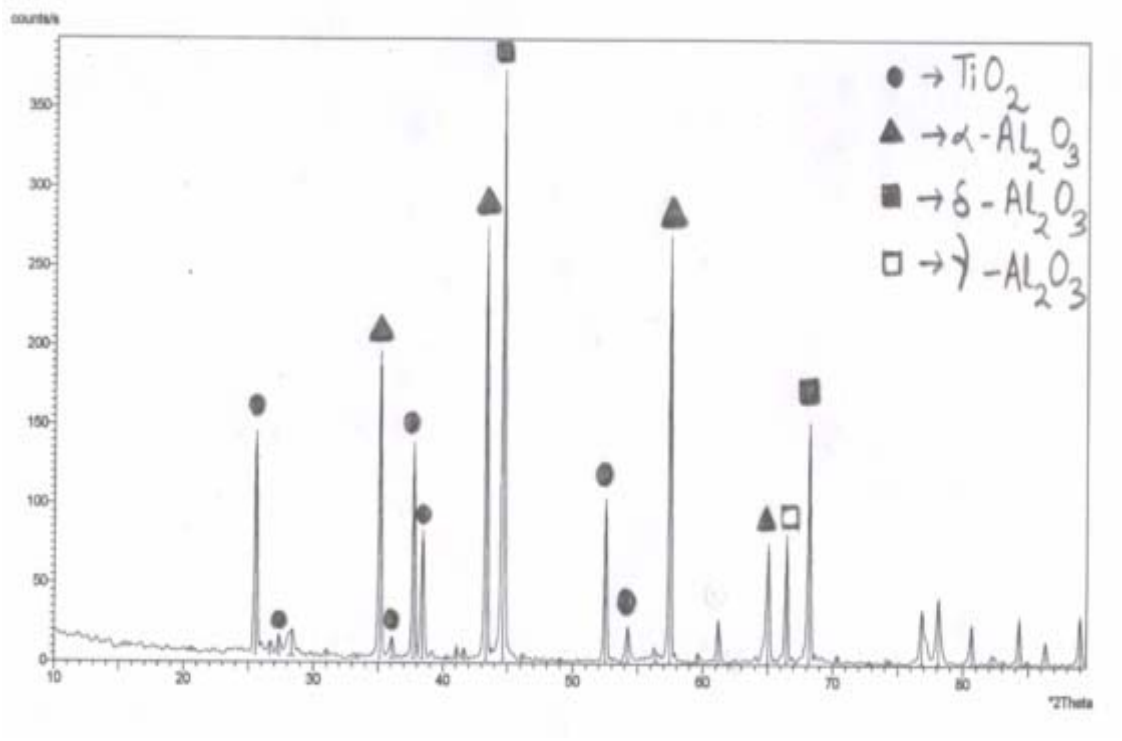

Fig.4.6 X-Ray Diffractogram of alumina titania raw powder.

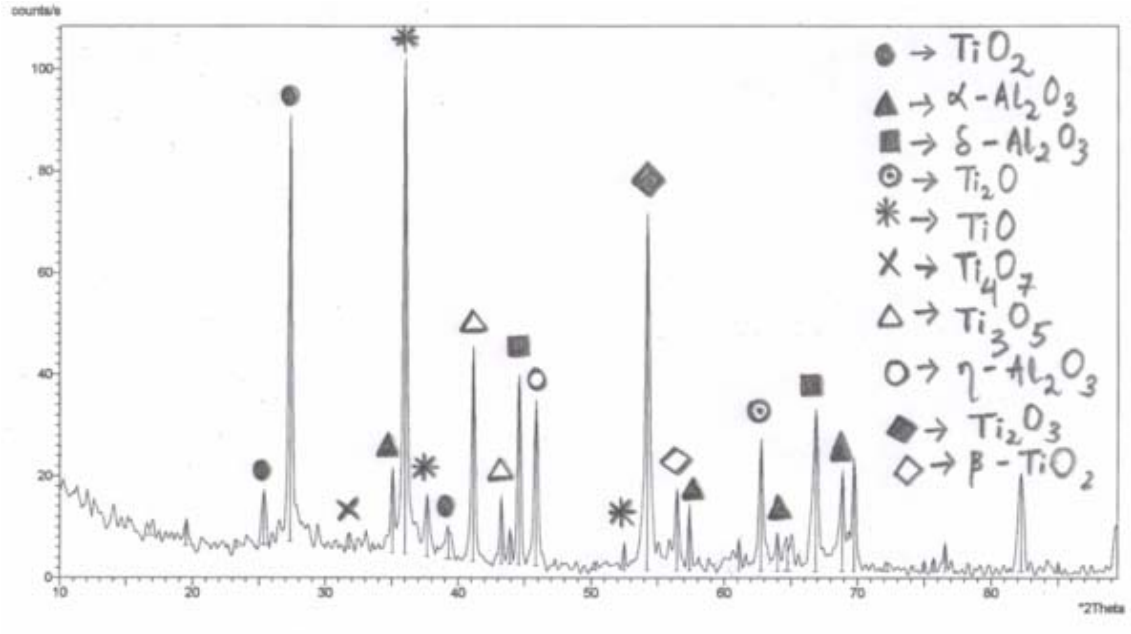

Fig.4.7 X-Ray Diffractogram of alumina titania coating deposited at 11kW power level.

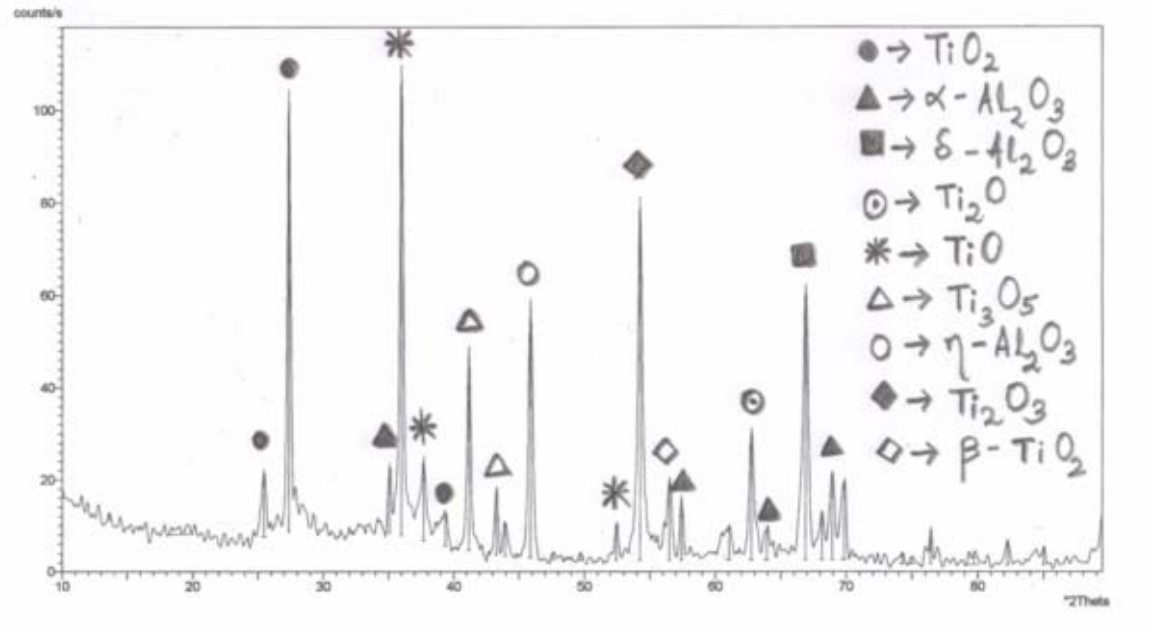

Fig.4.8 X-Ray Diffractogram of alumina titania coating deposited at 15 kW power level.

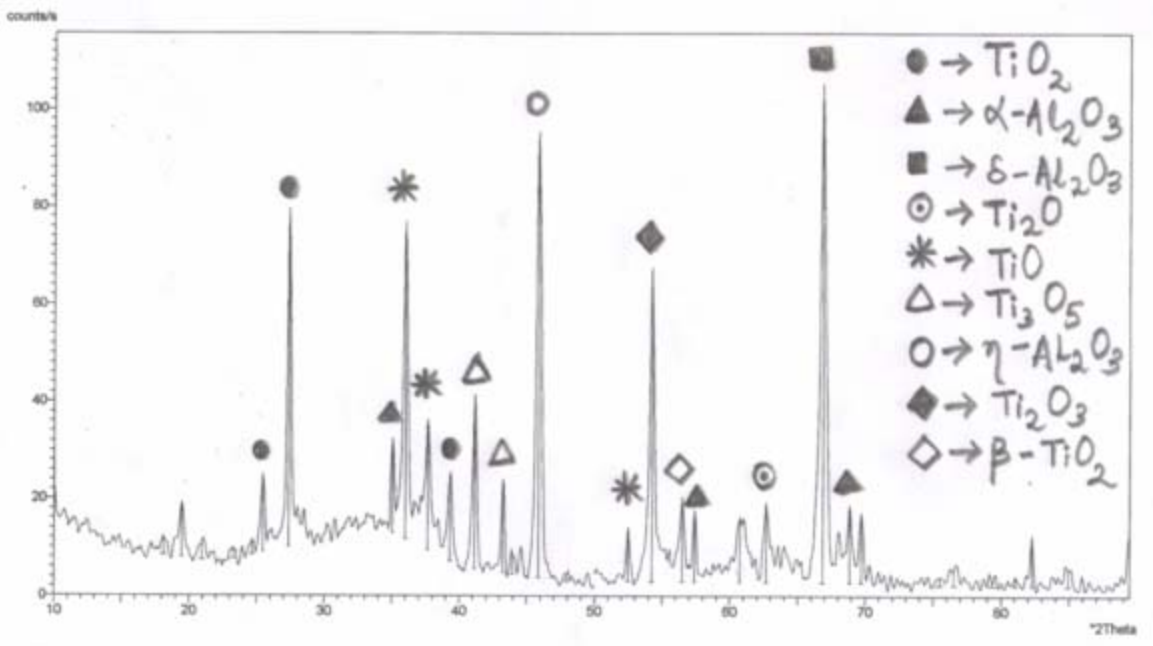

Fig.4.9 X-Ray Diffractogram of alumina titania coating deposited at 18 kW power level.

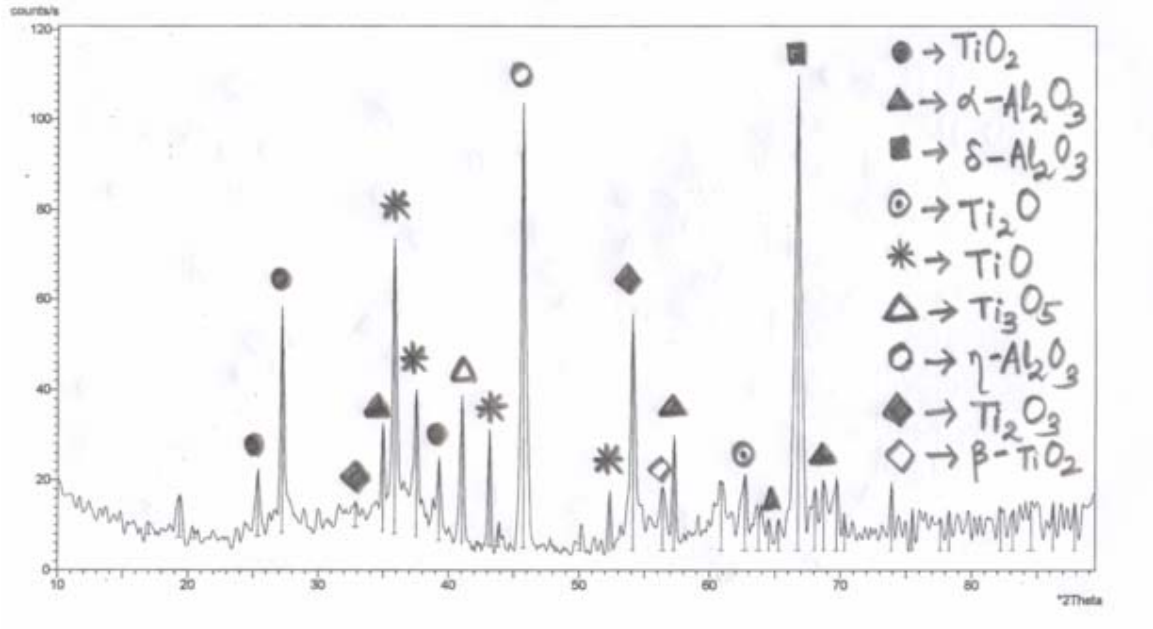

Fig.4.10 X-Ray Diffractogram of alumina titania coating deposited at 21kW power level.

The XRD of the feed material (fig. 4.6) shows the presence of α- Al_2O_3,δ- Al_2O_3, TiO_2 phases and some traces of γ - Al_2O_3 is also found to be present. Coating made at 11 kW power level (fig. 4.7), contain α- Al_2O_3,δ- Al_2O_3,η - Al_2O_3 and TiO_2 phases are present, where transformation of α- Al_2O_3 toη - Al_2O_3 and δ- Al_2O_3 is more. Besides the β -TiO_2 phase is also appeared. Generally Al_2O_3 transform to different allotropy phase forms but but TiO_2 reduces to Ti_3O_5, Ti_2O_3, Ti_2O, TiO, depending on enthalpy/environment and transformation conditions. The coating made at 15 kW power level contain α- Al_2O_3,δ- Al_2O_3,η - Al_2O_3, TiO_2 phases, where transformation of α- Al_2O_3 to η - Al_2O_3 and δ- Al_2O_3 is more, as compared to 11 kW, beside that β -TiO_2 phase is also present. From Fig. 4.9, coating made at 18 kW power level, transformation of α- Al_2O_3 to η - Al_2O_3 and δ- Al_2O_3 percentage goes on increasing for the coatings deposited at increased power levels but variation of percentage of TiO_2, Ti_3O_5, Ti_2O_3, Ti_2O, TiO do not show any significant change in oxides of titania. From Fig. 4.10, coating made at 21 kW power level, transformation of α- Al_2O_3 to η - Al_2O_3,δ- Al_2O_3 is maximum.

Generally α-Al_2O_3 transform to different phases η-Al_2O_3,δ-Al_2O_3 but TiO_2 is reduced toTi_3O_5, Ti_2O_3, Ti_4O_7, Ti_2O, TiO[**120**]. Ti_4O_7 phase is only present only for the coating deposited at 11kW, which can be justified from the free energy minimization plots [**121**]**.** Ti_4O_7 phase has lower free energy at lower power, next to it TiO (l) has lower free energy at lower power, so that it can be solidified to TiO(s), but at high power level TiO goes to gas

phase so it can not be condensed to solid phase of TiO having very high free energy. Reduction of TiO_2 to Ti_3O_5, Ti_2O_3 is also more at lower power level having lower free energy change.

4.9 SOLID PARTICLE EROSION WEAR BEHAVIOUR

Solid particle erosion is a wear process where particles strike against a surface and promote material loss. During flight, a particle carries momentum and kinetic energy, which can be dissipated during impact due to its interaction with a target surface. In case of plasma spray coatings encountering such situations, no specific model has been developed and thus the study of their erosion behavior has been mostly experimental data [**122**]. Erosion is a non-linear process with respect to its variables: either materials or operating conditions. To obtain the best functional output coatings exhibiting selected in-service properties and the right combinations of operating parameters are to be known. These combinations normally differ by their influence on the erosion wear rate or coating mass loss. Not much effort has been made to study the erosion wear behavior of plasma spray alumina-titania coatings yet. Here Erosion wear tests were carried out on the coatings to ensure its applicability under different operating conditions. The response of the coatings to the impingement of solid particles has been studied.

Erosion has been suggested as a suitable method to evaluate the cohesion of sprayed ceramic coatings [**123**]. A striking result in this work is that, although the wear rates spanned four orders of magnitude between the various erosion conditions, the ranking of the coatings stayed essentially the same. This suggests that the dominant wear mechanism, i.e. the basic mechanisms behind the formation and removal of wear fragments is similar for all coatings deposited at different power levels.

In this work, room temperature solid particle erosion trials on a few selected coated specimens are carried out using a compressed air blasting type rig under different test conditions at room temperature. For the coating which has shown maximum and minimum adhesion strength, is selected for study.

The coating made at 11kW power level, is eroded at different impact angles 30°and 90°. The nozzle (2.2 mm ID) is kept at 100mm, 125mm, 150mm, 175mm &200mm standoff distances from the target. Dry silica sand particles of 200,300 and 400μm average particle size at a feed rate of 50gm/min are used as erodent with an average velocity of 32m/s (as

measured by double disc method [**111**]) and pressure 4kgf/cm^2. The coating deposited at18 kW power level is eroded at 30°, 45^o, 60^o, 75^o and 90°angle at SOD of 150mm. Here, 200 & 400µm size dry silica sand particles are used as erodent with different velocities i.e. of 32m/sec, 38m/sec 45m/sec, 52m/sec and 58m/sec and at pressures of 4kgf/cm^2, 4.7kgf/cm^2, 5.5kgf/cm^2, 6.1kgf/cm^2, 6.5kgf/cm^2 with feed rate 50gm/min, 54gm/min, 58gm/min, 60gm/min and 62 gm/min. Amount of wear is determined on 'mass loss' basis [**112,113**]. It is done by measuring the weight change of the samples at regular intervals during the test duration. A precision electronic balance with + 0.01 mg accuracy is used for weighing. Erosion rate, defined as the coating mass loss per unit erodent mass (gm/gm) is calculated. The erosion rates are calculated at different erodent size, different erodent velocities, impingement angles, erodent dose and stand off distances.

The variations of cumulative mass loss with time, in case of the coating deposited at 18 kW, is illustrated in fig.4.11. The erodent particles having size 400µm strike the coated samples at 30^0 ,60^0 ,90^0 angle with stand of distance150mm; at a pressure of 6.5kgf/cm^2. It is seen that, the cumulative coating mass loss increases with increasing time of attack.

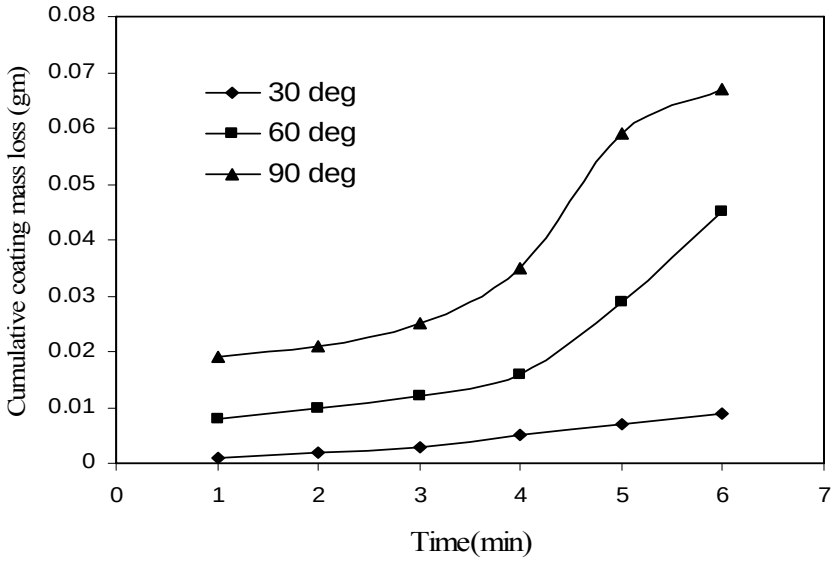

Fig.4.11 Variation of Coating mass loss with time for30^0, 60^0, 90^0 impact angles of 400µm size erodent at SOD of 150 mm, at pressure of 6.5 kgf/cm^2 for the sample Coated at 18 kW Power level.

The cumulative increment in material loss due to erosion wear of plasma sprayed coatings with exposure time (and erodent dose) has been studied by Levy [**124**]. In the present work such a trend is found in case of all coatings subjected to erosion test at all

impact angles. This can be attributed to the fact that, the fine protrusions on the top surface of the coating may be relatively loose and removed with less energy than what would be necessary to remove a similar portion/area of the coating from the bulk of the coating at later time. Consequently, the initial wear rate is high. With increasing exposure time the rate of wear starts decreasing and in the transient regime, a steady state in the wear rate is obtained. As the coating surface gradually gets smoothened, the rate of erosion tends to reach a steady state, as shown in fig.4.12 which contains variation of Erosion rate with Erodent dose of 400μm size erodent at impact angles of 30^0, 60^0 and 90^0 at SOD of 150 mm and at pressure of 4 kgf/cm^2 for the sample coated at 18 kW power level.

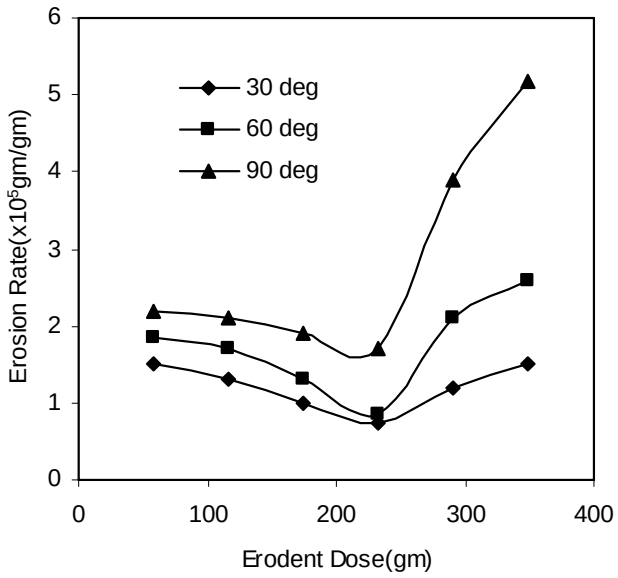

Fig. 4.12 Variation of Erosion rate with Erodent dose of 400μm size erodent at SOD of 150 mm and at pressure of 4 kgf/cm^2 for the sample coated at 18 kW power level.

With increase in the erodent dose, the erosion rate is affected tremendously. With higher erodent dose and with increasing the angle of impact from 30^0 to 90^0 the erosion rate increases sharply. The increase of erosion rate with erodent dose may be because of the cracks formed on the eroded sample, more amount of coating material comes out as debris. So the erosion rate increases and is maximum for 90^0 impact angle. Such trend in generally observed for brittle materials.

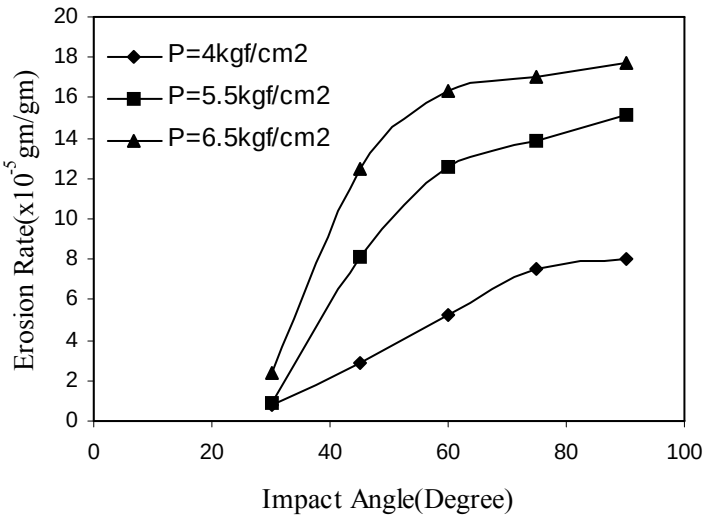

Fig. 4.13 Variation of Erosion rate with angle of impact for 400μm size erodent at 4.0, 5.5, 6.5 kgf/cm^2 pressures and at SOD of 150 mm after 6 minutes of impact for the sample coated at 18 kW power level.

Fig. 4.13, illustrates the effect of impact angle (α) on the erosion rate of coatings subjected to solid particle erosion for the coating deposited at 18kW. The erosion rate (mass loss of coating per unit wt of erodent (gm/gm)) is measured after the samples are exposed to the erodent stream for a fixed time i.e. for 6 minutes at SOD of 150mm. From the figure it is seen that, irrespective of the impact pressure of the erodent (of size 400μm), the erosion mass loss increases with increasing the angle of impact and maximum erosion takes place at $\alpha = 90^0$. Alahelisten [**125**] has studied erosion wear rate for diamond coating and found maximum erosion at for 90^0 impact angle and also erosion rate increases with increase in pressure of the erodent. This is typical of all brittle coatings. The relationship between erosion rate E and impact angle (α) is suggested by Bayer [**126**] as;

$$E = (K_d v^n \cos^n \alpha + K_b v^m \sin^m \alpha)M$$

For a particular test condition, velocity of impact v, erodent supply rate M is constant. The constants K_d, K_b m, n are determined by fitting the equation to experimental datas. For typical brittle materials $K_d = 0$ and the erosion rate is maximum at 90^0 impact angle. For typical ductile material, $K_b=0$ and erosion rate is largest at $20^0 – 30^0$ impact angles. The results obtained in the present work show that for 90^0 impact angle, alumina-13%titania coating loses 67 mg in 6 minutes (at 6.5kgf/cm^2 at SOD of 150 mm) for the alumina titania coating deposited at 18kW power level, while the mass loss is only 45 mg in case of $\alpha = 60^0$ and 9mg for $\alpha = 30^0$. This variation of erosion wear loss confirms that the angle at which the

stream of solid particles impinges the coating surface influences the rate at which the material is removed. It further suggests that, this dependency is also influenced by the nature of the coating material. The angle of impact determines the relative magnitude of the two components of the impact velocity namely, the component normal to the surface and parallel to the surface. The normal component determines/is responsible for the lasting time of impact (i.e. contact time) and the load. The product of this contact time and the tangential (parallel) velocity component determines the amount of sliding that takes place. The tangential velocity component also provides a shear loading to the surface, which is in addition to the normal load of the normal velocity component. Hence, as this angle changes the amount of sliding that takes place also changes as does the nature and magnitude of the stress system. Both of these aspects influence the way a coating wears. These changes imply that different types of material would exhibit different angular dependency.

Variation of Erosion rate with impact velocity of the 400µm erodent at 30^0, 60^0,90^0 angle of impact at SOD of 150 mm (after 6 minute) for the sample coated at 18kW power level is shown in fig. 4.14. It is seen that the erosion rate increases with increasing velocity of the erodent. It is obvious that, with increasing velocity the particles will have high kinetic energy, which will be dissipated (and transformed) at impact and hence will remove more particles from the impacted surface [**112**] and is maximum at 90^0 angles. Such findings are also reported by Lathabai et al for different coatings [**127**]. Shanov et.al. [**128**] have also observed that, alumina titania coating has better erosion resistant property than coating made with alumina only.

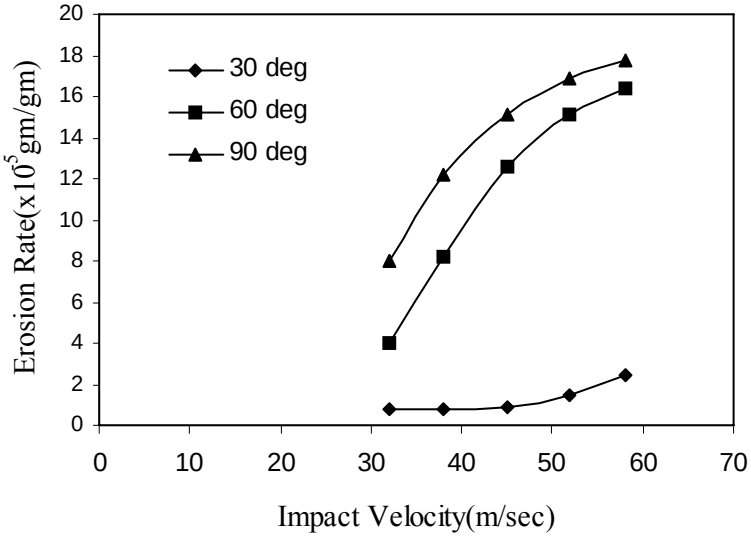

Fig. 4.14 Variation of Erosion rate with impact velocity of the 400µm size erodent at SOD of 150 mm after 6 minutes of impact, for the sample coated at 18kW power level.

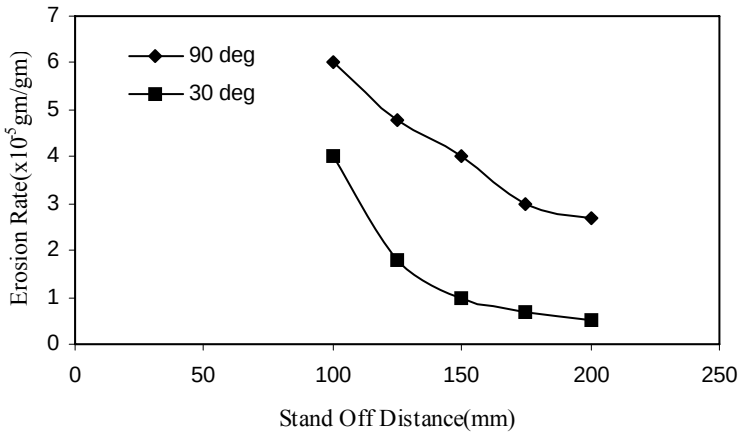

Fig. 4.15 Variation of Erosion rate with stand off distance of the 400µm size erodent at a pressure of 4kgf/cm^2 after 6 minutes of impact, for the sample coated at 11kw power level.

Variation of Erosion rate with stand off distance at 30^0, 90^0 angle of impact (after 6 minutes) at a pressure of 4kgf/cm^2 for the sample coated at 11kW power level is shown in fig. 4.15. It is seen that, erosion rate decreases with increasing stand off distance. It is obvious that the impact force will be less with increasing stand off distance so reduced rate of erosion. Similar observations are also reported by Chang-Jiu Li et.al. [**129**]. The rate of decrease of erosion rate with increase stand off distance is faster up to a certain stand off distance i.e. 150mm then take up a slow decreasing trend.

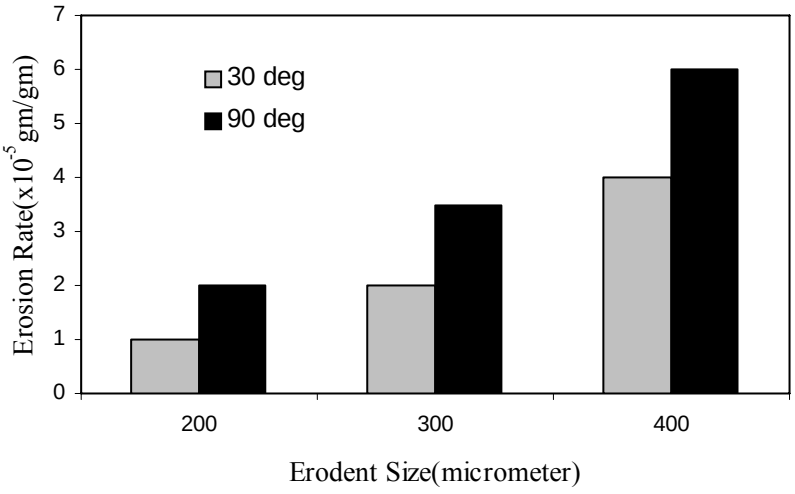

Fig. 4.16 Variation of Erosion rate with size of the erodent at a pressure of 4kgf/cm^2 and 100 mm SOD for the sample coated at 11kw power level.

Variation of Erosion rate with size of the erodent at 30^0, 90^0 angle of impact at a pressure of 4kgf/cm^2 at SOD of 100 mm after 6 minute for the sample coated at 11kw power level is shown in fig. 4.16. With increasing particle size of erodent, erosion rate increases and it is maximum for 90^0. Westergard et al [**130**] have reported that the erosion rates increased by three orders of magnitude with increasing the of the erodent size from 75 to 600 μm. The relative ranking of the materials, however, remained strikingly similar for all erosion conditions. Addition of 13% Titania has improved the erosion resistance compared to alumina only, has also been indicated else where [**130**].

4.10 MICROSTRUCTURAL INVESTIGATION

4.10.1 Powder morphology

SEM micrograph of alumina 13 wt% titania powders prior to coating is shown in fig.4.17. From the figure, it is seen that the particles are of varied particle sizes, irregular in shape. Some particles are elongated type and some are of multifaceted.

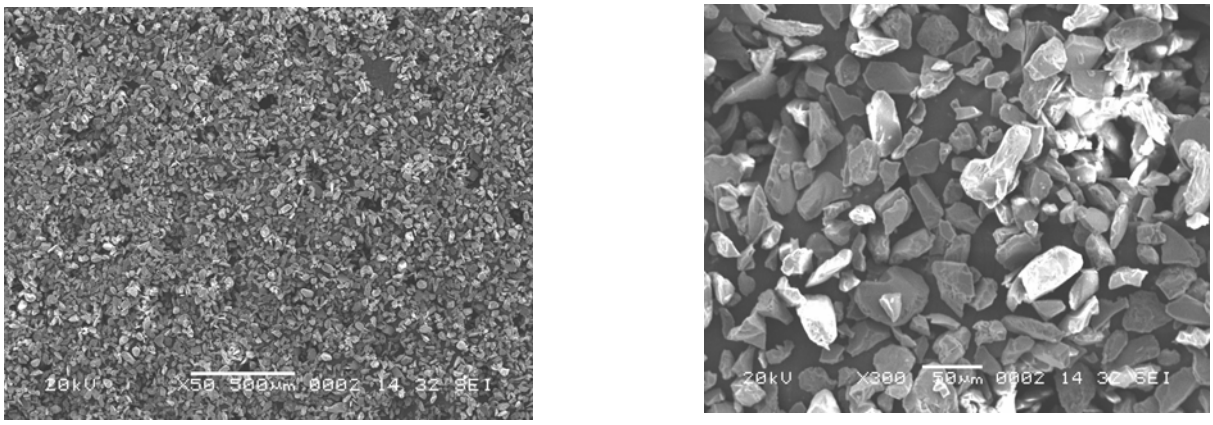

(a) **(b)**

Fig. 4.17 SEM micrograph of alumina 13 wt% titania raw powders (i.e. feed stock).

4.10.2 Structure of coating surface

The interface adhesion of the coatings depends on the coating morphology and inter-particle bonding of the sprayed powders. SEM micrograph of alumina titania coating surface deposited at 11kW, 15kW, 18kW and 21kW are shown in fig.4.18. The coating deposited at 11kW power level (fig.4.18 a), shows a uniform distribution of molten/semi molten particles. More amount of cavitations is observed, other than some large pores found on the inter particle boundaries and triple particle/grain junctions, which may have originated during

solidification of particles from molten/semi-molten state. The coating made at 15 kW (fig.4.18 b) bears a different morphology. A large number of globular particles and some flattened regions, indicative of particle melting during spray deposition. The grains/particles are mostly equi-axed type with little boundary mismatch between them. Amount of cavitations is less than that of the previous case. However, some cavity regions are seen along inter-particle/inter-grain boundaries. Coating deposited at further higher power level i.e. at 18 kW (fig.4.18c), bears a different morphology. Larger portions of the coatings exhibit flattened regions, which might have been formed during solidification of molten particles that have fused together in lumps. Less cavitations is observed at inter grain boundary.

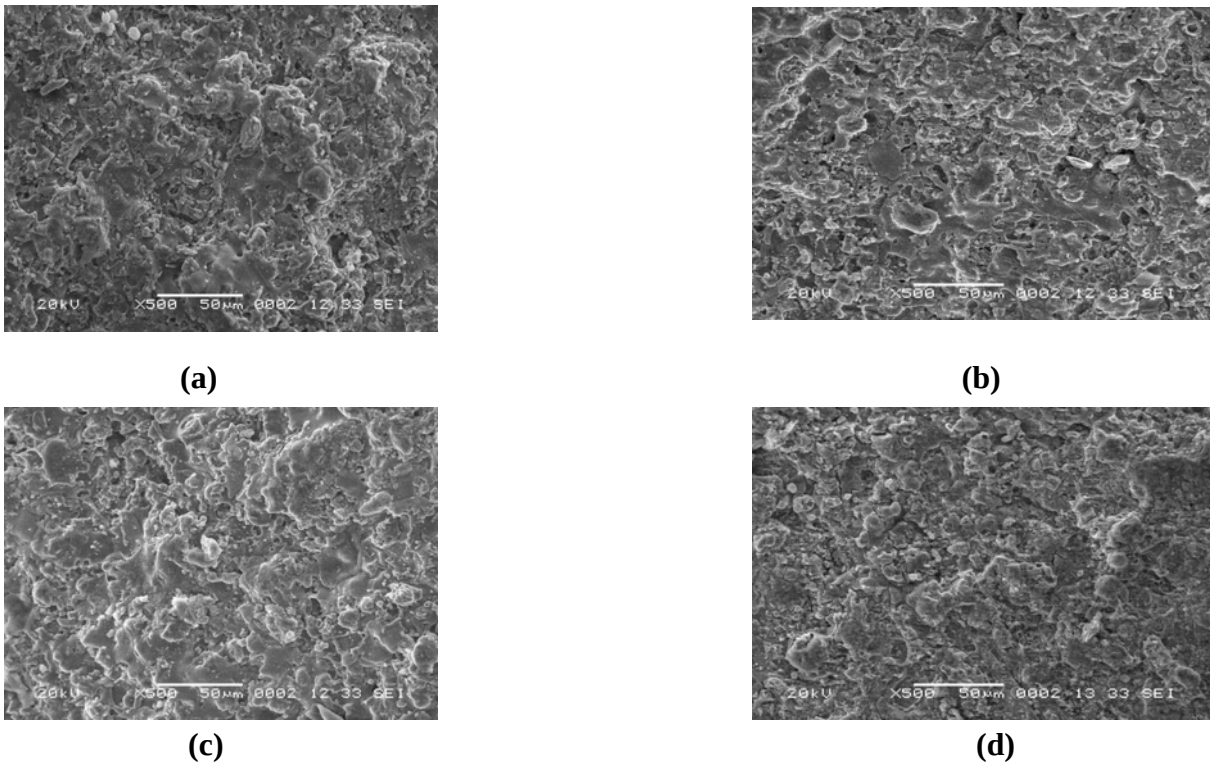

Fig.4.18 Surface morphology of alumina titania coatings deposited at different power level, i.e. (a) 11kW, (b) 15kW, (c) 18kW, (d) 21kW.

This may be the reason for increase of adhesion strength and hence is maximum for the coating deposited at 18kW power level. For the coatings deposited at further higher power level i.e. at 21 kW (fig.4.18 d), the surface morphology is completely different. A large number of spheroidal particles of varied diameters are seen, which might have been formed due to breaking / fragmentation of bigger particles which have melted during in flight traverse through the plasma jet and then solidified in form of spheres. The amount of porosity appears to have increased again. Amount of cavitations is more than that observed in

previous cases. This might be the cause for the improper inter-particle bonding and poor stacking to the substrate which have resulted in low interface bond strength. There is a drastic reduction in cavitations, which might be due to solidification of molten/semi molten particles forming flattened regions and reducing inter-particle mismatch and then by porosity. Splat formation due to higher cooling rate leads to maximum adhesion strength for the coating made at 18 kW power level. But the protruding surface on the coating might be the cause of increase in erosion rate. Hence, the erosion is less for the coating deposited at lower power level, i.e. at 11kW operating power.

4.10.3 Microstructure of coating interface

The coating substrate interface plays the most important role on the adhesion of the coating. The surface morphology of the coating cannot predict the interior (layer deposition) structures. The polished cross-sections of the samples are examined under SEM and a typical (which has shown maximum adhesion strength) is shown in fig. 4.19. From the micrograph good interface matching is seen. Lamellar structure confirms the solidification of molten particles to form splats during coating deposition. The coating is homogenous through out the length for the coating deposited at 18kW, hence has shown higher adhesion strength.

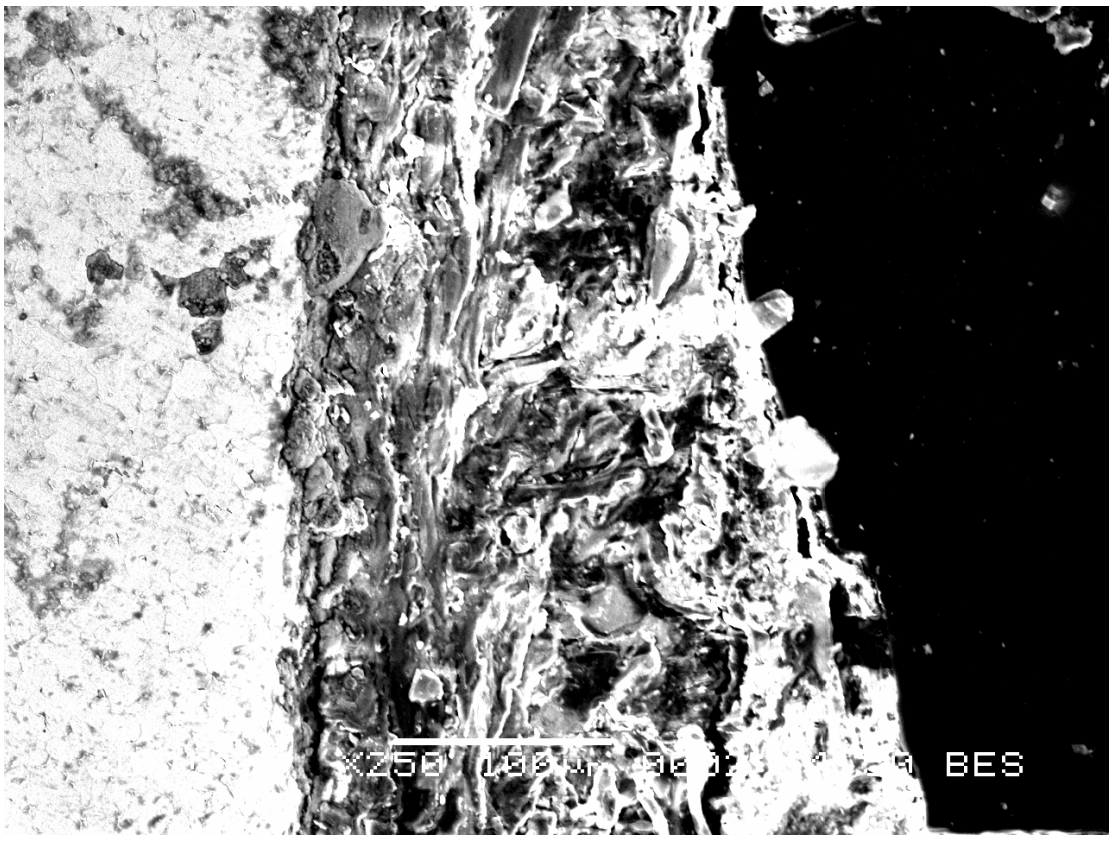

Fig. 4.19 Interface morphology of alumina titania coatings deposited on mild steel substrates at 18 kW power level.

4.10.4 Worn surfaces

Eroded Surface morphology (SEM micrographs) of alumina titania coating surface deposited at different power levels are shown in fig. 4.20. The rate of erosion is less for the coating deposited at 11kW power level (fig.4.20a) and more in case of coating deposited at 18 kW power level (fig.4.20b).

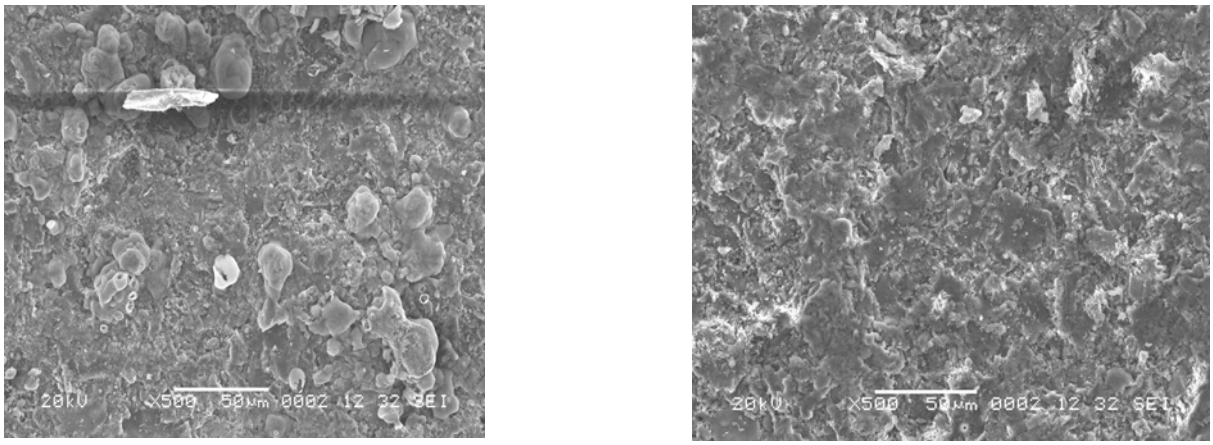

(a) **(b)**

Fig.4.20 Eroded Surface of coatings deposited at (a) 11kW and (b) 18kW.

SEM did not reveal any large differences in topographic features between the eroded surfaces of the coatings. Smaller particles resulted in more plastically deformed surfaces (Fig. 4.21a) and larger eroding particles produced sharp faceted grooves and surfaces with higher amounts of inter-splat debonding (Fig. 4.21b).

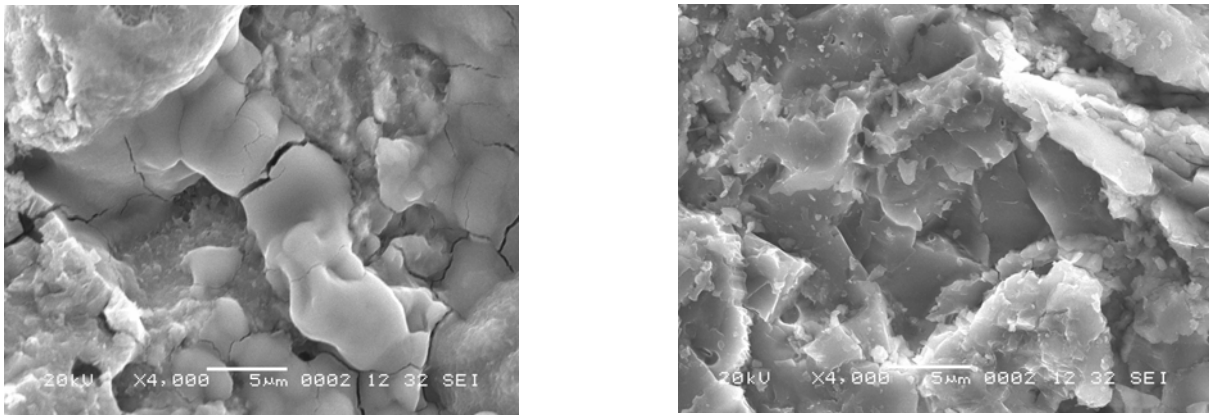

(a) **(b)**

Fig.4.21 Micrographs of (a) eroded with 200µm particle and (b) eroded with 400µm particles at normal impact for the coating deposited at 18kW.

All coatings showed the thermally induced cracks referred to normal cracks, within the splats. For low strains, presumably originating from relaxation of strained grains and splats by crack initiation and propagation; or by propagation of pre-existing cracks in the coating. When the coated beam is subjected to higher pressure/time, the most favorably oriented cracks are activated and start linking to nearby cracks. This linking process accelerates very rapidly and the cracks propagate through out the coating. When the crack reaches the coating/substrate interface, extensive coating delamination starts and the stress caused by the bending are relaxed. The appearance of the eroded surfaces also indicates that cracks tend to follow a variety of weak sites to produce wear debris. The thermal cracks normal to the surface, the interfaces between adjacent layers of splats and also the columnar boundaries within the individual splats can be identified as structural weaknesses for all the coatings, as been described in literature [**131,132**].

4.11 DISCUSSION

Thermal spraying is a highly complex deposition process with a large number of interrelated variables. Due to the high velocity and temperature gradients in the plasma plume, even small changes in the controllable or uncontrollable parameters can result in significant changes in the particle properties and thus in the microstructure of the coatings [**133,134**]. In thermal spray of oxide coatings developed using atmospheric plasma spray (APS) technique, particle deposition i.e. the coating thickness is influenced mainly by the input power to the plasma torch. With increase in power level, the plasma density increases leading to a rise in enthalpy and thereby the particle temperature. Hence more number of particles gets melted during in-flight traverse through plasma jet. When these molten species hit the substrate, get flattened and adhere to the surface. The deposition of layers is favored with availability of more number of molten / semi molten particles which is enhanced by increasing the torch input power. This increases the coating thickness. But, beyond certain limit of operating power level; fragmentation and vaporization of sprayed particles do occur simultaneously and some (powder) particles fly off during spraying restricting further increase in coating thickness.

In the present investigation, coatings are deposited on metal substrates of different thermal conductivity and thermal expansion coefficient. It is observed that the coating thickness varies with different substrate materials. This may be mainly due to thermal conductivity of the substrate material. When the sprayed particles impinge on the substrate

surface, heat transfer and dissipation takes place. The particles dissipate heat at a faster rate through the metal substrate. Subsequent particles accumulated / deposited on the top of the first layer restrict the heat transfer towards outside environment than through the metal surface. The dissipation of heat from the particles/coating layers is favored with increased heat dissipation rate through the substrate. So for the metals having higher thermal conductivity the layer deposition is faster. In this work, the observation of higher coating thickness and higher deposition rate on copper substrate than that on mild steel substrates may be attributed to this effect.

From the study of coating deposition, it is seen that deposition efficiency has increased with increase in torch input power up to an optimum level (about 18 kW), beyond which there is no significant change. This is a measure of the amount of materials deposited per unit surface area. Berger *et al*. [**135**] have also reported similar observation that, the deposition of high quality coating is favored at moderate temperature range.

The adherence of the coating to the substrate is of major concern. The bonding mechanism operative between the coating and substrate can be classified into three categories: mechanical, physical and physico-chemical. The molten particles striking a roughened surface conform to the surface topography can stick to the substrate. The mechanical interlocking between the coating and the protrusions on the substrate surface is termed as mechanical adherence. Substrate-coating adherence by Vander-walls force is classified as physical bonding.

In majority of the situations encountered, adhesion is physical bonding of the coating to the substrate. The formation of an inter-diffusion zone or an intermediate compound between the coating and substrate is generally termed as chemical or metallurgical bonding. The specific mechanism operative between a coating and substrate depends primarily on the materials used and the physical condition of these material particles on impact.

The analysis of coating - substrate bond strength of all the sprayed materials on different substrates, presented in table 4.3 envisages that; (i) there is an increase in adhesion strength with increase in plasma torch operating power (up to 18 kW) then with further increase in torch input power does not improve the adhesion strength for almost all the substrates and (ii) there is a variation in adhesion strength for different substrates.

Variation of adhesion strength with input power at constant TBD can be explained in terms of the thermal state of the particles striking the surface of the substrate. At lower power level, the plasma gas temperature is not high enough to effect complete melting of all the particles entering the plasma jet. It is also possible that un-melted particles get embedded within the molten ones. Such a situation naturally leads to poor coating adhesion. When the input power to the plasma torch is increased the plasma jet temperature and heat transfer coefficient of the plasma increases leading to complete melting of a large fraction of the injected feed stocks which on hitting the substrate get fused and flattened at a relatively faster rate. Therefore, there is better splat formation (of the molten species) and mechanical inter-locking on the substrate surface leading to increase in adhesion strength. Thiyagarajan et al [**136**] has computed the plasma temperature at the nozzle exit for different input power levels of the plasma torch. The results are summarized in Table 4.9. It can be seen that, as the input power increases, the plasma temperature at the nozzle exit as well as the mean flame temperature increases adding to the evidences of increased adhesion strength. However, at much higher power level, the amount of fragmentation and vaporization of the particles increase leads to lowering the deposition efficiency and coating adhesion as well.

The vapors and gaseous species of dissociated products can get entrapped in the coating and affect the porosity of the coatings. This can also lead to a decrease in the adhesion strength of the coating made at higher power level.

Input power (kW)	Plasma Temp. (K) at nozzle exit
8	5939
10	6358
12	6678
16	9446

Table 4.9 Mean plasma temperature of Ar-N_2 plasma at nozzle exit for different operating power [**136**].

It has been shown in previous investigations [**137**] that, for a given material the final coating properties depend on the velocity, temperature and type of particles just before impact on the substrate (or on the coating layers). The plasma power effectively changes the temperature and particle velocity profile and therefore affects the coating properties. The composition of the coating materials also affects the coating adhesion strength due to

transformation/formation of phases and inter-oxides that favor the inter particle bonding and adhesion to the substrate. In this investigation, higher adhesion strength in substrates of lower thermal conductivity (i.e. in mild steel) is observed. It is known that the oxides adhere weakly to a substrate of high thermal conductivity owing to a low contact temperature [**138**]. Hence the relatively lower adhesion strength on copper substrates as compared to mild steel substrate may be due to this effect.

From the microscopic studies it is seen that, the particle size and their appearance have changed with change in operating conditions of the plasma torch. Micro-cracks and cavities/pores are also seen in the deposited layers. This reflects in the type of reactions (indicative of whether the particles are molten, semi-molten, un- melted, fragmented and of possible phase transformation mechanisms) which might have taken place during in-flight traverse of the powders through plasma. The molten or semi-molten species bear equi-axed structure. The fragmented particles get melted completely exhibiting spheroidal shape and partially melted/un-melted powders get stacked in the coating layers during deposition. The formation of micro-cracks are possible in the coatings near to the substrate and open pores/cracks do originate along the direction of heat flow i.e. towards the substrate due to shrinkage of particles parallel to the surface of the substrate as been also found earlier [**139**]. Hence such microstructures affect the coating homogeneity and adhesion to the substrate. Measured values of coating porosity, presented in table 4.4. Maximum porosity of about 5.47 % is recorded for the coating deposited at 21kW and is very much within the limit as observed with plasma sprayed ceramic coatings [**119**].

Micro-hardness measurement is made on optically distinguishable phases present in the coatings. The existence of at least three different phases (which are optically distinguishable) might have been formed during plasma spraying. The hardness values are different for different phases and appear to be not much dependent on torch operating power level. On referring to the X Ray diffractograms taken on raw material and coated samples, it becomes evident that during coating deposition, formation, reduction and transformation of phases have taken place. So during spraying, the phase transformation and/or formation of inter oxides (transformation of α -alumina to δ -alumina, η-alumina and reduction of TiO_2 phase to Ti_3O_5, Ti_2O_3, Ti_2O, TiO phases) corroborate to different micro-hardness values obtained on various phases of the coatings.

To assess the suitability of these coatings for tribological applications, solid particle erosion wear behaviour is studied. From the observed results, it can be said that, the erosion wear rate varies with (i) erodent dose, (ii) impact angle of the solid particles on the coating surface, (iii) the velocity of erodent, (iv) stand off distance, (v) size of the erodent, (vi) input power of the plasma torch and also time dependant. With increase in impact angle, the erosion wear increases and is maximum at 90^0 of impact. Such type of observation of high rate of erosion wear is usual with plasma sprayed ceramic coatings [**140]**.

The erosion wear for different coatings can be attributed to the phase constituents of the coatings and type, volume and distribution of pores/cavities/cracks, protruding present in the coatings. The XRD study and micro-hardness results obtained in this investigation show that the different phase composition of the coatings exhibit different hardness. It is known that, with increase in the material hardness the erosion wear rate decreases [**141**]. So our findings on the wear behaviour of various coatings are at par with the concluding remarks of previous investigations.

Branco et al. [**142**] reported that, the coating porosity influences the erosion in three ways. Firstly, it reduces the material strength against plastic deformation or chipping since the material at the edge of a void lacks mechanical support. Secondly, the concave surface inside a void that is not under the shadow of some void edge will see an impinging particle at an angle higher than the average target surface to impact angle (which is detrimental for brittle materials). And finally, pores can impair strength by acting as stress concentrators and/or decreasing the load-bearing surface. The coatings under this investigation are though brittle in nature, the effect of pore volume fraction on erosion wear needs a more detailed investigation.

Chapter 5

ANALYSIS OF EXPERIMENTAL RESULTS USING STATISTICAL TECHNIQUES

- Introduction
- Taguchi Experimental Design
- Artificial Neural Network (ANN) Analysis
- Remarks

CHAPTER 5
ANALYSIS OF EXPERIMENTAL RESULTS USING STATISTICAL TECHNIQUES

5.1 INTRODUCTION

During spraying, various operating parameters are determined mostly based on past experience. It therefore does not provide the optimal set of parameters for a particular objective. In order to obtain the best result with regard to any specific coating quality characteristic, accurate identification of significant control parameters is essential. Solid particle erosion is considered as a non-linear process with respect to its variables: either materials or operating conditions. To obtain the best functional output coatings exhibiting selected in-service properties and the right combinations of operating parameters are to be known. These combinations normally differ by their influence on the erosion wear rate or coating mass loss. In order to control the wear loss in such a process one of the challenges is to recognize parameter interdependencies, co-relations and there individual effects on wear. This chapter is devoted to analyze the experimental results on the erosion wear behavior of alumina titania coatings made at different operational conditions. For this purpose, a statistical techniques Taguchi experimental design are used. Factors are identified according to their influence on the coating erosion rate. The most significant parameter is found. A prediction model using artificial neural network (ANN) is presented considering the significant factors. Beside that this analysis is made taking into account training and test procedure to predict the dependence of coating adhesion strength on different operating power levels on different substrates.

.

5.2 TAGUCHI EXPERIMENTAL DESIGN

Taguchi method of experimental design is a simple, efficient and systematic approach to optimize designs for performance and cost [**143**]. In the present work, this method is applied to the process of plasma spraying for identifying the significant process variables/interactions influencing coating erosion wear rate. The levels of these factors are also found out so that the process variables can be optimized within the test range.

5.2.1 Experimental Design

Experiments are carried out to investigate the influence of the four selected control parameters. The code and levels of control parameters are shown in table 5.1. This table shows that the experimental plan has two levels. A standard Taguchi experimental plan with notation **L16 (2^{15})** is chosen as outlined in table 5.2. In this method, experimental results are transformed into a signal-to-noise (S/N) ratio. It uses the S/N ratio as a measure the quality characteristics deviating from or nearing to the desired values. There are three categories of quality characteristics in the analysis of the S/N ratio, i.e. the lower-the-better, the higher-the-better, and the nominal-the-better. To obtain optimal spraying parameters, the lower-the-better quality characteristic for erosion wear rate is taken.

Parameter	Code	Level 1	Level 2
Impact Angle(Degree)	A	30	90
Impact Velocity(m/sec)	B	32	58
Stand Off Distance(mm)	C	100	150
Erodent Size(μm)	D	200	400

Table 5.1 Control factors and selected test levels.

Exp. No.	A	B	C	D	Coating erosion wear rate	S/N Ratio
1	1	1	1	1	10.00	-20.0000
2	1	1	1	2	11.00	-20.8279
3	1	1	2	1	11.5	-21.2140
4	1	1	2	2	12.20	-21.7272
5	1	2	1	1	14.40	. -23.1672
6	1	2	1	2	12.50	-21.9382
7	1	2	2	1	18.10	-25.1536
8	1	2	2	2	19.80	-25.9333
9	2	1	1	1	.6	4.4370
10	2	1	1	2	.8	1.9382
11	2	1	2	1	2.10	-6.4444
12	2	1	2	2	2.41	-7.6403
13	2	2	1	1	6.10	-15.7066
14	2	2	1	2	8.00	-18.0618
15	2	2	2	1	17.10	-24.6599
16	2	2	2	2	17.74	-24.9791

Table 5.2 Experimental lay out and results with calculated S/N ratios for coating erosion wear rate.

Level	A	B	C	D
1	-11.39	-11.43	-14.17	-16.49
2	-22.50	-22.45	-19.72	-17.40
Diff.	11.11	11.02	5.5	0.91
Rank	1	2	3	4

Table 5.3 The S/N response table for coating erosion wear rate.

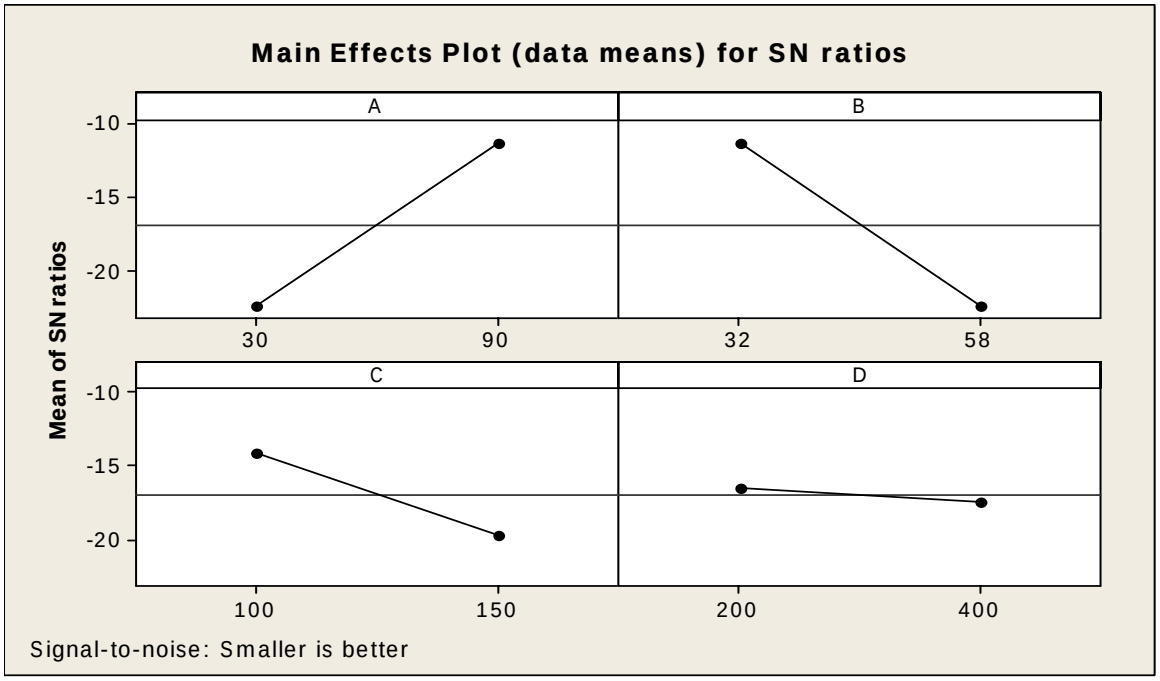

Fig.5.1 The S/N response graph for coating erosion wear rate.

5.2.2 Analysis of control factor

Table 5.2 shows experimental lay out and results with calculated S/N ratios for erosion wear rate of the coatings made at 18Kw power level. Analysis of the influence of each control factor on the coating efficiency is made with a signal-to-noise (S/N) response table, using MINITAB computer package. The response data of the testing process is presented in table 5.3. The S/N response graph for coating erosion wear rate is shown in fig.5.1.The influence of interactions between control factors is also analyzed in the response table. The control factor with the strongest influence is determined by differences values. The higher the difference, the more influential is the control factor or an interaction of two controls. The strongest influence on coating erosion wear rate is found out to be of impact angle (A) followed by impact velocity (B) and stand off distance (C) then size of the erodent (D) respectively.

It is interesting to note that the Taguchi experimental design method identified impact angle and impact velocity as the most powerful factor influencing the erosion wear rate of the alumina titania coatings. The stand off distance, size of the erodent emerge as the other significant factors affecting the coating erosion wear rate. The impact angle, thus is a significant process variable and in this work, is rightly taken as the basis for studying its effect on the coating erosion wear characteristics.

5.3 ARTIFICIAL NEURAL NETWORK (ANN) ANALYSIS

Plasma spraying is considered as a non-linear problem with respect to its variables: either materials or operating conditions. To obtain functional coatings exhibiting selected in-service properties, combinations of processing parameters have to be planned. These combinations differ by their influence on the coating properties and characteristics. In order to control the spraying process, one of the challenges nowadays is to recognize parameter interdependencies, correlations and individual effects on coating characteristics. Therefore a robust methodology is needed to study these interrelated effects. In this work, a statistical method, responding to the previous constraints, is implemented to correlate the processing parameters to the coating properties. This methodology is based on artificial neural networks (ANN), which is a technique that involves database training to predict property-parameter evolutions. This section presents the database construction, implementation protocol and a set of predicted results related to the coating erosion wear. ANNs are excellent tools for complex processes that have many variables and complex interactions. The analysis is made taking into account training and test procedure to predict the dependence of erosion wear behavior on angle of impact and velocity of erodent and the dependence of coating adhesion strength on different operating power levels on different substrates. This technique helps in saving time and resources for experimental trials. The details of this methodology are described by Rajasekaran and Pai [**144**].

5.3.1 Neural Network Model: Development and Implementation (for coating erosion wear rate)

An ANN is a computational system that simulates the microstructure (neurons) of biological nervous system. The most basic components of ANN are modeled after the structure of brain. Inspired by these biological neurons, ANN is composed of simple elements operating in parallel. It is the simple clustering of the primitive artificial neurons. This clustering occurs by creating layers, which are then connected to one another. The multilayered neural network which has been utilized in the most of the research works for material science, reviewed by Zhang and Friedrich [**145**]. A software package NEURALNET for neural computing developed by Rao and Rao [**146**] using back propagation algorithm is used as the prediction tool for coating erosion wear rate at different impact angles and impact velocity.

The database is built considering experiments at the limit ranges of each parameter. Experimental result sets are used to train the ANN in order to understand the input-output

correlations. The database is then divided into three categories, namely: a validation category, which is required to define the ANN architecture and adjust the number of neurons for each layer. A training category, which is exclusively used to adjust the network weights and a test category, which corresponds to the set that validates the results of the training protocol. The input variables are normalized so as to lie in the same range group of 0-1. To train the neural network used for this work, about 25 data sets at different angles and different velocities are taken. It is ensured that these extensive data sets represent all possible input variations within the experimental domain. So a network that is trained with this data is expected to be capable of simulating the plasma spray process. Different ANN structures (I-H-O) with varying number of neurons in the hidden layer are tested at constant cycles, learning rate, error tolerance, momentum parameter and noise factor and slope parameter. Based on least error criterion, one structure, shown in table 5.4, is selected for training of the input-output data. The learning rate is varied in the range of 0.001-0.100 during the training of the input-output data. The network optimization process (training and testing) is conducted for 1000,000 cycles for which stabilization of the error is obtained. Here the hidden layer number is 1 and neuron numbers in the hidden layer is varied and in the optimized structure of the network, this number is 6. The number of cycles selected during training is high enough so that the ANN models could be rigorously trained.

Input Parameters for Training	**Values**
Error tolerance	0.002
Learning parameter(ß)	0.001
Momentum parameter(α)	0.001
Noise factor (NF)	0.002
Maximum cycles for simulations	1000000
Slope parameter (£)	0.6
Number of hidden layer neuron	6
Number of input layer neuron (I)	2
Number of output layer neuron (O)	1

Table 5.4 Input parameters selected for training (Coating erosion wear).

The impact angles and impact velocity have already been identified (from the outcome of Taguchi analysis) as the parameter significantly affecting the coating erosion wear rate. Each of these parameters is characterized by one neuron and consequently the input layer in the ANN structure has two neurons and the output layer in the ANN structure

has one neuron. The optimized three-layer neural network having an input layer (I) with two input nodes, a hidden layer (H) with six neurons and an output layer (O) with one output node employed for this work is shown in fig. 5.2.

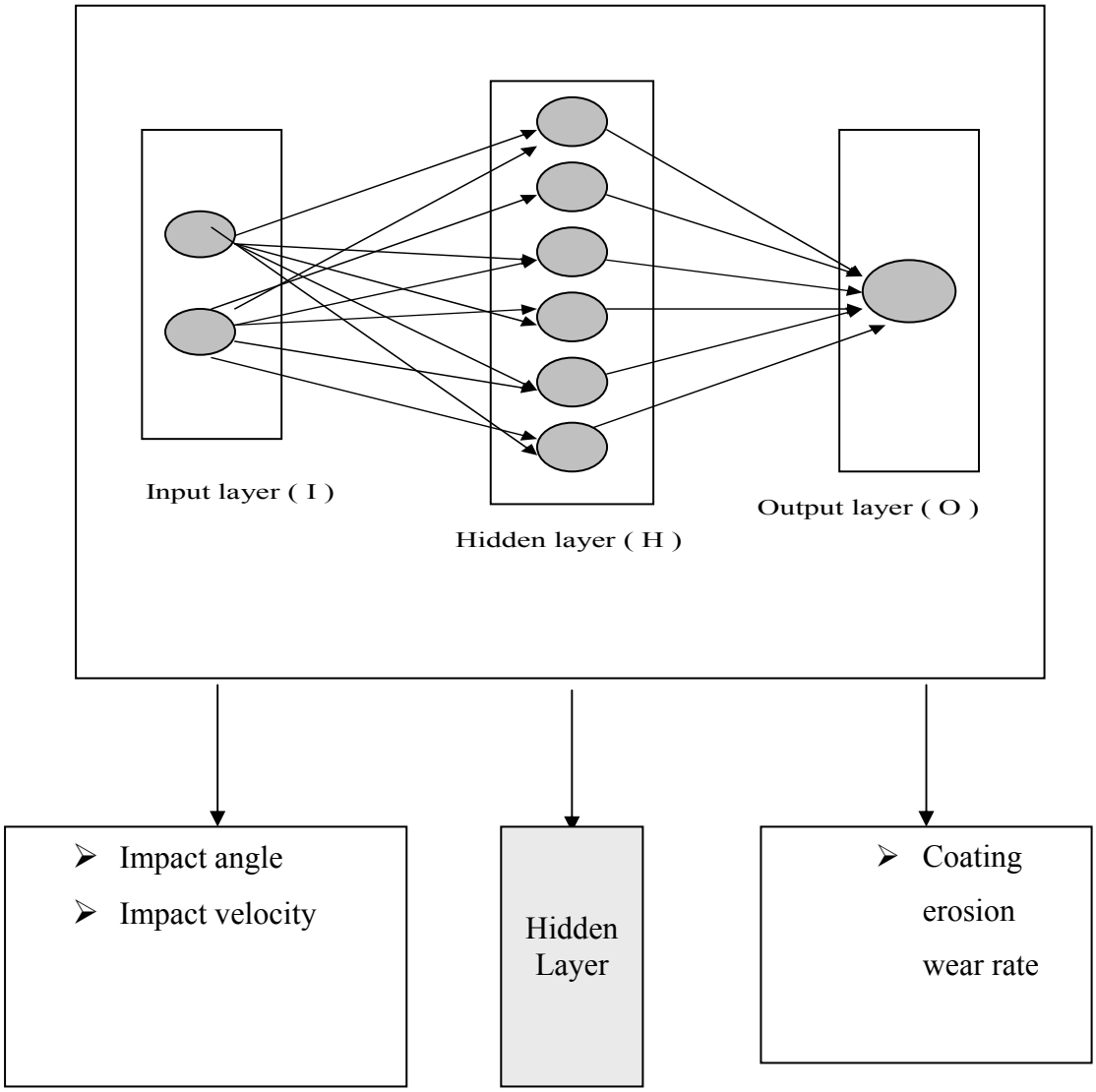

Fig.5.2 The three Layer Neural network.

5.3.2 ANN prediction of erosion wear rate

The prediction neural network is tested with four data sets from the original process data. Each data set contained inputs such as impact angle and impact velocity and an output value i.e. erosion wear rate is returned by the network. As further evidence of the effectiveness of the model, an arbitrary set of inputs is used in the prediction network. Results are compared to experimental sets that may or may not be considered in the training or in the test procedures. Fig.5.3 represents the comparison of predicted output values for erosion wear rate with those obtained experimentally at different impact angles of the erodent at different impact velocities i.e. 32m/sec , 45m/sec and 58 m/sec respectively.

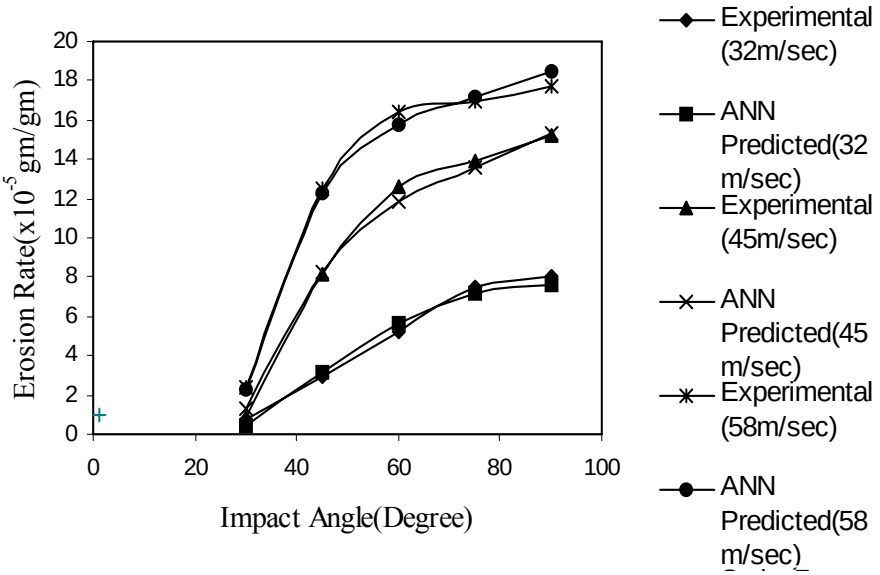

Fig.5.3 Comparison plot for predicted and experimental values of coating erosion wear rate at different impact angles of the erodent at impact velocity 32m/sec, 45m/sec and 58m/sec (time of exposure 6 min, SOD 150mm, size of the erodent 400μm for the sample coated at 18 kW power level).

Beside comparison of predicted and experimental values of erosion wear rate Fig.5.3 illustrates the effect of impact angle (α) on the erosion rate of coatings subjected to solid particle erosion. The erosion results for coatings of materials deposited at 18 kW operating power of the plasma torch at impact angles of 30^0,45^0, 60^0,75^0 and 90^0 for 32m/sec, 45m/sec and 58m/sec respectively at SOD of 150mm for size of the erodent 400μm are shown. Mass loss, then erosion rate (mass loss of coating (gm) per unit wt of erodent (gm)) is measured after the samples are exposed to the erodent stream for 6 minutes. It is seen from the graph that irrespective of the feed material, the erosion mass loss is higher at larger angle of impact

and the maximum erosion takes place at $\alpha = 90^0$. Such trend in generally observed for brittle materials.

It is interesting to note that the predictive results show good agreement with experimental sets realized after having generalizing the ANN structures. The optimized ANN structure further permits to study quantitatively the effect of the considered impact angle. The range of the chosen parameter can be larger than the actual experimental limits, thus offering the possibility to use the generalization property of ANN in a large parameter space. In the present investigation, this possibility was explored by selecting the impact angle in a range from 10^0 to 90^0 for velocities 32m/sec, 45m/sec, 58m/sec and a set of prediction for erosion wear rate is evolved. Fig.5.4 illustrates the predicted evolution of erosion wear rate of alumina titania coatings on mild steel substrates with the impact angle for velocities 32m/sec, 45m/sec, 58m/sec. From the predicted graph in fig.5.4 with increasing impact angle erosion rate increases for different impact velocity, and it is maximum at 58m/sec.

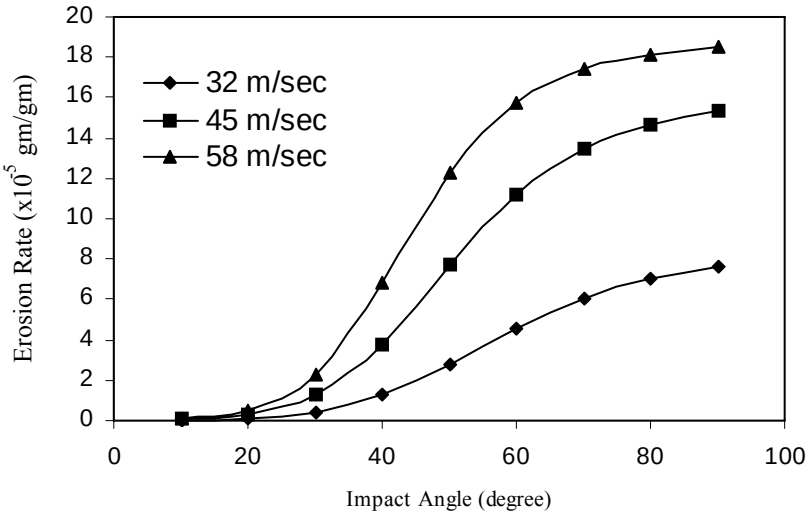

Fig.5.4 Predicted erosion wear rate of the coating at different impact angles of the erodent for different impact velocities (for 6 minute time of exposure, SOD150mm, size of the erodent 400μm for the sample coated at 18 kW power level).

In the present investigation, by selecting the impact velocity in a range from 20 to 70 m/sec at impact angles 30^0 , 60^0 and 90^0 and a set of prediction for erosion wear rate is evolved. Fig.5.5 illustrates the predicted evolution of erosion wear rate of alumina titania coatings on mild steel substrates with the impact velocity at impact angles 30^0, 60^0 and 90^0.

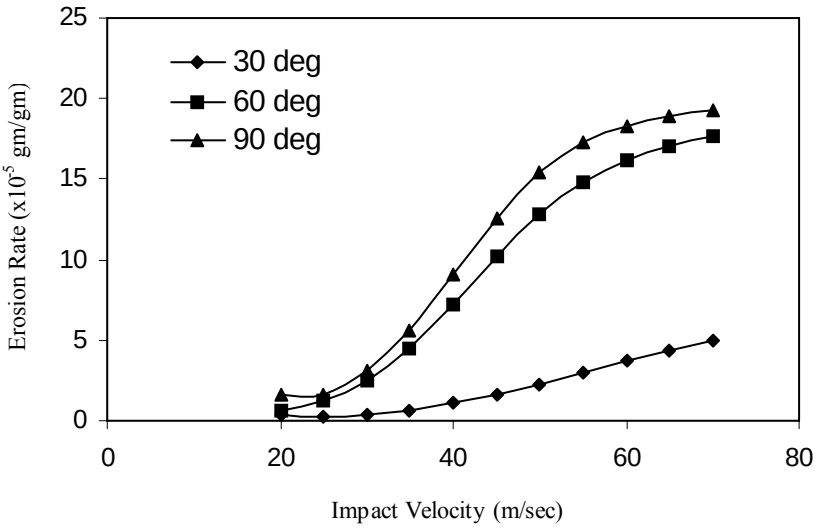

Fig.5.5 Predicted erosion wear rate at different impact velocities impacted at different angles (for exposure time 6 min, SOD150mm, size of the erodent 400μm, for the sample coated at 18 kW power level).

From the predicted graph in fig.5.4 with increasing velocity erosion rate increases for different angles. It is obvious that, with increasing velocity the particles will have high kinetic energy, which transformed at impact and hence remove more particles from the impacted surface and it is maximum at 90^0 angle. Beside that at low velocity and at low angle there may be one mechanism, so that the slope does not change much, but at high velocity and high angle there may be two mechanisms, so that may be the reason of large slope change.

5.3.3 Neural Network Model: Development and Implementation (for coating adhesion strength)

A software package NEURALNET for neural computing developed by Rao and Rao [**146**] using back propagation algorithm is used as the prediction of coating adhesion strength at different operating power levels for different substrates. To train the neural network used for this work, about 8 data sets at different operating power levels for different substrates are taken. Based on least error criterion, one structure, shown in table 5.5, is selected for training of the input-output data.

Input Parameters for Training	Values
Error tolerance	0.001
Learning parameter(ß)	0.002
Momentum parameter(α)	0.002
Noise factor (NF)	0.001
Maximum cycles for simulations	1000,000
Slope parameter (£)	0.6
Number of hidden layer neuron	6
Number of input layer neuron (I)	2
Number of output layer neuron (O)	1

Table 5.5 Input parameters selected for training (Coating adhesion strength).

The operating power levels and substrate materials are taken as the parameter significantly affecting the coating adhesion strength. Each of these parameters is characterized by one neuron and consequently the input layer in the ANN structure has two neurons and the output layer in the ANN structure has one neuron. The optimized three-layer neural network having an input layer (I) with two input nodes, a hidden layer (H) with six neurons and an output layer (O) with one output node employed for this work is as shown in fig. 5.2.

5.3.4 ANN prediction of coating adhesion strength

The prediction neural network was tested with three data sets from the original process data. Each data set contained inputs such as torch input power, substrate material and an output value i.e. coating adhesion strength was returned by the network. As further evidence of the effectiveness of the model, an arbitrary set of inputs is used in the prediction network. Results were compared to experimental sets that may or may not be considered in the training or in the test procedures. Fig.5.6 presents the comparison of predicted output values for coating adhesion strength with those obtained experimentally with different torch input power on different substrates.

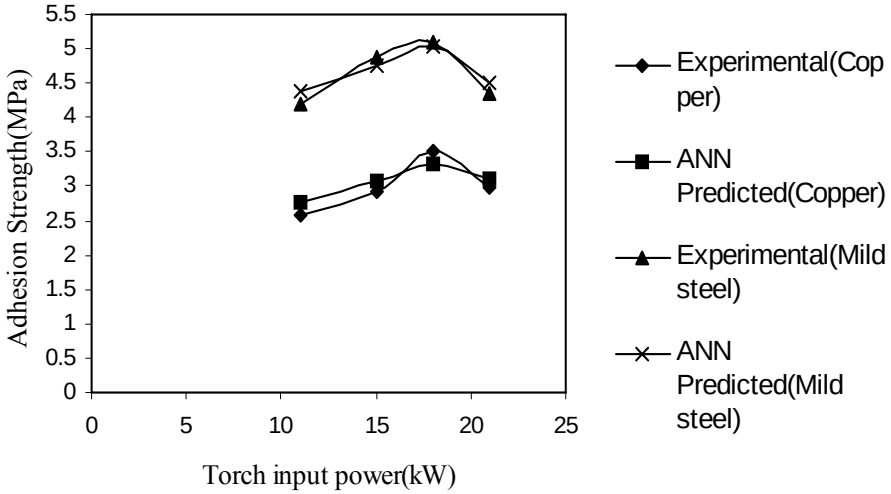

Fig.5.6 Comparison plot for predicted and experimental values of coating adhesion strength with different torch input power on different substrates.

It is interesting to note that the predictive results show good agreement with experimental sets realized after having generalizing the ANN structures. The optimized ANN structure further permits to study quantitatively the effect of the considered input power. The range of the chosen parameter can be larger than the actual experimental limits, thus offering the possibility to use the generalization property of ANN in a large parameter space. In the present investigation, this possibility was explored by selecting the torch input power in a range from 7 kW to 25 kW, and a set of prediction for coating adhesion strength is evolved.Fig.5.7 illustrates the predicted evolution of coating adhesion strength of alumina titania coatings on copper and mild steel substrates with torch input power.

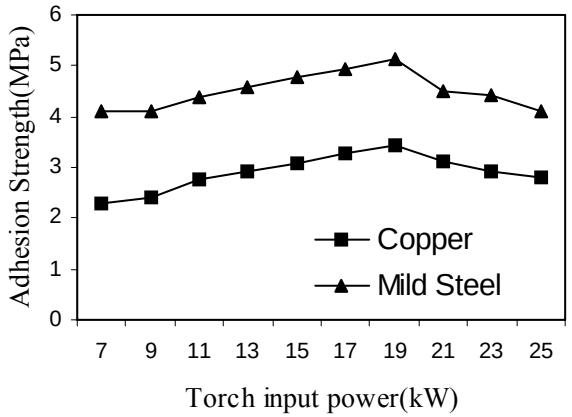

Fig.5.7 predicted values of coating adhesion strength of alumina titania coatings on copper and mild steel substrates at different torch input power.

From the figure it can be visualized that, the interface bond strength increases with the input power of the torch up to a certain power level and then shows a decreasing trend in coating adhesion, irrespective of the substrate material. This might be due to the fact that, when the operating power level is increased, larger fraction of particles attain molten state as well as the velocity of the particles also increase. Therefore there is better splat formation and mechanical inter-locking of molten particles on the substrate surface leading to increase in adhesion strength [**117**]. But, at a much higher power level, the amount of fragmentation and vaporization of the particles increase. There is also a greater chance to fly off of smaller particles during in-flight traverse during plasma spraying and results in poor adhesion strength of the coatings. Coating adhesion strength is more in case of mild steel substrate than that of copper substrate may be due to the dependence of thermal conductivity for melted particle, dissipation of heat at metal interface and also may be due to thermal expansion coefficient mismatch at the ceramic metal interface [**118**].

5.4 REMARKS

Functional coatings have to fulfill various requirements. The less erosion wear rate is one the main requirements of the coatings developed by plasma spraying. Solid particle erosion is considered as a non-linear process with respect to its variables: either materials or operating conditions. In order to achieve certain values of erosion rate accurately and repeatedly, the influence parameters of the process have to be controlled accordingly. Since the number of such parameters in plasma spraying is too large and the parameter-property correlations are not always known, statistical methods can be employed for precise identification of significant control parameters for optimization. Neural computation can be used as a tool to process very large data related to a spraying process like coating erosion wear rate and coating adhesion strength and to predict any desired coating characteristic the simulation can be extended to a parameter space larger than the domain of experimentation.

Chapter 6

CONCLUSIONS

- Conclusions
- Scope for Future Work

CHAPTER 6
CONCLUSIONS

The conclusions drawn from the present work are as follows:

- Commercial grade alumina & titania mixed powders in the size range 40 to 100μm is coatable on metal substrates employing thermal plasma spray technique. Coatings made with alumina titania possess desirable coating characteristics comparable to those of other conventional plasma sprayed ceramic coatings.

- Maximum coating thickness of ~ 200 micron on copper and ~ 190 micron on mild steel substrates is obtained with the coatings deposited at 18 kW power level. So it is evident that, there is an increase in coating thickness with increase in input power to the plasma torch; up to about 18 kW and then for further higher input power, no improvement in coating thickness is recorded. Coating thickness is higher in case of copper than that of mild steel substrate.

- Deposition efficiency for alumina titania coatings ranges from 21.6% to 41.73% in case of mild steel substrate and from 25.2% to 43.34% in the case of copper substrate. It is interesting to note that the deposition efficiency, in all cases, has increased in a step up fashion with the increase in torch input power.

- Adhesion strength of the coating varies with operating power. Maximum adhesion strength of 5.1 MPa on mild steel substrate and of 3.5Mpa on copper substrate is recorded at 18 kW. It is noted that invariably in all cases the interface bond strength increases with the input power of the torch up to a certain optimum power level and then shows a decreasing trend. Coating adhesion is higher in case of mild steel substrate than of copper substrate.

- It is observed that porosity volume fraction of these coatings lie in the range of from ~ 4 to ~ 6 %. The values obtained in the coatings under this study are well with in acceptable range for a good quality coating.

- The different phases observed in XRD studies, corroborates to the observation of different hardness values for different optically distinguished phases. High hard ness values may be due to the presence of different phase forms (i.e. allotropic transformations) of alumina phase having high hardness value. Low hard ness values may be of the titania phases.

- Due to phase transformations and inter-oxide formation during plasma spraying at different power levels, changes in the coating characteristics such as hardness etc. are observed.
- Operating power level of the plasma torch influences the coating adhesion strength, deposition efficiency, coating thickness and coating hardness to a great extent. The coating morphology is also largely affected by the torch input power.

- The microstructures of the coatings are dependent on operating power level of the plasma torch, the physical characteristics such as coating porosity, phase formation in the raw material during spraying.

- It is observed that, the erosion wear rate is dependent on erodent dose, angle of attack, velocity of erodent, stand off distance and size of the erodent. Cumulative coating mass loss varies with time of erosion. Maximum amount /rate of erosion occur at 90^0 impact angle. The trend of erosion of the coatings seems to follow the mechanism predicted for brittle materials. Coating deposited at 18 kW power level shows a higher erosion rate than that of the sample deposited at 11kW power level.

- Erosion wear behaviour is one of the main requirements of the coatings developed by plasma spraying for recommending specific application. In order to achieve tailored erosion wear rate accurately and repeatedly, the influence of the process parameters are to be controlled accordingly. The coating sustains erosion by solid particle impingement substantially and therefore alumina titania can be considered as a potential coating material suitable for various tribological applications.

- Impact velocity, impact angle, stand off distance and size of the erodent significantly affect the erosion wear rate of coating. Identification of these factors and their significance on the coating erosion wear rate is possible by statistical techniques like Taguchi experimental design. Artificial neural networks can be gainfully employed to

simulate property-parameter correlations in a space larger than the experimental domain. Neural computation can be gainfully employed as a tool to analyze, optimize and predict the erosion behavior, adhesion strength of the coatings purpose. It is evident that with an appropriate choice of processing conditions a sound and adherent ceramic coating is achievable using alumina and titania .

Scope for Future Work

The present work opens up a wide area for future investigators to explore many other aspects of alumina titania coatings. Evaluation of thermal stability of these coatings is to be evaluated to find high temperature applications. Sliding wear behaviour under different operating conditions can be investigated to identify suitable application areas. Post heat treatment of these coatings is to be made to ascertain further improvement in coating quality and properties.

References

REFERENCES

1. Taylor R. - "Thermal Plasma Processing of Materials"— Power Beams and Materials Processing PBAMP 2002, Ed. A. K. Das et al., Allied Publishers Pvt. Ltd., Mumbai, India: 2002. pp.13-20 .

2. Bandopadhyaya P.P. - Processing and Characterization of Plasma sprayed Ceramic coatings on Steel Substrate—Ph.D.Thesis, IIT, Kharagpur, India (2000).

3. Pawlowski L. The science and engineering of thermal spray coatings. New York, USA: Wiley, 1995. p. 432.

4. Normand B. , Fervel V., C. Coddet, Nikitine V., "Tribological properties of plasma sprayed alumina–titania coatings: role and control of the microstructure." Surf. Coat.Technol. Volume123, (2000) :p.278.

5. Fervel V., Normand B., Coddet C.," Tribological behavior of plasma sprayed Al_2O_3-based cermet coatings." Wear. Volume230, (1999): p.70.

6. Niemi K. , Vuoristo P. , Mantyla T., Lugscheider E., Knuuttila J., Jungklaus , in: Proceedings of the 8th National Thermal Spray Conference,Houston, TX: 1995, p. 645.

7. Ramchandran K. and Selvarajan P. A**.," "** In-flight particle behaviour and its effect on co-spraying of alumina–titania." Thin Solid Film. Volume 315, (1998): p.49.

8. Steffens H.D., Haumann D., Gramlich M., Wilden J., Wewel M., Hohle M., Nestler M.C. , in: Proceedings of the 8th National Thermal Spray Conference, Houston, TX: 1995, p. 677.

9. Ramachandran K. , Selvarajan V. , Ananthapadmanabhan P. V. , Sreekumar K.P., "Microstructure , adhesion, microhardness , abrasive wear resistance and electrical resistivity of the plasma sprayed alumina and alumina–titania coatings."Thin Solid Films .Volume 315, (1998): p. 144–152**.**

10. R.B. Heiman, 'Plasma Spray Coating, Principle and Application' , VCH, Weinheim, Germany, 1996.

11. Edwards R., "Cutting Tools", The Institute of Materials, UK,:1993.

12. Budinski K. G., Surface Engg. For Wear Resistance, N.J., USA:,1988.

13. Metco Plasma Spraying Manual, Metco, USA:1993.

14. Longo L. F., Thermal Spray Coatings, ASM, USA: 1985.

15. Meringolo V., Thermal Spray Coating, Tappi Press, Atlanta, USA:1983.

16. Tape N. A., Baker E. A. and Jackson B. C. , Plating and Surface finishing, 1976, October, p. 30.

17. Holm R., "The frictional force over the real area of Contact", Wiss. Vereoff. Siemens Werken, Volume17, No.4, (1938): p. 38-42.

18. Ashby M. F. and Lim S. C., 'Wear - mechanism maps.' Scripta Metallurgical et Materialia.Volume24, (1990): p. 805-810.

19. Wang Y., lei T.C. and Gao C.Q.,'Influence of isothermal hardening on the sliding wear behaviour of 52100 bearing steel.' Tribology International.Volume 23,No.1,(1990): p.47-63.

20. Soda N., 'Wear of some F.F.C metals during unlubricated sliding part-1.Effects of load, velocity and atmospheric pressure on wear'. Wear. Volume33, (1975):p. 1-16.

21. Burwell J.T. and Strang C.D, 'Metallic wear', Proc. Soc (London), 212A May 1953, p. 470-477.

22. Burwell J .T. , 'Survey of possible wear mechanisms.' Wear. Volume1, (1957/58): p.119-141.

23. K.H.Zumgahr, 'Microstructure and wear of materials' Elsevier , Amsterdam , 1987.

24. P.L.Ko, "Metallic wear-a review with special references to vibration-induced wear in power plant components." Tribology International. Volume 20, No. 1, (April 1987): p.66-78.

25. Eyre L.S., "Wear Characteristics of metals." Tribology International. (October 1976):p. 203- 212.

26. Dowson, "Wear oh where." International Conference on wear of Materials,Vancouver Canada, April 14-18, 1985.

27. Peterson.M. B, "Advanced in tribo-materials I Achievements in Tribology",Amer, Soc, Mech. Eng., Volume1, New York, 1990, pp. 91-109.

28. Blau J., "Fifty years of research on the wear of metals." Tribology International. Volume 30, No.5, (1997): p. 321-331.

29. WangY., " Sliding wear behavior of ceramic, plasma sprayed on casting aluminum alloy against SiC ball." Wear. Volume 161, (1993): p. 69.

30. Wang Y., Yuansheng J. and Shizhu W., "The tribological behaviour of various plasma-sprayed coatings against cast iron." Wear. Volume 128, (1988): p. 265.

31. Jainjun W. and Qunji X., "Tribological properties of $FeCl_3$ - graphite intercalation compound rubbed film on steel." Wear. Volume 162 ,(1993)**:** p. 229.

32. Lin J. F. and Li T. R., "Studies of Al_2O_3(p)- 6061 Al composites under dry sliding conditions using scanning electron microscopy, energy-dispersive spectrometry and X-ray diffractometry."Wear. Volume 160, (1990)**:** p. 201.

33. Ahn H.S. and Kwon O. K., "Classification of wear debris using a neural network." Wear.Volume 225, **(**1999): p. 814.

34. Jainjun W., Qunji X. and Huiling W., Wear. Volume 152, (1992) **:** p. 161.

35. L athabai S., Ottmuller M. , Fernandez I., **"**Solid particle erosion behaviour of thermal sprayed ceramic, metallic and polymer coatings." Wear. Volume 221, (1998): p. 93.

36. Zhou L., Gao Y. M., Zhou J.E. , Zhou Q. D., "Corrosion wear behaviour of ion-implanted steel." Wear . Volume176, (1994)**:** p. 39.

37. Ahn H. S. and Kwon O. K., "Wear behaviour of plasma-sprayed partially stabilized zirconia on a steel substrate." Wear. Volume 162 – 164, (1993):p. 636.

38. Quinn T. F. J. and Winer W. O., **"**The thermal aspects of oxidational wear.**"** Wear. Volume 102, (1985): p. 67.

39. Kim A. Y., Lim D. S. and Ahn H. S., J. Kor. Cer. Soc, Volume 30, (1993): p. 1059.

40. Ahn H. S. , Kim J. Y. and Lim D. S., "A study on wear and erosion of sialon-Si_3N_4 whisker ceramic composites.**"** Wear. Volume 203 – 204, (1997): p. 77.

41. Fu Y., Batchelor A. W., Xing H. and Gu Y., " Failure mechanisms of plasma nitrided Inconel 718 film." Wear. Volume 210, **(**1997): p. 157.

42. Sun Y., Li B.,Yang D., Wang T., Sasaki Y. and Ishii K., Wear. Volume 215, (1998): p. 232.

43. Song Y. S., Han J. C. , Park M.H., Ro B.H., Lee K. H., Byun E. S., Sasaki S., Proc. 15th International Thermal Spray Conference, 25th – 29th May 1998 , France , pp. 225.

44. Mendelson M. I., Wear. Volume 50, (1978)**:** p. 71.

45. Metco Technical Bulletin on TiO_2, Metco Inc., NY, USA:,1971.

46. Dai W. W., Ding C. X., Li J. F., Zhang Y.F. and Zhang P. Y., " Wear mechanism of plasma-sprayed TiO_2 coating against stainless steel ."Wear.Volume196, (1996)**:**p. 238.

47. Suh N. P., "The delamination theory of wear", Wear. Volume 25, **(**1973): p. 111.

48. H. So, "The mechanism of oxidational wear." Wear. Volume 184, (1995): p. 161.

49. Eyre T. S.," Effect of boronising on friction and wear of ferrous metals.",Wear.Volume 34,(1975)**:** p. 383.

50. Halling, Principles of Tribology, The Mcmillan Press Ltd, NY, USA:, 1975.

51. Guilmad Y., Denape J. and Patil J. A., " Friction and wear thresholds of alumina-chromium steel pairs sliding at high speeds under dry and wet conditions." Trib. Int. Volume 26, (1993): p. 29.

52. M. G. Gee, "The formation of aluminium hydroxide in the sliding wear of alumina." Wear. Volume 153, (1992): p. 201.

53. Mcpherson R., J. Mat. Sc., Volume 8, (1973) **:** p. 859.

54. Mcpherson R., J. Mat. Sc., Volume 15, (1980) **:** p. 3141.

55. Lopez A. R. D. A ., Faber K. T. , J. Am. Cer. Soc., Volume 82, No.8, (1999): p. 2204.

56. Ono H., Teramoto T. and Shinoda T., Mat and Mfg. Processes. Volume 8(4&5), (1993): pp.451.

57. Musikant S., What Every Engineer Should Know About Ceramics, Marcell Dekker Inc, NY, USA:. 1991.

58. Wahi R. P. and Lischner B., J. Material Science. Volume 15, (1980**):** p. 875.

59. Yamamota T., Olsson M. ,Hogmark S., "Wear mechanisms and tribo mapping of Al_2O_3 and SiC in dry sliding." Wear. Volume 174,(1994): p. 21.

60. Halling, Principles of Tribology, The Mcmillan Press Ltd, NY, USA:, 1975.

61. Guilmad Y. , Denape J. and Patil J. A., " Friction and wear thresholds of alumina-chromium steel pairs sliding at high speeds under dry and wet conditions." Trib. Int. Volume 26,(1993): p. 29.

62. Ramachandran K., Selvarajan V. , Ananthapadmanabhan P. V., Sreekumar K.P. "Microstructure,adhesion, microhardness, abrasive wear resistance of the plasma sprayed alumina and alumina – titania coatings." ,Thin solid film. Volume315**, (**1998): p. 144-152.

63. Krishnakumar V. and Swarnamani S., "Tribological Behaiour of plasma sprayed Al_20_3 and TiO_2 ceramic hard coating under dry contact.",IIT Madras,department of applied Mechanics,(1996).

64. Westergård R., Axén N., Wiklund U., Hogmark S., "An evaluation of plasma sprayed ceramic coatings by erosion, abrasion testing." Wear.Volume 246, (2000): p.12-19.

65. Normand B., Fervel V. , Coddet C. , Nikitine V. , "Tribological properties of plasma sprayed alumina–titania coatings:role and control of the microstructure." su rface and coatings technology.Volume123, **(**2000): p.278-287.

66. Vijayakumar K., Sharma Apurbba Kr., Mayuram M.M., Krishnamurthy R., "Response of plasma sprayed alumina – titania ceramic composite to high frequency impact loading."Materials letters. Volume 56, (2002): p. 252-262.

67. Ananthapadmanabhana P. V. , Thiyagarajana T .K., Sreekumara K. P., Satputea R.U., Venkatramania N., Ramachandran. K., "Co-spraying of alumina– titania: correlation of coating composition and properties with particle behaviour in the plasma jet." Surface and coatings technology.Volume168, (2003): p.231-240.

68. Bounazef Mokhtar,Guessasma Sofiane, Montavon Ghislain,Coddet Christian ,"Effect of APS process parameters on wear behaviour of alumina – titania coatings." Materials Letters. Volume 58,(2004): p. 2451-2455.

69. Xinhua Lin , Yi Zeng, Xiaming Zhou , Chuanxian Ding ," Microstructure of alumina /3wt.% titania coatings by plasma spraying with nanostructured powders." Materials science and engineering.Volume357, (2003): p. 228-234.

70. Sofiane Guessasma a, Mokhtar Bounazef b, Philippe Nardin c, Tahar Sahraoui, " Note on POD test parameters to study wear behaviour of alumina– titania coatings ." ceramics International. Volume52, (2006)**:** p. 13-19.

71. Okumus S. Cem, " Microstructural and mechanical characterization of plasma sprayed Al_2O_3 – TiO_2 composite ceramic coating on Mo / cast iron substrates ." materials Letters. Volume59, (2005): p. 2314-3220.

72. Habib K . A. , Saura J. J , Ferrer C. , Damra M. S. , Giménez E. , Cabedo L., "Comparison of flame sprayed Al2O3 / TiO2 coatings: Their microstructure, mechanical properties and tribology behaviour."surface and coatings technology. 2006.

73. Zhang Tiancheng , Luo Yichun , Li D.Y. , " Erosion behavior of aluminide coating modified with yttrium addition under different erosion conditions." Surface and Coatings Technology. Volume126, (2000):p.102-109.

74. Herman H., Sampath S., in: K.H. Stern (Ed.), " Thermal Spray Coatings", Metallurgical and Ceramic Protective Coatings, Chapman and Hall, London, UK,1996, p. 261.

75. Mishra S.B., Chandra K., Prakash S. , Venkataraman B. , "Characterisation and erosion Behaviour of a plasma sprayed Ni_3Al Coating on a Fe-based superalloy." Materials Letters. Volume59, (2005): p.3694 – 3698.

76. Westergard R., Erickson L. C., Axen N., Hawthorne H. M. , Hogmark S., Tribol. Int.Volume 31, No.5, (1998):p. 271.

77. Pfender E., "Fundamental studies associated with the plasma spray process." Surf. Coat. Technol. ,Volume34 (1988) :p.1.

78. O. Knotek , in: R.F. Bhushah (Ed.) , Handbook of Hard Coatings Deposition Technologies, Properties and Applications, 2001, p.92.

79. Guo D.Z., Li F.L.,Wang J.Y, Sun J.S., "Effects of post-coating processing on structure and erosive wear characteristics of flame and plasma spray coatings." Surf. Coat. Technol. ,Volume73, (1995):p. 73.

80. Restall J. E., Proc. 3rd Conf. on G as Turbine Materials in a Marine Environment, Bath, 1976, Ministry of Defence, London, Session V, Paper 10.

81. Galsworthy J. C., Restall J. E. and Booth G. C., Brunetaud in R., Coutsouradis D., Gibbons T. B., Lindblom Y., Meadowcroft D. B. and Stickler R. (eds.), Proc. Conf.on High Temperature Alloys for Gas Turbines, Liege, October 4 - 6, 1982, Reidel, Dordrecht, p. 207.

82. Kosel T.H. (Ed.), Friction, Lubrication and Wear Technology, ASM Handbook, Volume 18, (1992): p. 199.

83. Tabakoff W., "Erosion resistance of superalloys and different coatings exposed to particulate flows at high temperature." Surf. Coat. Technol. ,Volume 120– 121, (1999): p.542.

84. Levy A.V., "The erosion of carbide-metal composites", Surf. Coat. Technol. ,Volume36, (1988):p. 387.

85. Shipway P.H., Hutchings I.M., "Measurement of coating durability by s olid particle Erosion.", Surf. Coat. Technol.,Volume 71, (1995): p. 1.

86. Brunton J.H., Rochester M.C., Erosion of solid surfaces by the impact of liquid drops, in: C.M. Preece (Ed.), Erosion, Treatise on Materials Science and Technology, Volume 16,Academic Press, New York, 1979, p. 185–248.

87. Lesser M.B., Field J.E., "The impact of compressible liquids." Ann. Rev.Fluid Mech. Volume15 (1983):p. 97–122.

88. Field J .E. , ELSI conference: invited lecture—"liquid impact: theory, experiment, Applications." Wear.Volume233–235, (1999): p. 1–12.

89. Lee M.K., Kim W. W., Rhee C.K., Lee W.J., " Liquid impact erosion mechanism and theoretical impact stress analysis in TiN- coated steam turbine blade materials." Metal. Mater. Trans. VolumeA 30 (1999) : p.961–968.

90. Angle P. A. Impact Wear of Materials, (Elsevier; New York, 1976).

91. Tucker R.C. Jr., On the relationship between the microstructure and the wear characterstics of selected thermal spray coatings. Proceeding of ITSC, Kobe, Japan, 1995, pp. 477 – 482.

92. Alonso F., Fagoaga I. and Oregui P. .- "Erosion Protection of carbon – epoxy composites by plasma sprayed coatings." Suface & Coatings Technology. Volume 49, Issues 1 – 3, 10 Dec, (1991)**:** p.482 – 488.

93. Tabakoff W., Shanov. V. -- "Erosion rate testing at high temp. for turbo machinery use." Surface & Coatings Technologies. Volume 76 – 77, Part I, Nov (1995), p. 75 – 80.

94. Hawthrone F. M, Erickson L. C., Ross D., Tan H. and Trockzynsko T. , " The microstructural dependence of wear and indentation behaviour of some plasma-sprayed alumina coatings." Wear.Volume203 – 204, (1997)**:** p. 709.

95. Zhang X. S., Clyne T. W. and Hutchings I. M., Surf. Engg., Volume 13, No.5, (1997): p.393.

96. Roberto Jose, Branco Tavares, Gansert Robert , Sampath Sanjay , Christopher C. Berndt , Herman Herbert –" Solid Particle Erosion of Plasma Sprayed Ceramic Coatings. "Materials Research. Volume 7, No.1. (2004): p. 147-153.

97. Wrigren J., Surf. Coat. Tech. Volume 45, (1991): p. 263.

98. Nicholas M. G. and Scott K. T., Surfacing Journal. Volume 12,(1981**):** p.5.

99. Funk W. Goebe F.," Bond strength optimization of plasma-sprayed Cr_2O_3 layers by factorial two-level experiments." Thin Solid Film. Volume128, (1985): p. 45.

100. Wielage B., Hofmann V., Steinhauser A. , Zimmerman G., Wear. Volume 14, No.2, (1998): P.136.

101. Lee N. Y., Stinton D. P., Brandt C. C., Erdogan F., Lee Y. D. and Mutasim Z., J.Am. Cer. Soc., Volume 79,No.12, (1996): P. 3003.

102. Metco Plasma spraying Manual, 1993,Metco, USA.

103. Nash A.R., Weare N. E. and Walker D. L., July, J. Metals. July, 1961, p. 473.

104. Ramchandran K. and Selvarajan P. A., Thin Solid Film. Volume 315,(**1998):** p. 149.

105. Ingham H. S. and Fabel A. J., Welding Journal. (February, 1975)**:** p. 101.

106. Hennaut J., Othmezouri J. and Charlier J., Mat. Sc and Tech., Volume11,(1995): p. 174.

107. Elvers B., Hawkins S. and Schultz G. (eds), Ulhmann's Encyclopedia of Industrial Chemistry, Volume 1/16, VCH, (1990): p. 433.

108. Chen H., Lee S.W., Du Hao, Ding Chuan X and Cho Chul Ho; " Influence of feed stock and spraying parameters on the deposition efficiency. and microhardness of plasma sprayed zirconia coatings." -- Materials Letter .Volume 58, Issues 7 – 8, (March 2004)**:** p.241 – 1245.

109. Wojnar L., Image Analysis Applications In Materials Engineering, CRC Press, Boca Raton, 1999.

110. Cullity B.D.,Elements of X-Ray Diffraction,Addition-Wasley, Reading,MA, 1972, p.102.

111. Venkataraman B. – Evaluation of Tribological Coatings – Proc. of DAE-BRNS Workshop on Plasma Surface Engineering, BARC, Mumbai , (September 2004):, p. 217 – 235.

112. Nicholls J.R. , Deakin M.J. , Rickerby D . S. , " A comparison between the erosion behaviour of thermal spray and electron beam physical vapour deposition thermal barrier coatings." Wear. Volume 233–235, (1999):p.352–361.

113. Mishra S.B. , Chandra K. , Prakash S., Venkataraman B., " Characterisation and erosion behaviour of a plasma sprayed Ni_3Al coating on a Fe-based superalloy." Materials Letters.Volume59, (2005):p. 3694 – 3698.

114. Lalleman G . – Tallaron, " Study of Microstructure and adhesion of spinelles coatings formed by plasma spraying.", Ph. D. Thesis No. 96 – 58 (1996) E.C. Lyon, France.

115. Mishra S. C., Rout K. C., Ananthapadmanabhan P. V. and Mills B. , " Plasma Spray Coating of Fly Ash Pre-Mixed with Aluminium Powder Deposited on Metal Substrates.", J. Material Processing Technology.,Volume 102, 1 – 3 ,(2000): p. 9 – 13.

116. Lima C.R.C., Trevisan R.E., J.Themal Spray Tech.,Volume 62,(1997): p. 199.

117. Halling, Principles of Tribology, The Mcmillan Press Ltd, NY, USA, 1975.

118. Guilmad Y., Denape J. and Patit J . A.; " Friction and wear thresholds of alumina- chromium steel pairs sliding at high speeds underdry and wet condition; Trib.Int. Volume 26, (1993): p. 29-39.

119. Pawlowski Lech – The Science and Engineering of Thermal Spray. Coatings, JohnWiley & Sons, New York (1995): p.218.

120. Kitamura Toshihiro, Shibata Kiyoshi, and Takeda Koichi. In-flight reduction of Fe_2O_3,Cr_2O_3,TiO_2 and Al_2O_3 by Ar-H2 Plasma,Advanced Materials& Technology Research Laboratories, NIPPON STEEL CORPORATION, 1618 Ida, Nakahara Ku,KAWASAKI211,JAPAN.

121. Taylor Patrick R. and Pirzada Shahid A., Synthesis of ceramic carbide powders in a non transferred arc thermal Plasma reactor.College of Mines,University of Idaho,Moscow,Idaho 83843.

122. Roberto José, Branco Tavares, Gansert Robert, Sampath Sanjay, Berndt Christopher C., Herman Herbert, "Solid Particle Erosion of Plasma Sprayed Ceramic Coatings." Materials Research. Volume 7, No. 1, (2004): p.147-153.

123. Erickson L.C., Westergård R., Wiklund U., Hawthorne H.M., Axén N., Hogmark S., "Cohesion in plasma sprayed coatings — a comparison between evaluation methods." Wear.Volume214, (1998):p. 30–37.

124. Levy A. V., "The erosion corrosion behavior of protective coatings." Surf. and Coating Technology. Volume36, (1988): p. 387 – 406.

125. Alahelisten A., Hollman P., Hogmark S., "Solid particle erosion of hot flame-deposited diamond coatings on cemented carbide." Wear . Volume177,(1994): p.159-165.

126. Bayer G. –Mechanical Wear Prediction and Prevention – Marcel Dekkar, Inc., New York (1994): p. 396.

127. Lathabai S. , Ottmuller M., Fernandez I. , "Solid particle erosion behaviour of thermal sprayed ceramic, metallic and polymer r coatings."Wear.Volume 221,(1998): p.93–108.

128. Shanov V., Tabakoff W. and Metwally M., " Erosive wear of CVD ceramic coatings exposed to particulate flow." Surface and Coatings Technology. Volume 54/55, (1992):p. 25—31.

129. Li Chang-Jiu, Yang Guan-Jun , Ohmori Akira, "Relationship between particle erosion and lamellar microstructure for plasma- sprayed alumina coatings." Wear. Volume 260, (2006) : p.1166–1172.

130. Westergard R., Axén N., Wiklund U., Hogmark S., " An evaluation of plasma sprayed ceramic coatings by erosion, abrasion and bend testing." Wear.Volume 246 (2000): p. 12-19.

131. Wayne S.F., Sampath S., "Structure/ property relationships in sintered and thermally sprayed WC-Co." J. Thermal Spray Technol. , Volume1, (1992): p. 307– 315.

132. Hawthorne H. M., Erickson L. C. , Ross D. , Tai H., Troczynski T., "The Microstructural dependence of wear and indentation behaviour of some plasma sprayed alumina coatings." Wear.Volume 203/204 ,(1997):p. 709–714.

133. Sampath S., "bstrate temperature effects on splat formation, microstructure development and properties of plasma sprayed coatings Part I: Case study for partially stabilized zirconia.",er. Sci. Eng. ,VolumeA 167, (1993):p. 1.

134. Westergard R., Erickson L.C., Axen N., Hawthorne H.M., Hogmark S., "The erosion and abrasion characteristics of alumina coatings plasma sprayed under different spraying conditions.", Tribol. Int. ,Volume31,No.5, (1998):p. 271.

135. Berger L. M., Hermal W., Vuoristo P., Mantyla T., Lengaure W., Ettmayer P., "Structure,Properties and Potentials of WC – CO, Cr_3C_2 – NiCr and TiC – Ni Based Hard metal like Coatings – Proceedings of the 9th National Thermal Spray Conference, CC. Berndt (Ed.), Published by ASM International USA, (1996).

136. Padmanabhan P.V.A., Thiyagarajan T.K., Sreekumar K.P., Venkatramani N.; "-flight particle behaviour and its effect on co-spraying of alumina–titania."Scripta Materialia. Volume50, (2004):p. 143-147.

137. Vardelle A., Vardellet M., Pherson R. Mc., Fanchais P. – Proc. of 9th National Themal Spray Conference, (1980): p.155.

138. Pawlowski Lech – The Science and Engineering of Themal Spray Coatings,John Wiley & Sons, New York (1995): p. 235.

139. Johner H., Wilms V., Schweltzer K. K., Adam P. –" Experimental and Theoritical Aspects of Thick Themal Barrier Coatings for Turbine Applications." – Thermal Spray: Advances in Coatings Technology , David L. Houck (Ed.) Published by ASM Int. USA (1987): p.155– 166.

140. Bayer R. G. , Mechanical Wear Prediction and Prevention – Marcel Dekkar,Inc., New York (1994): p. 395.

141. Arata Y., Ohmori A., Li Chang Jiu – Fundamental Properties of the ACT – 5P (Arata Coating Test with Jet Particles) – Themal Spray : Advances in Coatings Technology, David L. Houck (Ed.), Published by ASM International, USA (1987**)**: p. 79 – 83.

142. Roberto Jose, Branco Tavares, Gansert Robert, Sampath Sanjay, Berndt Christopher , Herman Herbert – "Solid Particle Erosion of Plasma Sprayed Ceramic Coatings." Materials Research. ,Volume7, No.1,(2004): p.147-153.

143. Sahin Y.,"The Prediction of Wear Resistance Model for The Metal Matrix Composites." Wear .Volume 258, (2005): p. 1717-1722.

144. Rajasekaran S., Vijayalakshmi Pai G. A., 2003,--Neural Networks, Fuzzy Logic And Genetic Algorithms—Synthesis and Applications – Prentice Hall of India Pvt. Ltd., New Delhi.

145. Zhang Z., Friedrich K., Artificial neural network applied to polymer composites: a review, Comp. Sci. Technol., in press.

146. Rao V. and Rao H., 2000,'C++ Neural Networks and Fuzzy Systems',BPB Publications.